Muscle development and muscular abnormalities in the teleost fish larvae(Dissertation_全文)

AUTHOR(S):

Uji, Susumu

CITATION:

Uji, Susumu. Muscle development and muscular abnormalities in the teleost fish larvae. 京都大学, 2014, 博士(農学)

ISSUE DATE:

2014-09-24

URL:

https://doi.org/10.14989/doctor.r12861

Muscle development and muscular abnormalities in the teleost fish larvae

Susumu Uji

2014

CONTENTS

CHAPTER I GENERAL INTRODUCTION

The occurrence of malformed fish can cause significant problems during juvenile production because malformations are often associated with high mortality rates and growth depression (Barahona- Fernandes, 1982; Andrades *et al*., 1996). Additionally, malformed fish depress the market prices, lower market demand, and negatively affect the relationship of trust between a producer and buyer. Therefore, methods for early detection and decrease of abnormalities are required (Boglione *et al*., 2013).

A number of researchers have noted morphological and skeletal deformities in teleosts. However, little is known about the occurrence and/or causes of musculature deformities, in part because of the difficulties associated with detection of muscular abnormalities. Muscular defects can reduce growth and survival rates because muscles play important roles in feeding, respiration and swimming during not only adult stage but also larval stage in fish. In addition, muscular abnormalities may be a background of skeletal deformities (Akiyama *et al*. 1986*a*; Akiyama *et al*. 1986*b*; Sakaguchi *et al*. 1987; Yokoyama *et al*. 2005). Therefore, it is important to recognize muscular abnormalities.

The ability to detect developmental defects first requires a thorough understanding of the process of normal development. Recognition of normal development and the ability to detect developmental defects offers culturists the opportunity to address issues in a timely manner, such as instituting improvements in larval rearing techniques by modifying environmental conditions during juvenile production (Koumoundouros *et al*., 2001; Sfakianakis *et al*., 2004; Sfakianakis *et al*., 2006; Cobcroft and Battaglene 2009; Georgakopoulou *et al*., 2010). Larvae that have structural defects caused by unsuitable developmental conditions may have reduced growth and survival. Unfortunately, the effects of the environment on muscle development are often irreversible owing to the rapid pace of ontogenetic change during the embryonic and larval stages. Feeding and locomotor performance are influenced by muscle morphology and physiology. Thus, abnormalities in muscle morphology have consequences for survival during the embryonic and larval stage. I developed a modified whole mount immunohistochemical method to visualize muscle development. This method allows researchers to investigate environmental conditions that cause muscular abnormalities during larval culture.

Understanding the development of the fish cranial muscles is of value to both aquaculturists and researchers of comparative morphology (Edgeworth, 1935; Winterbottom, 1974). The cranial muscles play important roles in feeding and respiration throughout ontogeny, by controlling the opening and closing of the buccal and branchial cavities. However, the vast majority of studies investigating cranial muscle development only report on the adult system, which is probably based on the technical difficulty and complexity associated with the observation of embryos and larvae. Recently, the development of cranial musculature in larval fish has been reported using serial section reconstruction or immunohistochemical staining methods (Matsuoka, 1987; Schilling and Kimmel, 1997; Huysentruyt *et al*., 2007; Geerinckx and Adriaens, 2007, 2008; Diogo *et al*., 2008). However, the greater parts of these reports deal with the so-called superficial cranial muscles. In contrast, the development of branchial muscles has been poorly documented.

The branchial muscles include the branchial levators, levatores externi, levatores interni, and levator posterior (Winterbottom, 1974). Although several articles have described the branchial wall muscles termed branchial levators during zebrafish development (Schilling and Kimmel, 1997; Hernandez *et al*., 2005), the relationship between the branchial levators in larvae and the levatores externi, levatores interni, and levator posterior in the adult remains poorly understood. According to a report by Winterbottom (1974), the levatores externi muscles connect the epibranchials of the first four arches to the skull, whereas the levatores interni are generally observed as two or three muscles that connect the skull to the infrapharyngobranchials. Schilling and Kimmel (1997) define the branchial levators as a series of muscles that run along the ceratobranchial cartilages, and suggest that these muscles are the levatores interni described by Winterbottom (1974). On the other hand, Hernandez *et al*. (2005) term the branchial levators that insert on the epibranchial elements at 6 and 32 days post fertilization (dpf), as the levatores externi in zebrafish. Thus, the information regarding the dorsal branchial muscles in larval stages is limited and partially confusing. In addition, there appears to be a lack of articles that report on dorsal branchial muscle development in detail in fish for the period from embryo to fry. Therefore, it remains unclear whether the branchial levators in zebrafish are actually the levatores interni or the levatores externi. There are no reports on the development of the branchial levators present in other species that may be used to aid in the answering of this question.

Another issue further complicates the reporting of dorsal branchial muscle development (Table 1). The levator posterior is thought to represent the fifth levator externus (Edgeworth, 1935), even though the levator posterior is separated from the levator externus series by a distinct hiatus, and is innervated by the vagus nerve. It remains a point of contention as to whether the levator posterior should be actually classified as the fifth levator externus. Thus, at present, little is known about the development of dorsal branchial muscles in embryos and larvae of fishes, especially the relationship between the branchial levators and the levatores interni and externi, and between the levatores externi and the levator posterior (Table 1-1).

In the present study, I described the process of muscle development in the Japanese Flounder *Paralichthys olivaceus* (Temminck & Schlegel, 1846), Bamboo sole *Heteromycteris japonicus* (Temminck & Schlegel, 1846), greater amberjack *Seriola dumerili* (Risso), and seven-band grouper *Epinephelus septemfasciatus* (Thunberg) using the modified whole mount immunohistochemical method, focusing primarily on cranial muscles. In addition, I documented the presence of abnormal trunk musculature in cultured seven-band grouper larvae and determined the environmental factors that were associated with this phenomenon.

Table 1. Moot points about dorsal branchial muslces

larval stage		adult stage	
branchial levators (branchial wall muscles)	?	levators interni	(ref. Schilling and Kimmel, 1997)
	?	levators externi	(ref. Hernandez et al., 2005)
		levator posterior ? = fifth levator exterus	(ref. Edgeworth, 1935)

CHAPTER II Muscle development in the Japanese flounder *Paralichthys olivaceus* (Temminck & Schlegel, 1846) with special reference to some of the larval-specific muscles

It is generally difficult to precisely determine which of the larval cranial muscles correspond to those of the adult for a number of reasons. First, larvae are very small and, thus, are difficult to manipulate to observe the larval musculature. Second, the tissues associated with the cranial muscles including the dermal bones, are often not well formed in larvae, and third, some cranial muscles are positioned deep in the head, making access to the muscles difficult. To overcome these problems, I investigated cranial muscle development using a modified whole mount immunohistochemical method. As the whole mount immunostaining methods reported previously do not use a bleaching step, or use only hydrogen peroxide to reduce pigment (Schilling and Kimmel, 1997; Hernandez *et al*., 2005; Diogo *et al*., 2008; Patterson *et al*., 2008), it is often very difficult to visualize and identify some of the cranial muscles deeply positioned in the head due to melanin. Using a combination of potassium hydroxide, hydrogen peroxide, and trypsin to increase transparency, I was able to visualize the complete set of cranial muscles after whole mount immunostaining of teleost fish. This method allowed for the accurate identification of the larval cranial muscles.

The Japanese flounder *Paralichthys olivaceus* (Temminck & Schlegel, 1846) is a marine fish that experiences a long larval period followed by metamorphosis. In addition, Japanese flounder are unusual in that the right eye migrates to the left side of the head at metamorphosis (Fig. 2-1). The Japanese flounder is a highly valued fish species in marine aquaculture in Japan. As a result, egg collection and rearing techniques have been well established, allowing me to collect large numbers of fertilized eggs daily for approximately three months during the spawning season. In addition, the body of Japanese flounder larvae is very thin, thus allowing easy penetration of antibodies. Therefore, the Japanese flounder has several advantages over other fish species for observing muscle development.

In this chapter, I describe muscle development in the Japanese flounder during the period spanning from hatching to metamorphosis, focusing primarily on the cranial muscles.

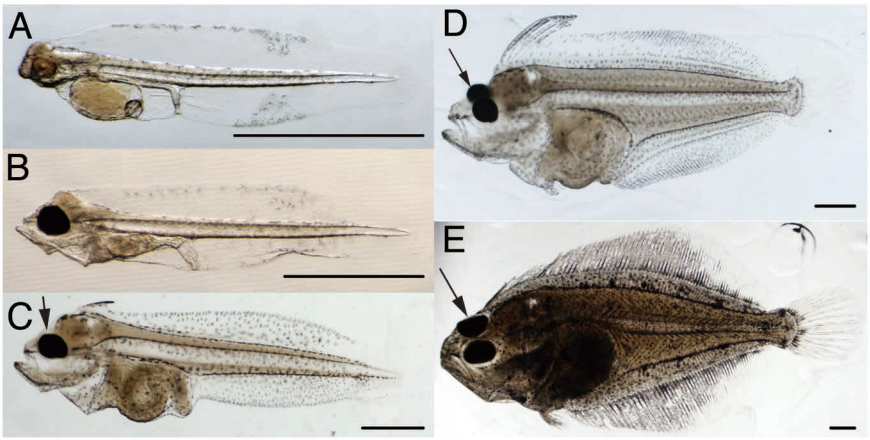

Figure 2-1. Development of the Japanese flounder, *Paralichthys olivaceus*, after hatching. Larvae at (A) 0 dph, (B) 4 dph, (C) 16 dph, (D) 32 dph and (E) 48 dph. The right eye (arrows) migrates to the opposite side during development. Scale bar = 1.0 mm.

Materials and methods

Japanese flounder samples

Fertilized eggs of *Paralichthys olivaceus* were obtained from a spawning tank. The temperature of the spawning tank was controlled at 16–18 °C and was housed at the National Research Institute of Aquaculture, Mie, Japan. Immediately after collection, the fertilized eggs were transferred and maintained in a 500 l plastic tank with running seawater at 20 °C. From this tank, a series of samples for 0, 1, 2, 4, 5, 7, 8, 10, 12, 14, 16, 20, 24, 28, 32, 36, 40, 44, 48 and 515 days post hatching (dph) was obtained. The numbers of specimens used for whole mount immunostaining and dissection at each dph were 15, 30, 32, 11, 10, 11, 31, 27, 43, 29, 44, 9, 17, 23, 19, 13, 19, 12, 12 and 3. Following anesthesia with 3-aminobenzoic acid ethyl ester (Sigma), larvae were fixed with 4% paraformaldehyde (PFA) in phosphate buffered saline (PBS) containing 0.3% Tween 20 (PBST), rinsed in PBST, dehydrated in a graded series of methanol (25, 50, 75 and 100%) and stored at –20 °C. The 515-dph samples used for dissection were fixed in 4% formalin in PBS after anesthesia with 3-aminobenzoic acid ethyl ester. After fixation, three samples of them were stained in Alizarin red S, dissected and observed under a stereoscopic microscope for myological examination.

Whole mount immunostaining and skeletal analysis

Stored larvae were rinsed in PBST, digested with 0.05% trypsin in a saturated solution of sodium tetraborate for 10 minutes to two hours either at room temperature or at 37 °C depending on age, and were then re-fixed with 4% PFA. After washing in PBST, the samples were submerged in 1% KOH supplemented with 0.9% H_2O_2 and gently agitated on a shaking platform to block for endogenous peroxidase activity and to remove melanin. The samples were incubated in Block Ace (Dainippon Pharm.) for two hours at room temperature. For immunohistochemical staining, samples were incubated with the primary anti-myosin antibody A4.1025 (1:200, Upstate), diluted in a mixture of Block Ace (Dainippon Pharm.), which had been previously diluted at 1:4 in PBST at 4 °C overnight, to identify myofibers. Following rinsing in PBST, the samples were submerged in Histofine Simple Stain PO (Nichirei) for two hours at room temperature, rinsed in PBST, and the color reaction developed using diaminobenzidine/H_2O_2 substrate or Vector VIP Substrate kit for Peroxidase (Vector Laboratories). After staining, samples were cleared in increasing concentrations of glycerol (25, 50 and 80%) and observed using a MZFL microscope (Leica) equipped with combi III (Leica), or Eclipse 90i microscope (Nikon). Micrographs were captured using a CCD camera DP70 (Olympus) and processed using Adobe Photoshop CS3 (Adobe Systems).

For visualization of cartilage tissue, larvae sampled at 20 and 24 dph were stained with Alcian blue according to the method described by Schilling *et al*. (1996). The numbers of larvae used were 10 and 11 respectively. For double staining of muscle and cartilage tissue, larvae sampled at 4, 8, 10, 12, 14, 16 and 24 dph were stained with Alcian blue and subsequently immunostained for muscle as described above. The numbers of larvae used for this double staining were 10, 10, 10, 9, 15, 13 and 16 respectively.

Results

The nomenclature of the muscles outlined in this study is primarily based on that used by Winterbottom (1974). The novel muscles discovered in the dorsal branchial arches of the flounder larvae were termed the larval branchial levators.

0 dph

At 0 dph, I could not identify the presence of any cranial muscle tissue even though the trunk myotomes have differentiated and the heart muscles have already looped (Fig. 2-2A).

1 dph

The superior rectus, lateral rectus and superior oblique of the extraocular muscles are detected as separate small muscles (Fig. 2-2C). In the cheek musculature, the adductor mandibulae A1 and the levator arcus palatini are found as relatively small muscles that are lying at the rear of the orbit (Fig. 2-2C). These muscles have not yet overlain each other. In the muscles located at the ventral part of the head, the intermandibularis posterior and interhyoideus are developing as paired small muscles respectively (Fig. 2-2D), even though they will become more deeply associated with each other to form the protractor hyoidei later on in development.

In the body region, the hypaxialis which is attached to the sixth myotome appears to be growing rostrally (Fig. 2-2B, C). The pectoral fin muscles are also detected, and appear as two muscle fiber masses (Fig. 2-2B, C).

2 dph

All six components of the extraocular muscles (superior oblique, inferior oblique, superior rectus, inferior rectus, medial rectus and lateral rectus) are clearly detected, even though the precise insertions remain obscure (Fig. 2-2E). These muscles appear to develop early and are followed by the musculature associated with the mandibular, hyoid and branchial arches. In the cheek muscles, in addition to the adductor mandibulae A1 and the levator arcus palatini, the adductor arcus palatini and the complex of the adductor operculi and the adductor hyomandibulae are present (Fig. 2-2E). The dorsal region of the adductor mandibulae A1 is overlain by fibers of the ventral part of the levator arcus palatini, and the adductor arcus palatini is situated posterior to the orbit and medial to the levator arcus palatini (Fig. 2-2F). The complex of the adductor operculi and the adductor hyomandibulae is present posteriorly to the levator arcus palatini (Fig. 2-2E). On the ventral surface of the head, the intermandibularis anterior and the intermandibularis posterior form a triangle. Transverse fibers of the intermandibularis anterior pass laterally between Meckel's

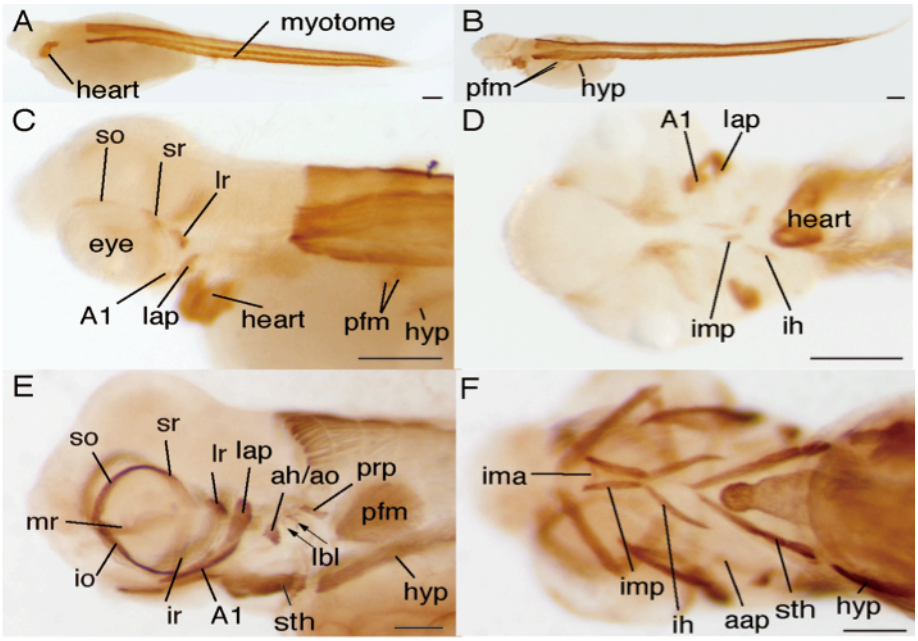

Figure 2-2. Larval musculature in the Japanese flounder head and trunk regions at 0–2 dph. Muscles were labeled with anti-myosin antibody. (A) Dorsolateral view of the musculature at 0 dph. (B) Dorsolateral view of the musculature at 1 dph. (C) Dorsolateral view of the cranial musculature at 1 dph. (D) Ventral view of the cranial musculature at 1 dph. (E) Lateral view of the cranial musculature at 2 dph. Arrows indicate the larval branchial levators. (F) Ventral view of the cranial musculature at 2 dph. aap, adductor arcus palatini; ah/ao, complex of adductor hyomandibulae and adductor operculi; A1, adductor mandibulae A1; hyp, hypaxialis; ih, interhyoideus; ima, intermandibularis anterior; imp, intermandibularis posterior; io, inferior oblique; ir, inferior rectus; lap, levator arcus palatini; lbl, larval branchial levator; lr, lateral rectus; mr, medial rectus; pfm, pectoral fin muscle; prp, protractor pectoralis; so, superior oblique; sr, superior rectus; sth, sternohyoideus. Scale bar = 0.1 mm.

cartilages to overlap the anterior ends of the intermandibularis posterior muscles (Fig. 2-2F). At this stage, the bilaterally symmetrical muscle straps of the intermandibularis posterior and the interhyoideus form an hourglass structure (Fig. 2-2F). In the dorsal portions of the branchial arches, the larval branchial levators are only very faintly detected (Fig. 2-2E). As I found that the present -mainly zebrafish-defined - terminology for teleost branchial muscles is rather confusing, I have refined this terminology for the purposes of the present work and created the term “larval branchial levators” for these muscles. In the ventral parts of the branchial arches, the sphincter oesophagi and a few obliqui ventrales are detected. In the muscles between the pectoral girdle and the skull, hyoid, and branchial arches, the paired sternohyoideus has arisen lateral to the heart tube (Fig. 2-2F). The sternohyoideus originates on the cranial face of the cleithrum and inserts onto the hyoid (Fig. 2-3E, F). The protractor pectoralis has also begun development as a small muscle. It appears to originate from the skull and

pass downwards in order to attach to the cleithrum (Fig. 2-2E). The muscles of the pectoral fin have grown as two plain pectoral fin plates. In the body region, a hypaxial muscle is attached to the sixth myotome and inserts on the posteroventral face of the cleithrum, opposite to the site where the sternohyoideus originates (Fig. 2-2E).

4 dph

The insertions of all the extraocular muscles are established (Fig. 2-3A, B). Whereas the adductor mandibulae A1 consists of a single mass at 2 dph, two masses of the adductor mandibulae can now be recognized in the cheek. The newly formed muscle represents the adductor mandibulae A2 and is located on the medial side of the adductor mandibulae A1 (Fig. 2-3D). The adductor mandibulae A1 originates from the hyosymplectic cartilage and inserts onto Meckel's cartilage (Fig. 2-3E). The levator arcus palatini appears conical in shape, with its apex lying anteroventrally, and occupies the area at the rear of the orbit between the neurocranium and the hyosymplectic cartilage (Fig. 2-3D, G). At this stage of development, the adductor hyomandibulae and the adductor operculi appear to be present as a single muscle mass that branches into two parts at the ventral end (Fig. 2-3D, J). The muscle originates on the ventral floor of the otic capsule of the neurocranium. It passes anteroventrally between the larval branchial levators 1 and 2, then inserts into the hyosymplectic cartilage and the opercle, which has not yet become ossified (Fig. 2-3G). This stage coincides with the time of the first feeding and so all components of the cheek muscles are developed, with the exception of the levator operculi and the dilatator operculi in the opercular region. On the ventral surface of the head, the positions of the intermandibularis anterior, intermandibularis posterior and interhyoideus have shifted anteriorly, coinciding with the anterior shift of the mouth. The hyohyoideus is faintly detected as paired thin muscle bands between the interhyoideus and the sternohyoideus muscles (Fig. 2-3E, F). In this chapter, I define the hyohyoideus inferior, hyohyoidei abductores and hyohyoidei adductores as hyohyoideus muscle types due to confusion in the literature over the classification of muscles located in the hyoid region, and because I was unable to identify the hyohyoidei abductores and the hyohyoidei adductores clearly.

The larval branchial levators are clearly detected (Fig. 2-3C, D, G and H), even though these muscles are only rudimentary in the 2-dph larvae. With the exception of the larval branchial levator 1, these muscles originate from the lateral side of the otic

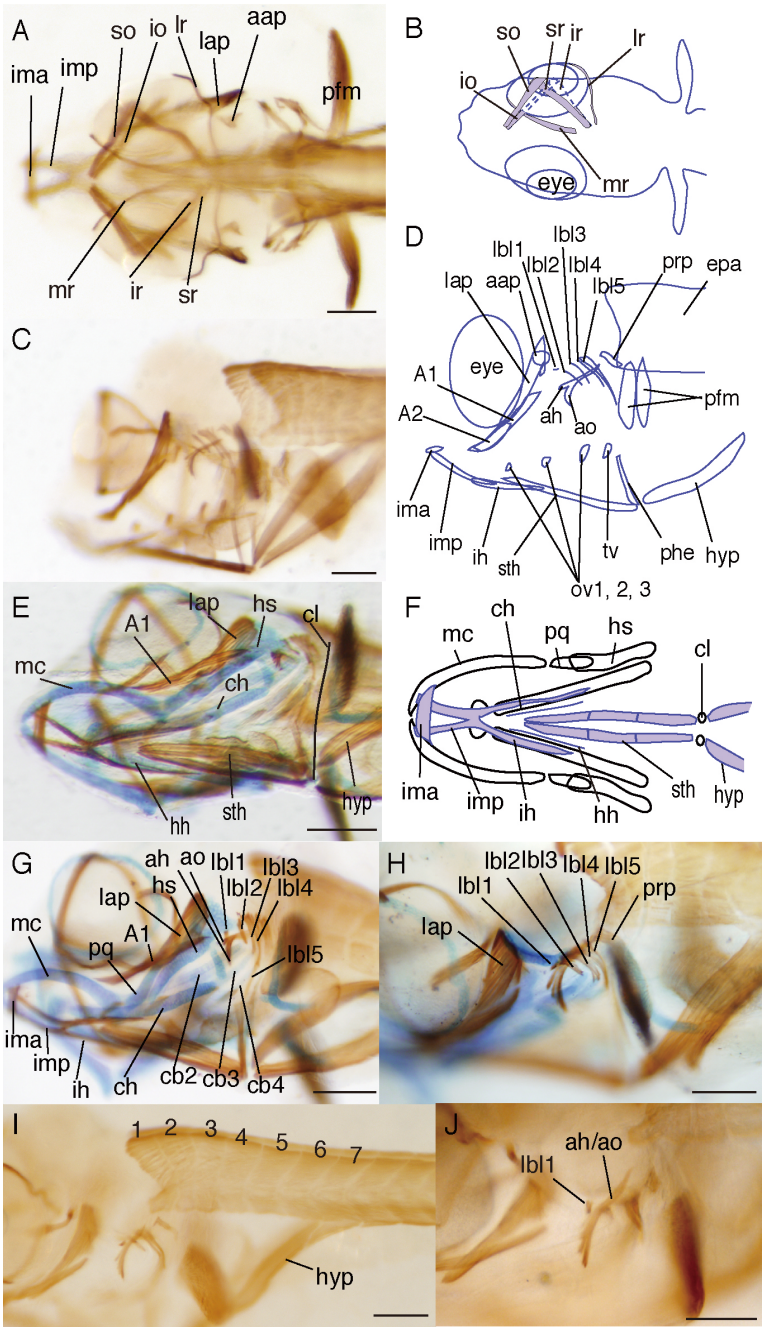

Figure 2-3

vesicle and insert onto the corresponding ceratobranchial cartilage along the branchial arch (Fig. 2-3G, H). The larval branchial levator 1 originates from the lateral side of the otic vesicle and points medially towards the region where epibranchial cartilage 1 or infrapharyngobranchial cartilages are to be formed (Fig. 2-3D, G, H, J). I was unable to precisely judge to what the larval branchial levator 1 connected, as there is no definitive cartilage tissue present. In later stages, the larval branchial levator 1 is found

Figure 2-3. Larval musculature of the Japanese flounder at 4 dph. Muscles were labeled with anti-myosin antibody and cartilage was stained with Alcian blue. (A) Dorsal view of the cranial musculature at 4 dph. (B) Schematic dorsal view of the extraocular musculature at 4 dph. (C) Lateral view of the cranial musculature at 4 dph. (D) Schematic representation of musculature in (C). (E) Ventrolateral view of the cranial musculature (brown) and cartilage (blue) at 4 dph. (F) Schematic representation of the ventral head muscles at 4 dph. (G) Ventrolateral view of the cranial musculature (brown) and cartilage (blue) at 4 dph. (H) Dorsolateral view of the cranial musculature (brown) and cartilage (blue) at 4 dph. Note the position of the larval branchial levators and the protractor pectoralis, and the complex of the adductor hyomandibulae and the adductor operculi. (I) Lateral view of the musculature at 4 dph. The figures show the number of myotomes. (J) Dorsolateral view of the cranial musculature at 4 dph, focusing on the adductor hyomandibulae and the adductor operculi. aap, adductor arcus palatini; ah, adductor hyomandibulae; ah/ao, complex of adductor hyomandibulae and adductor operculi; ao, adductor operculi; A1, adductor mandibulae A1; A2, adductor mandibulae A2; cb, ceratobranchial cartilage; ch, ceratohyal cartilage; cl, cleithrum; epa, epaxialis; hh, hyohyoideus; hs, hyosymplectic cartilage; hyp, hypaxialis; ih, interhyoideus; ima, intermandibularis anterior; imp, intermandibularis posterior; io, inferior oblique; ir, inferior rectus; lap, levator arcus palatini; lbl, larval branchial levator; lr, lateral rectus; mc, Meckel's cartilage; mr, medial rectus; ov, obliqui ventrales; pfm, pectoral fin muscle; phe, pharyngoclavicularis externus; pq, palatoquadrate; prp, protractor pectoralis; so, superior oblique; sr, superior rectus; sth, sternohyoideus; tv, transversus ventralis. Scale bar = 0.1 mm.

---

to be identical to the levator internus 1, which inserts onto infrapharyngobranchial 2. In the ventral region of the branchial arches, the obliqui ventrales and the transversus ventralis are clearly detected (Fig. 2-3C, D). The obliqui ventrales 1–3 interconnect with the corresponding hypobranchials and ceratobranchials. The transversus ventralis is identified in arch 4, and interconnects the left and right cartilaginous fourth hypobranchial. In the region between the pectoral girdle and branchial arches, the pharyngoclavicularis externus is detected, connecting ceratobranchial 5 and the cleithrum. In the body region, the hypaxial muscles are attached to the sixth myotome and a new small hypaxial muscle mass is detected at the seventh myotome (Fig. 2-3I).

8 dph

In the 4-, 5- and 7-dph larvae, the adductor mandibulae is composed of the adductores mandibulae A1 and A2. However, in the 8-dph larvae, three different adductor mandibulae portions termed A1, A2 and Aω are recognized. The newly appearing adductor mandibulae muscle Aω may have subdivided from the adductor mandibulae A1; the posterior portion of this muscle appear to be partially continuous with the anterior portion of the adductor mandibulae A1 (Fig. 2-4A). The dilatator operculi is located lateral to the levator arcus palatini, and appears as a very thin muscle band at

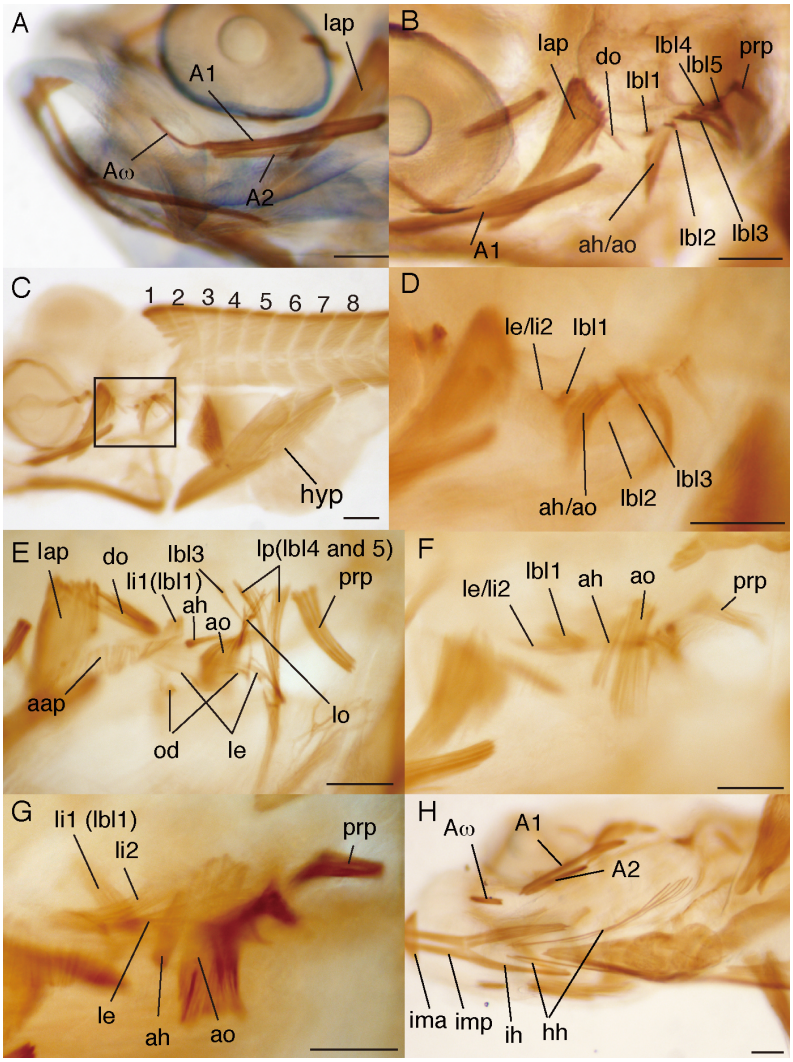

Figure 2-4. Larval musculature of the Japanese flounder at 8 and 12 dph. Muscles were labeled with anti-myosin antibody and cartilage was stained with Alcian blue. (A) Ventrolateral view of the cranial musculature (brown) and cartilage (blue) at 8 dph. (B) Dorsolateral view of the cranial musculature at 8 dph. (C) Lateral view of the musculature at 8 dph. The figures show the number of myotomes. (D) Magnification of the boxed area in (C). (E) Lateral view of the cranial musculature at 12 dph. Note that the branchial levator 3 remains in part at 12 dph. (F) Dorsolateral view of the cranial musculature at 12 dph, focusing on the adductor hyomandibulae and the adductor operculi. (G) Dorsolateral view of the cranial musculature at 12 dph, focusing on the levator externus and levator internus 2. (H) Ventrolateral view of the cranial musculature at 12 dph. aap, adductor arcus palatini; ah, adductor hyomandibulae; ah/ao, complex of adductor hyomandibulae and adductor operculi; ao, adductor operculi; A1, adductor mandibulae A1; A2, adductor mandibulae A2; Aω, adductor mandibulae Aω; do, dilatator operculi; hh, hyohyoidei; hyp, hypaxialis; ih, interhyoideus; ima, intermandibularis anterior; imp, intermandibularis posterior; lap, levator arcus palatini; lbl, larval branchial levator; le, levator externus; li, levator internus; lo, levator operculi; lp, levator posterior; od, obliqui dorsales; prp, protractor pectoralis. Scale bar = 0.1 mm.

this stage (Fig. 2-4B). The anterior portion of this muscle is partially continuous with the levator arcus palatini. The adductor hyomandibulae and the adductor operculi appear to remain as a single muscle strap, whose ventral tip has divided into two parts. The intermandibularis anterior, intermandibularis posterior, interhyoideus and hyohyoideus muscles that are located in the ventral surface region of the head, do not change their shape or position, even though they have grown in size. In the dorsal parts of the branchial arches, the anlage of the levatores externi and the levator internus 2 muscle mass are faintly detected only as a small muscle at this stage (Fig. 2-4D). In the region between the pectoral girdle and branchial arches, the pharyngoclavicularis internus is also detected. In the body region, the hypaxial muscles, growing as two clear muscle bands, insert on the cleithrum and are attached to the seventh and eighth myotome (Fig. 2-4C).

12 dph

In the cheek muscles, the levator operculi is detected (Fig. 2-4E). The levator operculi develops behind the dilatator operculi. This former muscle originates from the lateral side of the otic capsule and inserts on the opercle (Fig. 2-5E). The dilatator operculi grows into a conical shape, with the apex pointing caudoventrally. The adductor operculi and the adductor hyomandibulae are separated at this stage clearly (Fig. 2-4F). All of the cheek muscles have developed (Table 2-1). On the ventral surface of the head, the hyohyoidei are subdivided into two separate muscle bands (Fig. 2-4H), and the most posterior part of the hyohyoideus has reached the posterior region of the opercle. The 12-dph larvae have the developing branchial levators (the levatores externi and the levator internus 2)(Fig. 2-4F, G), and the regressing larval branchial levator 3 (Fig. 2-4E). The 8-dph larvae have all of the larval branchial levators（Fig. 2-5A, E）. At 10 dph, the larval branchial levator 2 gradually disappears in the dorsal part of the branchial arches, while the levator operculi has not yet developed (Fig. 2-5B). By 12 dph, the larval branchial levator 2 disappears completely and the larval branchial levator 3 begins to disappear, while the levator operculi starts to appear in the dorsal part of the branchial arches (Fig. 2-5C, E). By 14 dph, the larval branchial levator 3 almost completely disappears (Fig. 2-5D, E). The larval branchial levators, with the exception of the larval branchial levator 1, are located lateral to the adductor operculi and the adductor hyomandibulae, and insert on the ceratobranchial cartilages. The newly

Table 2-1. Timing of cranial muscle development in the Japanese flounder.

Muscles of the eye	0 dph	1 dph	2 dph	4 dph	8 dph	12 dph	16 dph	20 dph	24 dph	28 dph	32 dph	36 dph	40 dph	44 dph
superior oblique	×	○	○	○	○	○	○	○	○	○	○	○	○	○
inferior oblique	×	×	○	○	○	○	○	○	○	○	○	○	○	○
superior rectus	×	○	○	○	○	○	○	○	○	○	○	○	○	○
inferior rectus	×	×	○	○	○	○	○	○	○	○	○	○	○	○
medial rectus	×	×	○	○	○	○	○	○	○	○	○	○	○	○
lateral rectus	×	○	○	○	○	○	○	○	○	○	○	○	○	○
Muscles of the cheek														
adductor mandibulae	×	○	○	○	○	○	○	○	○	○	○	○	○	○
levator arcus palatini	×	○	○	○	○	○	○	○	○	○	○	○	○	○
dilatator operculi	×	×	×	×	○	○	○	○	○	○	○	○	○	○
levator operculi	×	×	×	×	×	○	○	○	○	○	○	○	○	○
adductor arcus palatini	×	×	○	○	○	○	○	○	○	○	○	○	○	○
adductor operculi	×	×	ah/ao	ah/ao	ah/ao	○	○	○	○	○	○	○	○	○
adductor hyomandibulae	×	×	ah/ao	ah/ao	ah/ao	○	○	○	○	○	○	○	○	○
Muscles serving the ventral surface of the head														
intermandibularis anterior	×	×	○	○	○	○	○	○	○	○	○	○	○	○
intermandibularis posterior	×	×	○	○	○	○	○	○	○	○	○	○	○	○
interhyoideus	×	×	○	○	○	○	○	○	○	○	○	○	○	○
hyohyoideus	×	×	×	○	○	○	○	○	○	○	○	○	○	○
Muscles serving the dorsal parts of the branchial arches														
larval branchial levator	×	×	○	○	○	△	-*	-*	-*	-*	-*	-*	-*	-*
levatores externi	×	×	×	×	○	○	○	○	○	○	○	○	○	○
levatores interni	×	×	×	○(lbl1)	○(lbl1)	○(lbl1)	○	○	○	○	○	○	○	○
levator posterior	×	×	○(lbl4)	○(lbl4)	○(lbl4)	○(lbl4)	○	○	○	○	○	○	○	○
obliqui dorsales	×	×	×	×	×	○	○	○	○	○	○	○	○	○
obliquus posterior	×	×	×	×	×	×	○	○	○	○	○	○	○	○
adductores	×	×	×	×	×	×	×	○	○	○	○	○	○	○
retractor dorsalis	×	×	×	×	×	×	○	○	○	○	○	○	○	○
interbranchiales	×	×	×	×	×	×	×	×	○	○	○	○	○	○
Muscles serving the ventral parts of the branchial arches														
sphincter oesophagi	×	×	○	○	○	○	○	○	○	○	○	○	○	○
obliqui ventrales	×	×	○	○	○	○	○	○	○	○	○	○	○	○
transversus ventralis	×	×	×	○	○	○	○	○	○	○	○	○	○	○
rectus communis	×	×	×	×	×	×	○	○	○	○	○	○	○	○
Muscles between the pectoral girdle and the skull, hyoid, and branchial arches														
sternohyoideus	×	×	○	○	○	○	○	○	○	○	○	○	○	○
pharyngoclavicularis externus	×	×	×	○	○	○	○	○	○	○	○	○	○	○
pharyngoclavicularis internus	×	×	×	×	○	○	○	○	○	○	○	○	○	○
protractor pectoralis	×	×	○	○	○	○	○	○	○	○	○	○	○	○
levator pectoralis	×	×	×	×	×	×	○	○	○	○	○	○	○	○

×, no muscle fibers; ○, differentiated muscle fibers; △, faint regression of muscle fibers; ah/ao, the complex of the adductor hyomandibulae and the adductor operculi; ○(lbl1), detected as a larval branchial levator 1; ○(lbl4), detected as a larval branchial levator 4

-* After 16 dph, I use the terms the “levator internus 1” and the “levator posterior” instead of the “larval branchial levator 1” and the “larval branchial levator 4 (and possibly 5)”, respectively.

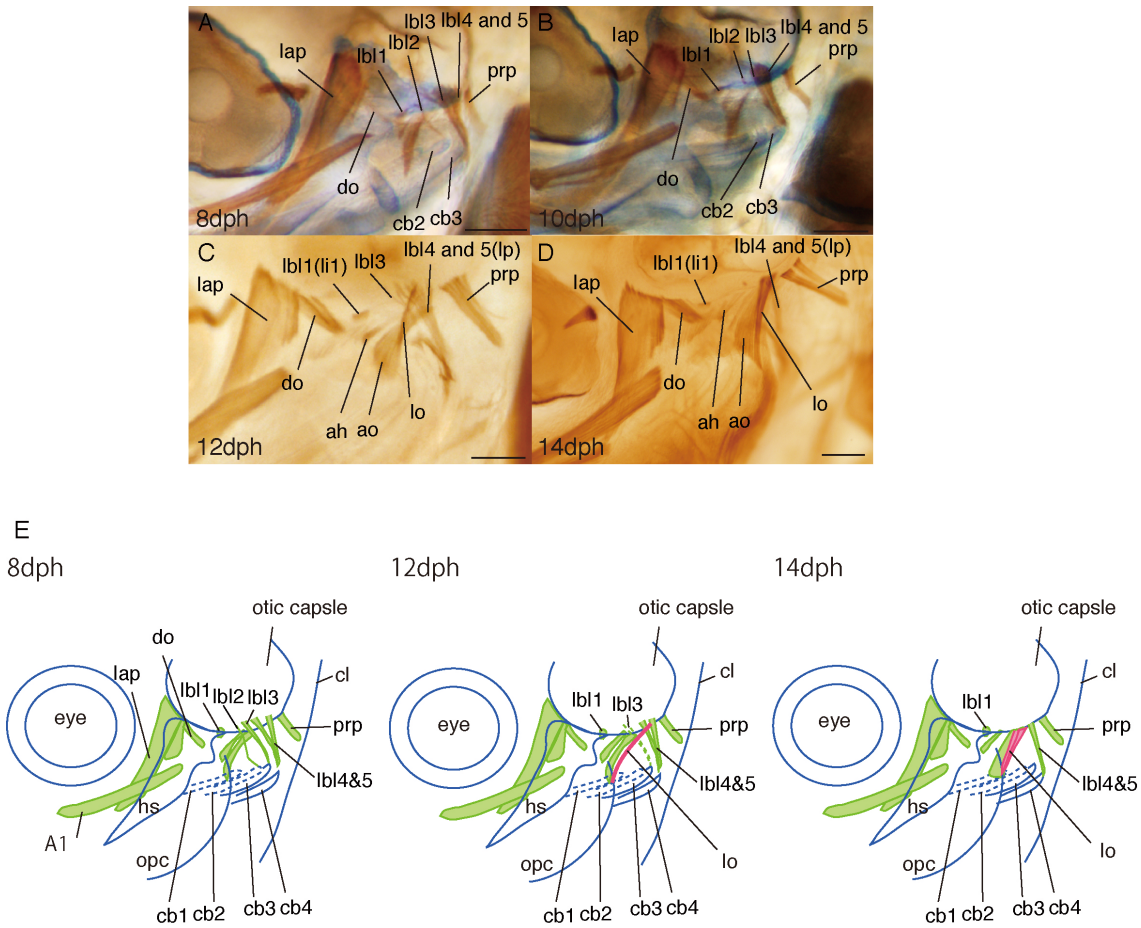

Figure 2-5. The disappearance of larval branchial levators and the development of levator operculi. Muscles were labeled with anti-myosin antibody and cartilage was stained with Alcian blue. (A) Lateral view of the cranial musculature (brown) and cartilage (blue) at 8 dph. (B) Lateral view of the cranial musculature (brown) and cartilage (blue) at 10 dph. (C) Lateral view of the cranial musculature at 12 dph. (D) Lateral view of the cranial musculature at 14 dph. (E) Schematic lateral representation of the larval branchial levators and levator operculi at 8, 12 and 14 dph. ah, adductor hyomandibulae; ao, adductor operculi; A1, adductor mandibulae A1; cb, ceratobranchial cartilage; cl, cleithrum; do, dilatator operculi; hs, hyosymplectic cartilage; lap, levator arcus palatini; lbl, larval branchial levator; li, levator internus; lo, levator operculi; lp, levator posterior; opc, opercle; prp, protractor pectoralis. Scale bar = 0.1 mm.

developed levator externus muscle is positioned medial to the adductor operculi and the adductor hyomandibulae (Fig. 2-4E), and insert on the epibranchial cartilages. Therefore, this new paired muscle, presumably moving the branchial arches, is clearly distinct from the larval branchial levators, even though the function of this muscle in the lifting of the branchial arches seems to be similar. Two dorsal muscles are detected on

branchial arches 2 and 3 at this stage (Fig. 2-4E). Given the insertion from these muscles on epibranchial cartilages and the origin of infrapharyngobranchials 2 and 3, I termed these muscles the obliqui dorsales. The 515-dph adults have two obliqui dorsales that insert on infrapharyngobranchials 2 and 3. In the body region, the hypaxial muscles are increasing in number and are covering the abdominal region. The muscles are attached to the seventh to the 11th myotomes.

16 dph

In the cheek musculature, the levator operculi is detected as two parts (Fig. 2-6C), and merges into one muscle later on in development. The adductor mandibulae A2 shifts its position to ventral side of the A1 (Fig. 2-6G, J). The Aω develops into a thick, short muscle (Fig. 2-6G). The adductor arcus palatini have developed into a thin muscle sheet, the posterior portion of which is located close to the anterior portion of the adductor hyomandibulae (Fig. 2-6F, J). In the ventral surface region, both intermandibularis posteriores are arranged in parallel (Fig. 2-6G). The larval branchial levators 2 and 3 have disappeared completely by this stage, while portions of the larval branchial levators 1, 4 and possibly 5 remain (Fig. 2-6F). By this stage, the levatores externi and the levator internus 2 are well developed. After this stage, I use the terms “levator internus 1” and “levator posterior” as the designations of the muscles that up till now were named “larval branchial levator 1” and “larval branchial levator 4 (and possibly 5)”, respectively. Branchial arches 1, 2, 3 and 4 receive insertions of the levator externus (Fig. 2-6H). This muscle appears to be a single muscle that originates on the anteroventral side of the otic capsule, and diverges to insert on the epibranchial cartilages (Fig. 2-6C, D, H and I). The shape of this muscle is similar to that of the sternoptychid *Argyropelecus* described previously by Winterbottom (1974). The levatores externi 1 and 2 insert on the dorsolateral face of the epibranchial cartilages 1 and 2, and the levatores externi 3 and 4 insert on the dorsal face of the epibranchial cartilages 3 and 4, respectively (Fig. 2-6H, I). The levator internus 2 is also clearly detected. This muscle develops from the levatores externi muscles and points towards infrapharyngobranchial cartilage 3 (Fig. 2-6D). At this stage, all four levatores externi and the two levatores interni, also present in adult fish, are clearly detected. The obliquus posterior is detected, and connects ceratobranchial 5 to epibranchial 4 (Fig. 2-6H). The retractor dorsalis is also detected at this stage (refer Fig. 2-8G). The retractor

dorsalis is identified by the position, orientation and the results of dissection of the adult specimens; however, its precise insertion and origin remain unclear at this stage of

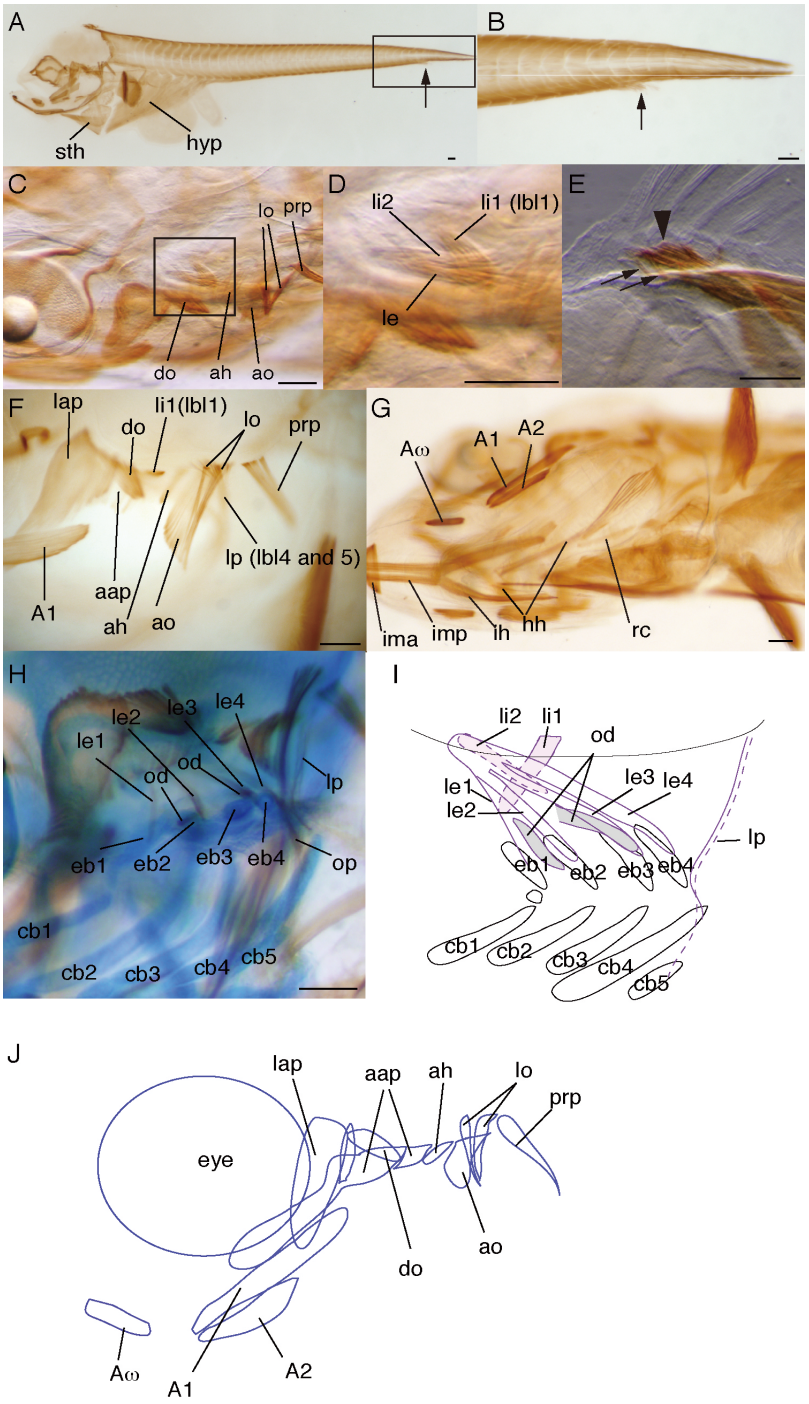

Figure 2-6

Figure 2-6. Larval musculature in the Japanese flounder head and trunk at 16 dph. Muscles were labeled with anti-myosin antibody and cartilage was stained with Alcian blue. (A) Lateral view of the musculature at 16 dph. Arrows indicate muscles extending from the myotome. (B) Magnification of the boxed area in (A). Arrows indicate muscles extending from the myotome. (C) Dorsolateral view of the cranial musculature at 16 dph. (D) Magnification of the boxed area in (C). (E) Lateral view of the dorsal fin musculature at 16 dph. Arrows show the lateral parts of the dorsal fin muscle and the arrowhead shows the midline part of the dorsal fin muscle. (G) Ventrolateral view of the cranial musculature at 16 dph. (H) Lateral view of the cranial musculature (brown) and cartilage (blue) at 16 dph. (I) Schematic lateral representation of the branchial musculature at 16 dph. (J) Schematic lateral representation of the cheek musculature at 16 dph. aap, adductor arcus palatini; ah, adductor hyomandibulae; ao, adductor operculi; A1, adductor mandibulae A1; A2, adductor mandibulae A2; Aω, adductor mandibulae Aω; cb, ceratobranchial cartilage; do, dilatator operculi; eb, epibranchial cartilage; hh, hyohyoidei; hyp, hypaxialis; ih, interhyoideus; ima, intermandibularis anterior; imp, intermandibularis posterior; lap, levator arcus palatini; lbl, larval branchial levator; le, levator externus; li, levator internus; lo, levator operculi; lp, levator posterior; od, obliqui dorsales; op, obliquus posterior; prp, protractor pectoralis; rc, rectus communis; sth, sternohyoideus. Scale bar = 0.1 mm.

development. In the ventral part of the branchial arches, the rectus communis is also detected (Fig. 2-6G). This muscle connects the ceratobranchial of the respective arch to the hypobranchial of the preceding one. The hypaxial muscles continue to grow in size in the abdominal region and the seventh to 13th myotome join to form the hypaxial muscles (Fig. 2-6A). The paired sternohyoideus halves have grown in a dorsoventral direction and combine on the ventral midline to form a large triangular shaped muscle (Fig. 2-6A).

In the caudal region, several muscles of the 39th and 40th myotomes have partially extended from the trunk (Fig. 2-6A, B). These muscles will become the caudal fin muscles in later stages of development. The position of muscle extension is coincident with the position of cell condensations that generate the caudal cartilage tissues (refer Fig. 2-7M). The muscles that control the dorsal fin rays arise from the anteriormost portion of the dorsal fin (Fig. 2-6E).

24 dph

Whereas all extraocular muscles of 20-dph larvae are thin, those of the 24-dph larvae have grown to take on a relatively thick appearance, with the exception of the medial rectus. There are no differences in shape between the left and right sides of the extraocular muscles, even though the cartilage of the neurocranium near the eye shows asymmetry due to cartilage resorption in these stages (Fig. 2-7G, H). In the 24-dph

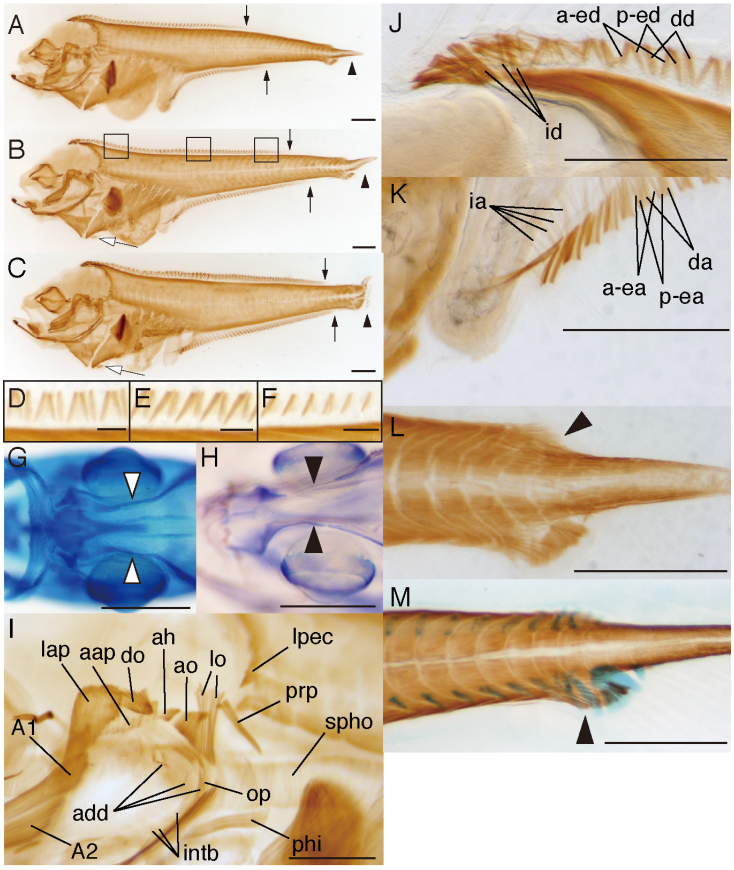

Figure 2-7. Larval musculature in the Japanese flounder head and trunk regions at 24 dph. Muscle was labeled with anti-myosin antibody and cartilage was stained with Alcian blue. (A-C) Lateral view of the musculature at 24 dph. Black arrows show the posterior end of the dorsal and anal fin muscles. Black arrowheads show the notochord curvature. White arrows show the pelvic muscle. (D) Magnification of the anteriormost boxed area in (B). (E) Magnification of the middle boxed area in (B). (F) Magnification of the posteriormost boxed area in (B). (G) Dorsolateral view of the cranial cartilage at 20 dph. No asymmetric cranial cartilage is observed (white arrowheads). (H) Dorsolateral view of the cranial cartilage at 24 dph. The cartilage of the neurocranium shows asymmetry due to cartilage resorption (arrowheads). (I) Lateral view of the cranial musculature at 24 dph. (J) Lateral view of the dorsal fin musculature at 24 dph. (K) Lateral view of the anal fin musculature at 24 dph. (L) Lateral view of the caudal musculature at 24 dph. Arrowhead shows the muscles that extend from the dorsal myotome. (M) Lateral view of the caudal musculature (brown) and cartilage (blue) at 24 dph. Arrowhead shows that the caudal cartilage and caudal muscle develop at the same position. aap, adductor arcus palatini; add, adductores; ah, adductor hyomandibulae; ao, adductor operculi; A1, adductor mandibulae A1; A2, adductor mandibulae A2; do, dilatator operculi; a-ea, anterior erectors anales; a-ed, anterior erectors dorsales; da, depressores anales; dd, depressores dorsales; ia, inclinatores anales; id, inclinatores dorsales; intb, interbranchiales; lap, levator arcus palatini; lo, levator operculi; lpec, levator pectoralis; op, obliquus posterior; phi, pharyngoclavicularis internus; prp, protractor pectoralis; p-ea, posterior erectors anales; p-ed, posterior erectors dorsales; spho, sphincter oesophagi. Scale bar = 0.5 mm except fig.7C-E, in which scale bar = 0.1mm.

larvae examined, the adductor mandibulae Aω is subdivided into dorsal and ventral elements (refer Fig. 2-8A, C). In the branchial arches, the adductores and the interbranchiales now appear (Fig. 2-7I). The adductores interconnect the epibranchial and ceratobranchial elements of the branchial arches. The adductores 2 and 3 are thin muscles, and are located on the dorsolateral side of the second and third arch respectively. The adductor 4 is a thick muscle, and is located on the medial side of the fourth arch. The interbranchiales are small muscles associated primarily with the gill filaments. In the region between the pectoral girdle and the neurocranium, the levator pectoralis has arisen from the epaxialis body musculature (Fig. 2-7I).

A few individuals with somewhat varying degrees of morphological development are present (Fig. 2-7B, C). Considering the degree of flexion of the notochord, these individuals appear to have developed faster than the other 24-dph larvae. However, with the exception of the fin muscles, no difference is observed in the muscle composition of these specimens. Hence, I use these individuals to describe the development of the dorsal and anal fin muscles. A report by Takahashi (1917) suggested that there were three types of muscles in the dorsal and anal fins, termed the erector, depressor and inclinator muscles. According to the Takahashi report, I have subsequently classified four muscles into the erector, depressor and inclinator muscle groups, considering the insertion and direction of the muscles in relation to the pterygiophore. In the dorsal fin muscles, the anteriormost and the middle muscles on the midline are the anterior and the posterior erectores dorsales, and the posteriormost ones on the midline are depressores dorsales (Fig. 2-7J). The muscles that insert laterally on the pterygiophores are the inclinatores dorsales. Equally, in the anal fin musculature, the anteriormost and the middle muscles on the midline are the anterior and the posterior erectores anales, and the posteriormost ones on the midline are depressores anales (Fig. 2-7K). The muscles that insert on the pterygiophore laterally are the inclinatores anales. In the dorsal and anal fins, muscles develop in an anterior to posterior direction during development (Fig. 2-7A, B and C). On each pterygiophore, dorsal and anal fin muscles also develop in an anterior to posterior direction (Fig. 2-7D, E and F). That is, the first muscles to develop are the anterior erectores, the second are the posterior erectores and the last are the depressores. After that, the inclinatores develop more laterally (Fig. 2-7J). Unlike the caudal fin muscles, these muscles do not appear to originate from the myotome. The development of these muscles seems to correlate with the degree of

curvature in the caudal end of the notochord, which is an important landmark of staging (Minami, 1982).

In the caudal region, several muscle fibers start to extend from the dorsal side of the 39th and 40th myotomes of the trunk, which are the same myotomes where several muscle fibers extended from the ventral side in the 16-dph larvae (Fig. 2-7L).

28 dph

At this stage of development, the right eye has begun to migrate dorsally (Fig. 2-8A, B). As a result of this migration, the extraocular muscles are positioned differently on the left and right sides. The right eye has rotated slightly (Fig. 2-8A, B), and the superior oblique is divided into two parts at the dorsal tip and insert at two points on the eye (refer Fig. 2-8L). In the cheek musculature, the adductor mandibulae Aω is further subdivided into three elements in some of the specimens. The new portion develops from the posterior edge of the adductor mandibulae Aω (Fig. 2-8C). In 28-dph larvae, I detect different shapes between the bilateral muscles for the first time. The adductor mandibulae A1 demonstrates a different shape between the left and right sides (Fig. 2-8A, B); the right adductor mandibulae A1 appearing as a thin rectangle, and the left adductor mandibulae A1 appearing as a thin trapezoid-shaped muscle. In the ventral surface of the head, the hyohyoideus has generated several short muscle bands inserting on the branchiostegal rays (Fig. 2-8D). These muscle bands interconnect the branchiostegal rays. In the dorsal and anal fins, the inclinatores join to form the fin muscles from the lateral side (Fig. 2-8E). In the 28-dph F-stage larvae, the pelvic fin muscles are detected in three parts (Fig. 2-8F).

32 dph–44 dph

Eye migration is initiated at 28 dph and has ceased by 44 dph (Fig. 2-8B, H and L). There is no further change in muscle composition after this time; only some minor modifications occur. The extraocular muscles have grown into short, thick muscles, with the exception of the medial rectus (Fig. 2-8L, M). At 44 dph, and when eye migration is complete, the adductor mandibulae A1 on the right side is relatively larger than that of the left side, when compared to that of the 28-dph larvae (Fig. 2-8H, I). The dilatator operculi is subdivided into two portions in the 44-dph larvae (Fig. 2-8O). The newly subdivided muscle connects the opercle and the hyomandibular, and the timing of

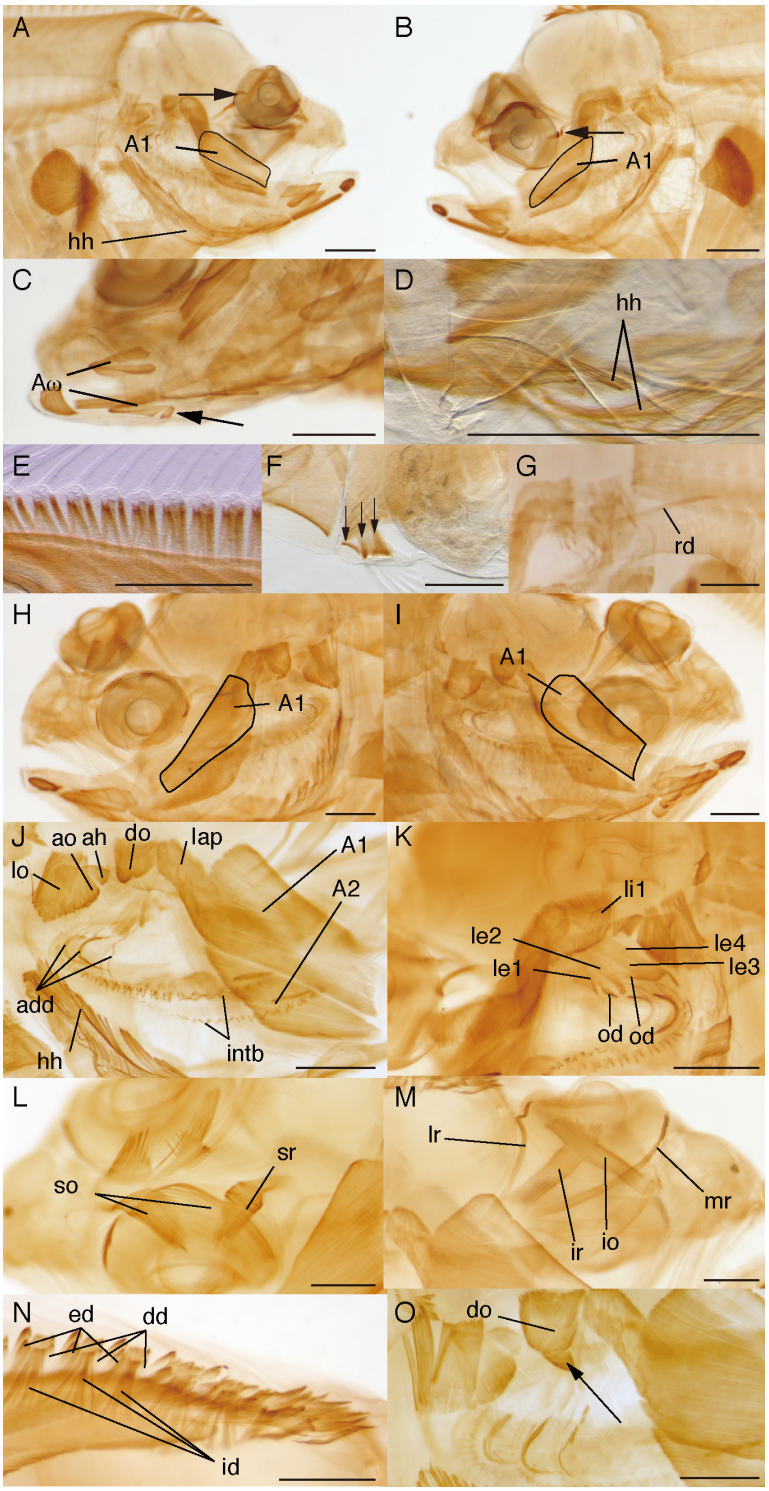
A
A1
hh
B
A1
C
Aω
D
hh
E
F
G
rd
H
A1
I
A1
J
ao ah
do
lap
lo
A1
A2
add
hh
intb
K
li1
le2
le4
le1
le3
od od
L
sr
so
M
lr
mr
ir
io
N
ed
dd
id
O
do

Figure 2-8

Figure 2-8. Larval musculature in the Japanese flounder head and trunk regions at 28, 36, 40 and 44 dph. Muscles are labeled with anti-myosin antibody. (A, B) Lateral view of the cheek musculature at 28 dph. Arrows show the position where the lateral rectus inserts on the eye. The adductores mandibulae A1 on both sides of the specimen are outlined in black. (C) Ventrolateral view of the cranial musculature at 28 dph. (D) Lateral view of the cranial musculature at 28 dph. (E) Lateral view of the dorsal fin musculature at 28 dph. (F) Lateral view of the pelvic fin musculature at 28 dph. Arrows show three parts of the pelvic fin muscles. (G) Lateral view of the musculature at 28 dph, focusing on the retractor dorsalis. (H, I) Lateral view of the musculature at 36 dph. The adductores mandibulae A1 on both sides of the specimen are outlined in black. (J) Lateral view of the cranial musculature at 36 dph. (K) Lateral view of the cranial musculature at 40 dph. (L) Dorsolateral view of the extraocular musculature at 44 dph. (M) Lateral view of the extraocular musculature at 44 dph. (N) Dorsolateral view of the dorsal fin musculature at 44 dph. (O) Lateral view of the cranial musculature at 44 dph. The dilatator operculi is subdivided into two sections (arrow). add, adductores; ah, adductor hyomandibulae; ao, adductor operculi; A1, adductor mandibulae A1; A2, adductor mandibulae A2; Aω, adductor mandibulae Aω; do, dilatator operculi; dd, depressores dorsales; ed, erectores dorsales; hh, hyohyoidei; id, inclinatores dorsales; intb, interbranchiales; io, inferior oblique; ir, inferior rectus; lap, levator arcus palatini; le, levator externus; li, levator internus; lo, levator operculi; lr, lateral rectus; mr, medial rectus; od, obliqui dorsales; rd, retractor dorsalis; so, superior oblique; sr, superior rectus; Scale bar = 0.5 mm.

---

subdivision in the dilatator operculi appears to be random between the left and right sides in the individuals.

Discussion

The cranial muscles termed the recti ventrales, a group of muscle that interconnects the hypobranchial and the ceratobranchial, or both elements of one arch to the preceding one, were the only muscle that I am unable to detect in the larvae samples. Having detected all of the cranial muscles in larvae and having determined that investigated larvae and 515-dph adults lack the recti ventrales, I concluded the Japanese flounder does not possess this muscle. The number of recti ventrales has been reported to vary in teleosts (Winterbottom, 1974), with these muscles being reduced in number and represented only by a single pair in many taxa (Stiassny, 2000). To my knowledge, this is the first study to report the absence of recti ventrales in a teleost species. The functional implications of the lack of this muscle are currently unclear.

Development of the cheek muscles

The adductor mandibulae is the largest of the muscles located in the head and is primarily responsible for closing of the jaws. The adductor mandibulae consists of three parts termed A1, A2 and Aω. The first stage at which the asymmetric shape of this muscle could be detected was in 28-dph larvae and was observed in the adductor mandibulae A1. The right adductor mandibulae A1 was larger than that located on the left side at 28 dph, and was probably due to the large space generated on the right side following migration of the eye to the opposite side of the head. Hence, muscle size and shape may depend not only on the timing of differentiation as suggested by Schilling and Kimmel (1997), but also on the space surrounding the developing muscle. Interestingly, the timing of subdivision of the adductor mandibulae Aω appeared to be random between the left and right side (Fig. 2-8C). Among 23 larvae observed at 28 dph, larvae could be grouped in four types according to the subdivision of Aω. Eight larvae had Aω without subdivision on both side of the body. Four had subdivided Aω only on the right side. Seven had subdivided Aω only on the left side. The remaining four had subdivided Aω on both sides. This result suggests that the development of the adductor mandibulae Aω is not related to the direction of eye migration in the Japanese flounder. All of the asymmetric muscle development that I identified occurs subsequent to any asymmetric cartilage development, strongly suggesting that muscle asymmetry develops as the result of asymmetric morphogenesis in other tissues.

A considerable variety of larval development patterns among species have been reported (Blaxter, 1988). In this study, the dilatator operculi and levator operculi, which are the muscles associated with the opercle, develop considerably later in Japanese flounder compared with those of zebrafish. In zebrafish, the dilatator operculi and levator operculi develop at 62 and 85 hours post fertilization (hpf) respectively (Schilling and Kimmel, 1997), and the opercle ossifies very early from mesenchymal condensation at 3 dpf (Javidan and Schilling, 2004). On the other hand, the opercle in Japanese flounder only slightly ossifies at 10 dpf (data not shown). Hence, the difference in the timing of development of the dilatator operculi and the levator operculi between these two species seems to result from the difference in the developmental timing of the opercle.

Development of the branchial arch muscles

There are few published reports that describe the development of the dorsal branchial

muscles (Hernandez *et al*., 2005; Schilling and Kimmel, 1997), likely due to the complexity of these muscles and their position deep in the head region. For these reasons, it is difficult to accurately identify some of the dorsal branchial muscles including the retractor dorsalis, oblique dorsales, branchial levator 1 (levator internus 1) and levator internus 2 in larval stages of Japanese flounder. Thus, the origin and insertion of these muscles remains unclear. However, I was able to identify these muscles in different larval and adult stages. According to Winterbottom (1974), the transversus dorsalis generally develops via the subdivision of the sphincter oesophagi, and connects the dorsal elements of the branchial arches across the midline. In larval stages of the Japanese flounder, the muscle that appears continuous with the sphincter oesophagi was not considered a separate transversus dorsalis, but separates from the sphincter oesophagi in later (adult) stages.

Relationship between the larval branchial levators and the levatores externi, the levatores interni and the levator posterior

In the present study, I report that in the Japanese flounder; (1) the larval branchial levators are distinct from the levatores externi, (2) the larval branchial levator 1 appears equal to the levator internus 1, (3) the larval branchial levator 4, and possibly the larval branchial levator 5 represent the levator posterior, and (4) the larval branchial levators 2 and 3, which are larval-specific muscles, regress soon after the larval stages of development.

As the infrapharyngobranchials did not appear to have segmented at 4 dph-larval stage, it seems that the larval branchial levator 1 may pull the infrapharyngobranchials as one plate in early larval stages. Each of the larval branchial levators 2–5 subsequently insert on the ceratobranchial cartilage along each branchial arch, respectively. As 4 dph coincides with the initial feeding period, the muscles required for feeding and respiration should ideally develop prior to this time. Normally, the dilatator operculi and the levator operculi function as the opercular abductors against the adductor operculi in the adult. However at this earlier stage in development, there is no ossified opercle, and neither the dilatator operculi nor the levator operculi are associated with the opercle. Thus, the larval branchial levators 2–5 may be the sole muscles to abduct the branchial arches against the complex of the adductor operculi and the adductor hyomandibulae, and the larval branchial levator 1. The larval branchial

levators 2–5 are also thought to play a role in the expansion of the buccal chamber required to take up food at this stage. As the larvae grow, the larval branchial levators 2 and 3 regress and the levatores externi and the levator internus 2 develop from the anterior region of the branchial arches.

Dorsal, anal and caudal fin muscle development

Although the zebrafish caudal fin has been shown to originate, at least in part, from the trunk neural crest (Smith *et al*., 1984), there is limited information as to how the caudal fin muscles arise. Thus, this is the first report to describe that the muscles derived from the 39th and 40th myotomes may extend in order to form part of the caudal fin musculature. The differentiated muscle of the myotome extends directly into the fin, to provide the fin musculature. The position of the extension events also coincides with the location of the cell condensations that generate the caudal cartilages. Therefore, the cell condensations may aid in the determination of cartilage position and induce the extension signals.

In the dorsal and anal fins, muscle development occurs at the definitive position in which each muscle functions. Muscle tissue extension from any of the myotomes is not detected unlike in the caudal fin. The order of differentiation from anterior to posterior is true for the muscle and cartilage in the dorsal and anal fin. The differentiation of cranial muscles is coordinated with that of the cartilage (Schilling and Kimmel, 1997). The same rule may also be applicable for muscle development in the dorsal and anal fin tissues.

CHAPTER III **Muscle development in the bamboo sole *Heteromycteris japonicus* (Temminck & Schlegel, 1846) with special reference to larval branchial levators**

It is useful to study the bamboo sole in comparison with the Japanese flounder in order to understand the common mechanism of flatfish muscle development, as the two fish belong to the same taxonomic order, *Pleuronectiformes*. In addition, the following features give bamboo sole the potential to be a good model organism for understanding the developmental biology of flatfishes in general. The first is size: the size at maturity can be as low as 7 cm standard length (Ochiai, 1966). Therefore, these fish can be reared in small tanks. The second is the life cycle: only one year (Ochiai, 1966). Thus, the fish lends itself to rapid genetic analysis of all stages of its life cycle. The third is the spawning period: the bamboo sole spawn in rearing tanks from June to November under conditions of natural temperature and photoperiod. Controlling the rearing temperature and photoperiod will lead to spawning over all seasons under laboratory conditions.

The presence of larval-specific muscles in the Japanese flounder has been described in the chapter II, but it is not clear whether they are common to all flatfishes or if they are unique to the Japanese fluounder. In this chapter, I describe muscle development in the bamboo sole from hatching to metamorphosis and investigates whether this species also has larval-specific muscles at the dorsal branchial arches.

Materials and methods

Bamboo sole samples

Specimens of bamboo sole were collected off the coast of Tottori prefecture and bred in a temperature-controlled (22 °C) 500 l tank at the National Research Institute of Aquaculture, Mie, Japan, and the eggs removed after fertilization. Immediately upon collection, the fertilized eggs were transferred and maintained in a 50 l plastic tank with running seawater maintained at 22 °C. From this tank, a series of samples was obtained at 0, 1, 2, 3, 5, 7, 11, 14, 17 and 21 dph, from which 13, 26, 9, 16, 21, 22, 20, 21, 26 and 40 specimens, respectively, were used for whole mount immunostaining. Following

terminal anesthesia with 3-aminobenzoic acid ethyl ester (Sigma), larvae were fixed with 4% paraformaldehyde (PFA) in phosphate buffered saline (PBS) containing 0.3% Tween 20 (PBST), rinsed in PBST, dehydrated in a graded series of methanol (25, 50, 75 and 100%) and stored at –20 °C.

Whole mount immunostaining

Stored larvae were used for whole mount immunohistochemical staining following the protocol of the chapter II. Some of larvae were cut with a sharp-edged razor before staining to visualize clearly some of the cranial muscles positioned deep in the head. For double staining of muscle and cartilage tissue, samples were first stained with Alcian blue and subsequently immunostained for muscle as described above. After staining, samples were cleared in increasing concentrations of glycerol (25, 50 and 80%) and observed using an MZFL microscope (Leica) equipped with combi III (Leica), or an Eclipse 90i microscope (Nikon). Micrographs were captured using a CCD camera DP70 (Olympus) and processed using Adobe Photoshop CS3 (Adobe Systems). The nomenclature of the muscles outlined in this study is based on that used in the chapter II.

Results

Muscle of the eye

At 0 dph, any cranial muscle tissue including eye muscles are not detected (Fig. 3-1A). At 1 dph, all six components of the extraocular muscles (superior oblique, inferior oblique, superior rectus, inferior rectus, medial rectus and lateral rectus) are visible faintly (Fig. 3-1B-D). At 2 dph, all six components of the extraocular muscles are detected clearly, somewhat surprisingly for this early stage (Fig. 3-1E). These muscles appear to develop early and are followed by the musculature associated with the mandibular, hyoid and branchial arches. There is no further change in eye muscle composition after this time (Table 3-1).

Muscle of the cheek

At 1 dph, the adductor mandibulae A1 and the levator arcus palatini are found as

relatively small muscles at the rear of the orbit (Fig. 3-1C, D). These muscles are seen to overlay each other at this stage. The adductor operculi are found behind the levator arcus palatini (Fig. 3-1C, D). At 2 dph, the adductor mandibulae A2, the dilatator operculi and the adductor hyomandibulae are present, in addition to the adductor mandibulae A1, the levator arcus palatini and the adductor operculi (Fig. 3-1F-H). The dorsal region of the adductor mandibulae A1 is overlain by fibers of the ventral part of the levator arcus palatini, and the adductor mandibulae A2 is located on the medial side of the adductor mandibulae A1 (Fig. 3-1G). The adductor hyomandibulae is situated posterior to the orbit and medial to the levator arcus palatini (Fig. 3-1H). The dilatator operculi is located lateral to the levator arcus palatini, and appears as a very thin muscle band at this stage (Fig. 3-1F, H). The adductor operculi passes anteroventrally between the larval branchial levators 1 and 2, then inserts onto the hyosymplectic cartilage and the opercle, which has not yet become ossified. At 3 dph, the adductor mandibulae muscle Aω, the adductor arcus palatini and levator operculi begin to develop (Fig. 3-1I-K). It appears that the newly appearing adductor mandibulae muscle Aω may have subdivided from the adductor mandibulae A1 since the posterior portion of this muscle seems to be partially continuous with the anterior portion of the adductor mandibulae A1 (Fig. 3-1I). The adductor arcus palatini is situated posterior to the orbit, medial to the levator arcus palatini and close to the adductor hyomandibulae (Fig. 3-1J). The levator operculi is a very thin muscle and develops behind the dilatator operculi (Fig. 3-1K). While the adductor mandibulae Aω exists as a single element at 14 dph, it is subdivided at 17 dph into two elements in the left side of body (future blind side) but not in the right side (future ocular side) (Fig. 3-1L-N). The new element develops at the ventral side of the original adductor mandibulae Aω (Fig. 3-1M). This is the first asymmetric muscle development realized during metamorphosis of the bamboo sole. This left-right asymmetric structure of the adductor mandibulae Aω is maintained at least until the completion of metamorphosis (at 21 dph)(refer Fig. 3-3J, L).

Table 3-1. Timing of cranial muscle development in the bamboo sole

	0dph	1dph	2dph	3dph	5dph	7dph	11dph	14dph	17dph	21dph
Muscles of the eye										
Superior oblique	×	○	○	○	○	○	○	○	○	○
Inferior oblique	×	○	○	○	○	○	○	○	○	○
Superior rectus	×	○	○	○	○	○	○	○	○	○
Inferior rectus	×	○	○	○	○	○	○	○	○	○
Medial rectus	×	○	○	○	○	○	○	○	○	○
Lateral rectus	×	○	○	○	○	○	○	○	○	○
Muscles of the cheek										
Adductor mandibulae	×	○	○	○	○	○	○	○	○	○
Levator arcus palatini	×	○	○	○	○	○	○	○	○	○
Dilatator operculi	×	×	○	○	○	○	○	○	○	○
Levator operculi	×	×	×	○	○	○	○	○	○	○
Adductor arcus palatini	×	×	×	○	○	○	○	○	○	○
Adductor operculi	×	○	○	○	○	○	○	○	○	○
Adductor hyomandibulae	×	×	○	○	○	○	○	○	○	○
Muscles serving the ventral surface of the head										
Intermandibularis anterior	×	×	○	○	○	○	○	○	○	○
Intermandibularis posterior	×	×	○	○	○	○	○	○	○	○
Interhyoideus	×	○	○	○	○	○	○	○	○	○
Hyohyoideus	×	×	○	○	○	○	○	○	○	○
Muscles serving the dorsal parts of the branchial arches										
Larval branchial levators	×	×	○	○	-*	-*	-*	-*	-*	-*
Levatores externi	×	×	×	×	○	○	○	○	○	○
Levatores interni	×	×	○(lbl1)	○(lbl1)	○	○	○	○	○	○
Levator posterior	×	×	○(lbl4)	○(lbl4)	○	○	○	○	○	○

Obliqui dorsales	×	×	×	×	×	○	○	○	○	○
Obliquus posterior	×	×	×	×	×	×	×	×	○	○
Adductores	×	×	×	×	×	×	○	○	○	○
Retractor dorsalis	×	×	×	×	×	×	×	○	○	○
Interbranchiales	×	×	×	×	×	×	○	○	○	○
Muscles serving the ventral parts of the branchial arches										
Sphincter oesophagi	×	×	○	○	○	○	○	○	○	○
Obliqui ventrales	×	×	○	○	○	○	○	○	○	○
Transversi ventrales	×	×	×	○	○	○	○	○	○	○
Rectus communis	×	×	×	○	○	○	○	○	○	○
Recti ventrales	×	×	×	×	×	×	×	○	○	○
Muscles between the pectoral girdle and the skull, hyoid, and branchial arches										
Sternohyoideus	×	○	○	○	○	○	○	○	○	○
Pharyngoclavicularis externus	×	×	○	○	○	○	○	○	○	○
Pharyngoclavicularis internus	×	×	×	×	○	○	○	○	○	○
Protractor pectoralis	×	○	○	○	○	○	○	○	○	○
Levator pectoralis	×	×	×	×	×	×	○	○	○	○

×, no muscle fibers; ○, differentiated muscle fibers; ○(lbl1), detected as a larval branchial levator 1; ○(lbl4), detected as a larval branchial levator 4

-* After 5 dph, the terms “levator internus 1” and “levator posterior” are used instead of “larval branchial levator 1” and “larval branchial levator 4 ”, respectively.

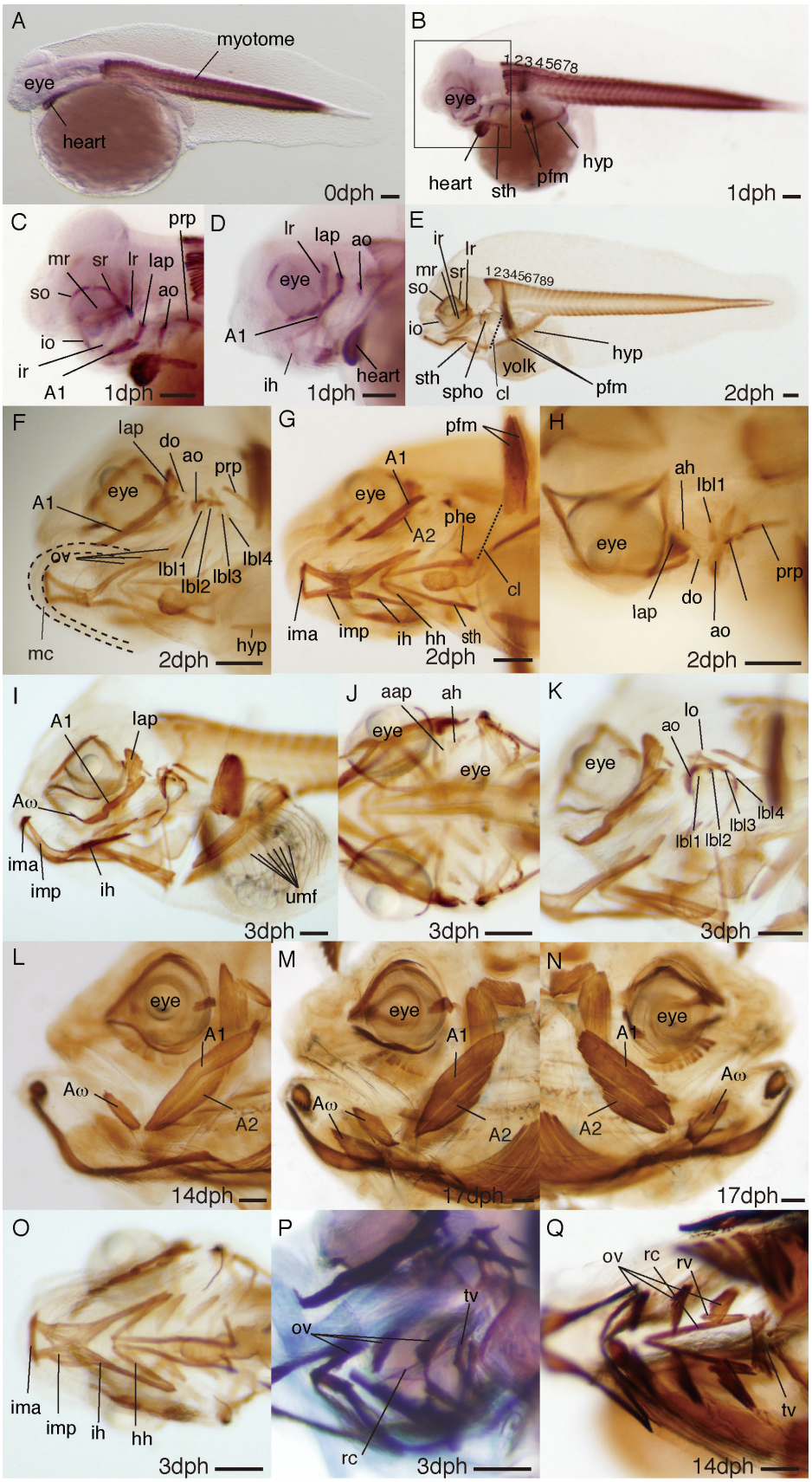
A
myotome
eye
heart
0dph
B
1 2 3 4 5 6 7 8
eye
heart
sth
pfm
hyp
1dph
C
prp
mr
sr
lr
lap
so
ao
io
ir
A1
1dph
D
lr
lap
ao
eye
A1
ih
heart
1dph
E
ir
lr
mr
sr
1 2 3 4 5 6 7 8 9
so
io
hyp
sth
spho
yolk
cl
pfm
2dph
F
lap
do
ao
prp
eye
A1
ov
lbl1
lbl2
lbl3
lbl4
mc
hyp
2dph
G
pfm
A1
eye
phe
A2
cl
ima
imp
ih
hh
sth
2dph
H
ah
lbl1
eye
prp
lap
do
ao
2dph
I
A1
lap
Aω
ima
imp
ih
umf
3dph
J
aap
ah
eye
eye
3dph
K
lo
ao
eye
lbl4
lbl3
lbl1
lbl2
3dph
L
eye
A1
Aω
A2
14dph
M
eye
A1
Aω
A2
17dph
N
eye
A1
Aω
A2
17dph
O
ima
imp
ih
hh
3dph
P
tv
ov
rc
3dph
Q
ov
rc
rv
tv
14dph

Figure 3-1

Figure 3-1. Muscles of the eye and cheek, and muscles serving the ventral surface and those serving the ventral parts of branchial arches in *Heteromycteris japonicus*. The muscles were labeled with anti-myosin antibody, and cartilage was stained with Alcian blue. (A) Lateral view of the musculature at 0 dph. (B) Lateral view of the musculature at 1 dph. The figures show the number of myotomes. (C) Magnification of the boxed area in (B). (D) Ventrolateral view of the cranial musculature at 1 dph. The figures show the number of myotomes. (E) Lateral view of the musculature at 2 dph. (F) Ventrolateral view of the cranial musculature at 2 dph. (G) Ventrolateral view of the cranial musculature at 2 dph, focusing on the adductor mandibulae A2 and pharyngoclavicularis externus. (H) Dorsal view of the cranial musculature at 2dph. (I) Lateral view of the musculature at 3 dph. (J) Dorsal view of the cranial musculature at 3 dph. (K) Ventrolateral view of the musculature at 3 dph, focusing on the larval branchial levators. (L) Lateral view of the cranial musculature at 14 dph, focusing on the left adductor mandibulae Aω. (M) Lateral view of the cranial musculature at 17 dph, focusing on the left adductor mandibulae Aω. (N) Lateral view of the cranial musculature at 17 dph, focusing on the right adductor mandibulae Aω. (O) Ventral view of the cranial musculature at 3 dph. (P) Ventral view of the cranial musculature at 3 dph, focusing on the rectus communis. (Q) Ventral view of the cranial musculature at 14 dph. aap, adductor arcus palatini; ah, adductor hyomandibulae; ao, adductor operculi; A1, adductor mandibulae A1; A2, adductor mandibulae A2; Aω, adductor mandibulae Aω; cl, cleithrum; do, dilatator operculi; hh, hyohyoideus; hyp, hypaxialis; ih, interhyoideus; ima, intermandibularis anterior; imp, intermandibularis posterior; io, inferior oblique; ir, inferior rectus; lap, levator arcus palatini; lbl1-4, larval branchial levator 1-4; lo, levator operculi; lr, lateral rectus; mc, Meckel's cartilage; mr, medial rectus; ov, obliqui ventrales; pfm, pectoral fin muscle; phe, pharyngoclavicularis externus; prp, protractor pectoralis; rc, rectus communis; rv, recti ventrales; so, superior oblique; spho, sphincter oesophagi; sr, superior rectus; sth, sternohyoideus; tv, transversus ventralis; umf, unidentified muscle fibers. Scale bar = 0.1 mm.

Muscles serving the ventral surface

At 1dph, the interhyoideus develops as small paired muscles (Fig. 3-1D). At 2 dph, the intermandibularis anterior, intermandibularis posterior and hyohyoideus are newly visible (Fig. 3-1F, G). The intermandibularis anterior and the two intermandibularis posterior muscles form a triangle. Transverse fibers of the intermandibularis anterior pass laterally between Meckel's cartilages to overlap the anterior ends of the intermandibularis posterior muscles. The bilaterally symmetrical muscle straps of the intermandibularis posterior and the interhyoideus form an hourglass structure (Fig. 3-1G). There is no further change in muscle composition serving the ventral surface after this time (Table 3-1). At 3 dph, the intermandibularis posterior and the interhyoideus become more deeply associated with each other to form the protractor hyoidei in development (Fig. 3-1O).

Muscles serving the ventral parts of branchial arches

At 2 dph, the sphincter oesophagi and a few obliqui ventrales are detected (Fig. 3-1E, F). At 3 dph, the transversus ventralis and rectus communis are clearly detectable (Fig. 3-1P). The obliqui ventrales 1–3 interconnect with the corresponding hypobranchials

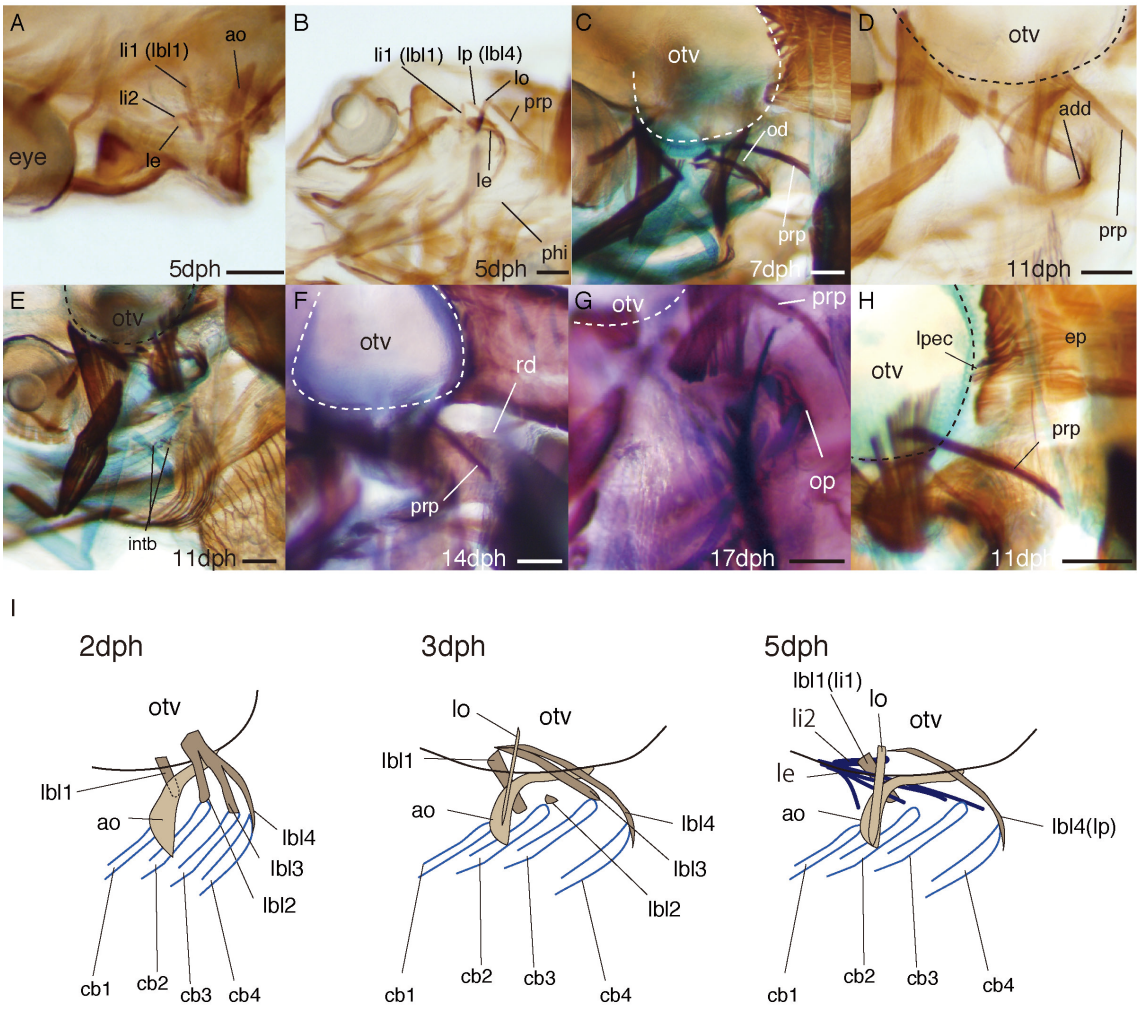

Figure 3-2. Muscles serving the dorsal parts of branchial arches and muscles between the pectoral girdle and the skull, hyoid, and branchial arches in the bamboo sole. Muscles were labeled with anti-myosin antibody and cartilage was stained with Alcian blue. (A) Dorsal view of the cranial musculature at 5 dph, focusing on the levator externus and levator interni. (B) Ventrolateral view of the cranial musculature at 5 dph, focusing on the levator externus, levator internus 1 and levator posterior. (C) Dorsolateral view of the musculature at 7 dph, focusing on the obliqui dorsales. (D) Lateral view of the cranial musculature at 11 dph, focusing on the adductores. (E) Dorsolateral view of the cranial musculature at 11 dph, focusing on the interbranchiales. (F) Dorsal view of the musculature at 14 dph, focusing on the retractor dorsalis. (G) Lateral view of the cranial musculature at 17 dph, focusing on the oblique posterior. (H) Lateral view of the musculature at 11 dph, focusing on the levator pectoralis. (I) Schematic lateral representation of the larval branchial levators and levator operculi at 2, 3 and 5 dph. add, adductores; ao, adductor operculi; cb, ceratobranchial cartilage; ep, epaxialis; intb, interbranchiales; lbl1-4, larval branchial levator 1-4; le, levatores externi; li1 and 2, levator internus 1 and 2; lo, levator operculi; lp, levator posterior; lpec, levator pectoralis; od, obliqui dorsales; op, obliquus posterior; otv, otic vesicle; phi, pharyngoclavicularis internus. prp, protractor pectoralis; rd, retractor dorsalis. Scale bar = 0.1 mm.

and ceratobranchials. The transversus ventralis is identified in the fourth arch, and interconnects the left and right cartilaginous fourth hypobranchials. There is no further change in muscle composition serving the ventral parts of branchial arches until 14 dph, at which time, the recti ventrales are detected (Fig. 3-1Q). The recti ventrales interconnect the third and fourth hypobranchials.

Muscles serving the dorsal parts of branchial arches

At 2 dph, the larval branchial levators are very faintly detected (Fig. 3-1F, H). With the exception of larval branchial levator 1, these muscles originate from the lateral side of the otic vesicle and insert onto the corresponding ceratobranchial cartilage along the branchial arch (Fig. 3-1F, H; 2I). The larval branchial levator 1 originates from the lateral side of the otic vesicle and points medially towards the region where epibranchial cartilage 1 or infrapharyngobranchial cartilages, are to be formed (Fig. 3-1H, I). At 3 dph, larval branchial levators are the only muscles controlling the branchial arches in this region until 5 dph (Fig. 3-1K, 2I). At this time, the larval branchial levator 2 has begun to atrophy. The levatores externi and levator internus 2 are not present at this stage; these develop at 5 dph (Fig. 3-2A, B). The newly developed levatores externi are positioned medially to the adductor operculi and insert on the epibranchial cartilages. The larval branchial levators 2 and 3 have disappeared completely by this stage, while portions of the larval branchial levators 1 and 4 remain (Fig. 3-2B, I). After this stage, the terms “levator internus 1” and “levator posterior” are used as the designations of the muscles that until now were named “larval branchial levator 1” and “larval branchial levator 4”, respectively. At 7 dph, the obliqui dorsales are detected (Fig. 3-2C). At 11 dph, the adductor 4 and interbranchiales are detected (Fig. 3-2D, E). The adductor 4 is a thick muscle, and is located on the medial side of the fourth arch. The interbranchiales are small muscles associated primarily with the gill filaments. At 14 dph, the retractor dorsalis is detected (Fig. 3-2F). At 17 dph, the obliquus posterior is detected, and connects the fifth ceratobranchial to the fourth epibranchial (Fig. 3-2G).

Muscles between the pectoral girdle and the skull, hyoid, and branchial arches

At 1 dph, the paired sternohyoideus are faint and located lateral to the heart (Fig. 3-1B). The protractor pectoralis has also begun development as a small muscle at this stage (Fig. 3-1C). At 2 dph, the paired sternohyoideus is situated lateral to the heart (Fig.

3-1E, G). The sternohyoideus originates on the anterior face of the cleithrum and inserts on the hyoid. The protractor pectoralis is clearly visible at this stage (Fig. 3-1F), and appears to originate from the skull and pass ventrally in order to attach to the cleithrum. The pharyngoclavicularis externus is also visible, connecting the fifth ceratobranchial and the cleithrum (Fig. 3-1G). At 5 dph, the pharyngoclavicularis internus is visible (Fig. 3-2B). At 11 dph, the levator pectoralis is detected, which may have been derived from the epaxialis at the trunk (Fig. 3-2H).

Muscles of the body and fins

At 0 dph, the trunk myotomes and heart muscles have differentiated (Fig. 3-1A). At 1dph, the hypaxialis which is attached to the eighth myotome appears to be growing rostrally below the pectoral fin (Fig. 3-1B). The pectoral-fin muscles are also detected, and appear as two muscle fiber masses (Fig. 3-1B). At 2 dph, a hypaxial muscle is attached to the ninth myotome and inserts on the posteroventral face of the cleithrum, opposite to the site where the sternohyoideus originates (Fig. 3-1E-G). The muscles of the pectoral fin have grown as two plain pectoral-fin plates (Fig. 3-1F). At 3 dph, the muscle fibers are detected on the epidermal tissue and are covering the abdominal region (Fig. 3-1I). This muscle could not be identified. Furthermore, there is no description of this muscle in reports of muscle development in the Japanese flounder (the Chapter II) and the zebrafish (Schilling & Kimmel, 1997). In this study the muscle is referred to as 'unidentified muscle fibres (umf)'. At 5 dph, the hypaxial muscles have increased in number and now cover the abdominal region. These muscles are attached to the eighth through 11th myotomes (Fig. 3-3A). Simultaneously, the hypaxial muscles have increased in number and cover the abdominal region during development (Fig. 3-3B, D). At 11dph, the muscles that control the dorsal and anal-fin rays arise from the anteriormost portion of each fin (Fig. 3-3B). In the caudal region, several muscles of the 39th and 40th myotomes have partially extended from the trunk (Fig. 3-3B, C). These muscles will become the caudal-fin muscles in later stages of development. At 17 dph, the eyes of most of the fish were still symmetrically situated, except for a few individuals where the left eyes had already migrated dorsally at varying degrees. These individuals appear to have developed faster than the other 17-dph larvae. They are different in the developmental stage of fin muscles from other individuals, although no difference was seen in the other muscles of these fish. Therefore, these

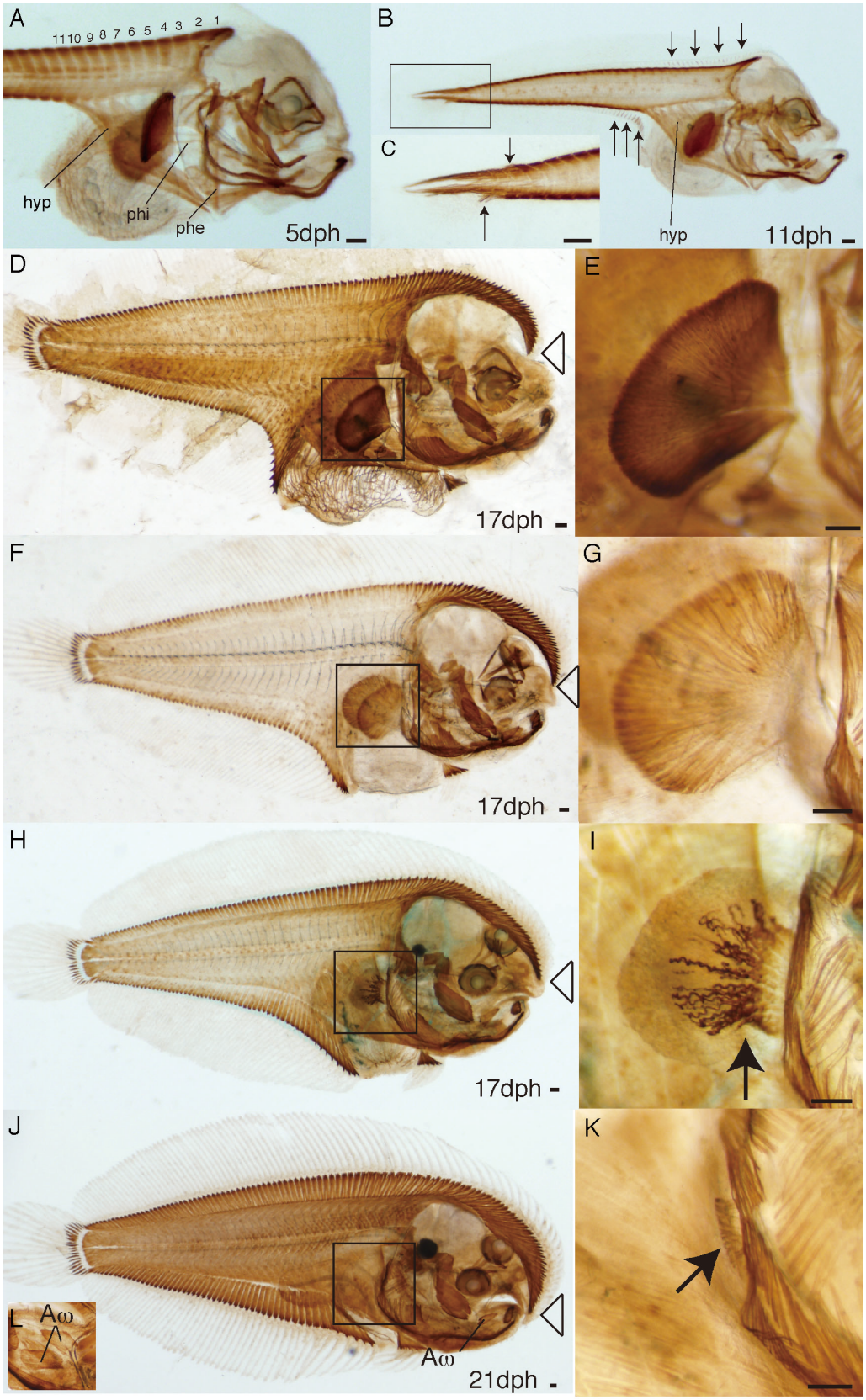
A
1110 9 8 7 6 5 4 3 2 1
hyp
phi
phe
5dph
B
C
hyp
11dph
D
17dph
E
F
17dph
G
H
17dph
I
J
Aω
Aω
21dph
K

Figure 3-3

Figure 3-3. Muscles of the body and fins in the bamboo sole. Muscles were labeled with anti-myosin antibody. (A) Lateral view of the cranial musculature at 5 dph. The figures show the number of myotomes. (B) Lateral view of the musculature at 11 dph, black arrows show the dorsal and anal fin muscles. (C) Magnification of the boxed area in (B), black arrows indicate muscles extending from the myotome. (d, f, h) Lateral view of the musculature at 17 dph, triangular arrows indicate the tip of dorsal fin muscles. (E) Magnification of the boxed area in (D). (G) Magnification of the boxed area in (F). (I) Magnification of the boxed area in (H), black arrow indicates pectoral fin muscles regressing. (J) Lateral view of the musculature at 21 dph, triangular arrow indicates the tip of dorsal fin muscles (K) Magnification of the boxed area in (J), black arrow indicates regenerated pectoral fin. (L) Lateral view of the left adductor mandibulae Aω at 21 dph. Aω, adductor mandibulae Aω; hyp, hypaxialis; phe, pharyngoclavicularis externus; phi, pharyngoclavicularis internus. Scale bar = 0.1 mm.

---

individuals are used to describe the development of the dorsal and anal fin muscles. In these fish, the dorsal-fin muscles are seen to grow rostrally, and the left eye migrates dorsally between the growing dorsal fin and head (Fig. 3-3D, F, H). As the eye migrates, the pectoral-fin muscles regress (Fig. 3-3E, G, I). At 21 dph, eye migration has almost ceased. The dorsal fin muscles reach the mouth (Fig. 3-3J), such that there is no more space between the dorsal fin muscle and the head. The pectoral fin has almost completely regressed (Fig. 3-3K), and the muscle composition of 21 dph larvae is the same as 17 dph larvae.

Discussion

This chapter reveals that the bamboo sole possesses larval-specific muscles in the dorsal branchial arches, as in the case of the Japanese flounder. These muscles might be common among flatfishes, since the bamboo sole and Japanese flounder belong to two distinct families. However, the phylogenetic relationships of the order Pleuronectiformes are still controversial (Chapleau, 1993; Pardo *et al.*, 2005; Azevedo *et al.*, 2008) and more species need to be studied to draw a firm conclusion.

This is the second study to report the presence of larval-specific muscles in a teleost species. I reported the presence of larval-specific muscles in the dorsal branchial arches of Japanese flounder in chapter II. These muscles were previously thought to be unique to the Japanese flounder. Although the larval branchial levators 2 and 3 exist only for a very short period of time in the development of bamboo sole compared with those of Japanese flounder (Fig. 3-2I), the larval branchial levators do develop first before development of the levatores externi and levator internus 2.

There are six differences between the bamboo sole and Japanese flounder: (1) the position where the adductor hyomandibulae develop is different; (2) the bamboo sole has a recti ventralis muscle, whereas the Japanese flounder does not; (3) there is an asymmetric composition of the adductor mandibulae Aω between the left and right sides only in the bamboo sole*;* (4) the muscle fibers covering the abdominal region are found only in the bamboo sole*;* (5) the muscle fibers of the pectoral fin atrophy during metamorphosis only in the bamboo sole*;* (6) the dorsal-fin muscles extend rostrally only in the bamboo sole.

Referring to the different position of development of the abductor hyomandibulae (#1 above), Winterbottom (1974) reported that this muscle is derived from the adductor arcus palatini or the adductor operculi. This difference in origin is responsible for the difference in the position of the adductor hyomandibulae between bamboo sole and Japanese flounder. The adductor hyomandibulae develops from the adductor operculi in Japanese flounder and from the adductor arcus palatini in bamboo sole.

Referring to difference #2 above, while the recti ventrales are present in most teleosts, their number has been reported to vary (Winterbottom, 1974), with these muscles being reduced in number and represented only by a single pair in many taxa (Stiassny, 2000). Thus the condition in Japanese flounder, which has no recti ventrales, is unique among teleosts.

With reference to #3 above, the asymmetry of the adductor mandibulae Aω of bamboo sole was initially observed in 17 dph larvae, when the left eye had just begun to migrate. Thus, the differential formation of the adductor mandibulae Aω is one of the earliest asymmetric tissue developments in metamorphosis of this species. On the other hand, the adductor mandibulae Aω of Japanese flounder do not show such asymmetry observed in the bamboo sole. This probably reflects the difference in the feeding habits of the two species. Although the two species are both carnivorous, the Japanese flounder is usually nektonic in feeding and mostly preys upon fish, whereas the bamboo sole feeds benthically on diverse range of prey, such as small shrimp, fish, and molluscs (Ochiai, 1966). Although many body parts develop asymmetrically between the ocular and blind side of Pleuronectiformes, the size of the jaws of piscivorous flatfishes such as the genus *Hippoglossus* is virtually the same between both sides (Norman, 1934). On the other hand, the size of the jaws on the blind side is generally larger than those on the ocular side in the benthically feeding Pleuronectiformes including the genus

Pleuronectes (Norman, 1934). The difference in the size of the jaws of these fish apparently corresponds to the asymmetry of the adductor mandibulae Aω.

With reference to the point #4 above, the muscle fibers covering the abdominal region are found only in the bamboo sole; there is no documentation of their presence in any other teleosts. The functional implications of this muscle are currently unclear.

Referring to the fifth and sixth points above, it is known that some members of Soleidae have no pectoral fin on both sides in the adult stage and the pectoral fins of bamboo sole atrophy during metamorphosis (Minami, 1981). On the other hand, adult Japanese flounder have pectoral fins on both sides. Thus, the regression of muscle fibers occurs in accordance with the regression of the pectoral fins. The rostral extension of the dorsal-fin muscles is evidently the result of the rostral extenstion of the dorsal fin.

CHAPTER IV Visualization of musculature of the larval greater amberjack *Seriola dumerili* (Risso) using whole-mount immunostaining with special reference to cranial muscles.

The greater amberjack *Seriola dumerili* (Risso) (Perciformes: Carangidae) is an important aquaculture species in Japan. Mass seed production of this fish is still difficult because of early mortality, malformations and cannibalism (Shiozawa *et al*., 2003; Kolkovski and Sakakura 2007; Takemaru *et al*., 2009), but some studies have been published on various aspects of this species to understand normal development and to prevent early mortality and malformations (Liu 2001; Sawada *et al*., 2006a; Hamasaki *et al*., 2009; Hirata *et al*., 2009; Teruya *et al*., 2009; Laggis *et al*., 2010; Imai *et al*., 2011).

Some studies regarding skeletal development and skeletal abnormalities in the greater amberjack are available, but little is known about muscular development. In addition, so-called malformations are not always caused by bone tissue abnormalities in some fish (Sakaguchi *et al*., 1987; Yokoyama *et al*., 2005). For instance, in the scoliosis of cultured yellowtails *S. quinqueradiata* and Japanese mackerel *Scomber japonicus* by the parasitism of *Myxobolus acanthogobii* and viral deformity in yellowtail *S. quinqueradiata*, it is likely that the parasite and virus in the brain interfere with the nervous system, leading to myopathy of axial muscles and asymmetrical changes in muscle tone, finally leading to skeletal abnormalities. Hence, it follows that muscular abnormalities in the greater amberjack may be a background of skeletal deformities; therefore, it is important to recognize muscle development in detail.

Describing muscle development in the greater amberjack is also important for developmental studies because the presence of larval-specific muscles in the Japanese flounder and bamboo sole has been described in the chapter II and III, but it is unclear whether larval-specific muscles are common to all fish or unique to flatfish. Investigating muscle development in the greater amberjack, a member of Perciformes and one of the largest orders of vertebrates, will help elucidate this issue.

In this chapter, I describe muscle development in the larval greater amberjack from 0 to 12 dph, when all cranial muscles appear, using the modified whole mount immunohistochemical method, focusing primarily on cranial muscles.

Materials and methods

Amberjack samples

Larvae for whole mount immunostaining were sampled from a 80 kl rearing tank used for actual mass aquaculture production at the Shibushi Laboratory of the National Research Institute of Aquaculture, Fisheries Research Agency in Kagoshima, Japan. Water temperature was maintained at 23 °C before hatching; thereafter, it was increased to 26 °C by 3 dph and was maintained at 26 °C during the rearing period. Larvae were fed S-type rotifers at a density of 20 individuals/ml from 3–6 dph and L-type rotifers at a density of approximately 20 individuals/ml thereafter. All rotifers were cultured with Chlorella (Chlorella V12; Chlorella Industry) and were enriched with HUFA enriched Chlorella (Super Chlorella V12; Chlorella Industry) for 6–12 hours prior to feeding. Five hundreds ml Super Chlorella V12 was added to the rearing tank twice daily to prevent starvation of the rotifers. A series of samples from this tank at 0, 1, 2, 3, 4, 5, 6, 8, 10 and 12 dph was obtained. The numbers of specimens used for whole mount immunostaining at each dph were 11, 14, 18, 14, 21, 22, 25, 25, 20 and 18. Individuals that have the dominant developmental stage of each day were used to document normal muscle development. Larvae were anesthetised with 0.01% 3-aminobenzoic acid ethyl ester (Sigma) and were fixed with 4% paraformaldehyde (PFA) in phosphate buffered saline (PBS) containing 0.3% Tween 20 (PBST), rinsed in PBST, dehydrated in a graded series of methanol (25%, 50%, 75% and 100%) and stored in 100% methanol at −20 °C.

Whole mount immunostaining

Stored larvae in 100% methanol at −20 °C for two years were used for whole mount immunohistochemical staining based on the methods described in the chapter II. The primary anti-myosin antibody A4.1025 (1:200, Upstate) was used for visualization of muscle tissues. Some larvae were cut with a sharp-edged razor before staining to clearly visualize the cranial muscles deeply positioned in the head. For double staining of muscle and cartilage tissue, samples were stained with Alcian blue and subsequently immunostained for muscle according to the methods described in the chapter II. After

staining, samples were cleared in increasing concentrations of glycerol (25%, 50% and 80%) and observed using a MZFL microscope (Leica) equipped with Combi III (Leica) or an Eclipse 90i microscope (Nikon). Micrographs were obtained using a CCD camera DP70 (Olympus) and processed using Adobe Photoshop CS3 (Adobe Systems). The muscle nomenclature outlined in this study is based on that used in the chapter II.

Results

0 dph (3.2 mm total length (TL)) - 1 dph (3.6 mm TL)

No cranial muscle tissue is found, even though the trunk myotomes and the heart muscles have differentiated at 0 dph (Fig. 4-1A). The superior rectus, lateral rectus and inferior rectus of the extraocular muscles are detected as separate small muscles at 1 dph (Fig. 4-1B, C). The hypaxialis, which is attached to the sixth myotome, appear to be growing rostrally in the body region (Fig. 4-1B, D).

2 dph (3.6 mm TL)

In the eye musculature, all six components of the extraocular muscles (superior oblique, inferior oblique, superior rectus, inferior rectus, medial rectus and lateral rectus) are clearly detected (Fig. 4-1E, F). No further changes in eye muscle composition are observed after 2 dph (Table 4-1). In the cheek musculature, the adductor mandibulae A1 and A2, levator arcus palatini, adductor arcus palatini, adductor operculi and adductor hyomandibulae are found (Fig. 4-1F, G). The adductor mandibulae A1 and the levator arcus palatini are lying at the rear of the orbit (Fig. 4-1G). These muscles overlaid each other; the dorsal region of the adductor mandibulae A1 is overlaid by fibres of the ventral part of the levator arcus palatini. The levator arcus palatini appears conical in shape, with its apex lying anteroventrally, and occupy the area at the rear of the orbit between the neurocranium and the hyosymplectic cartilage. The adductor arcus palatini is situated posterior to the orbit and medial to the levator arcus palatini (Fig. 4-1F). The adductor mandibulae A2 is located on the medial side of the adductor mandibulae A1 (Fig. 4-1F). The adductor hyomandibulae and the adductor operculi

Table 4-1. Timing of cranial muscle development in the greater amberjack

	0dph	1dph	2dph	3dph	4dph	5dph	6dph	8dph	10dph	12dph
Total length	3.2 mm	3.6 mm	3.6 mm	3.8 mm	3.7 mm	4.1 mm	4.2 mm	4.5 mm	5.0 mm	5.8 mm
Muscles of the eye										
Superior oblique	×	○	○	○	○	○	○	○	○	○
Inferior oblique	×	×	○	○	○	○	○	○	○	○
Superior rectus	×	○	○	○	○	○	○	○	○	○
Inferior rectus	×	×	○	○	○	○	○	○	○	○
Medial rectus	×	×	○	○	○	○	○	○	○	○
Lateral rectus	×	○	○	○	○	○	○	○	○	○
Muscles of the cheek										
Adductor mandibualae	×	×	○	○	○	○	○	○	○	○
Levator arcus palatini	×	○	○	○	○	○	○	○	○	○
Dilatator operculi	×	×	×	○	○	○	○	○	○	○
Levator operculi	×	×	×	×	×	○	○	○	○	○
Adductor arcus palatini	×	×	○	○	○	○	○	○	○	○
Adductor operculi	×	×	○	○	○	○	○	○	○	○
Adductor hyomandibulae	×	×	○	○	○	○	○	○	○	○
Muscles serving the ventral surface of the head										
Intermandibularis anterior	×	×	○	○	○	○	○	○	○	○
Intermandibularis posterior	×	×	○	○	○	○	○	○	○	○
Interhyoideus	×	×	○	○	○	○	○	○	○	○
Hyohyoideus	×	×	×	○	○	○	○	○	○	○
Muscles serving the dorsal parts of the branchial arches										
Larval branchial levators	×	×	○	○	○	○	○	-*	-*	-*

Levatores externi	×	×	×	×	×	○	○	○	○	○
Levatores interni	×	×	○(lbl1)	○(lbl1)	○(lbl1)	○(lbl1)	○(lbl1)	○	○	○
Levator posterior	×	×	○(lbl4&5)	○(lbl4&5)	○(lbl4&5)	○(lbl4&5)	○(lbl4&5)	○	○	○
Obliqui dorsales	×	×	×	×	×	×	○	○	○	○
Obliquus posterior	×	×	×	×	×	×	○	○	○	○
Adductores	×	×	×	×	×	×	×	○	○	○
Retractor dorsalis	×	×	×	×	×	○	○	○	○	○
Interbranchiales	×	×	×	×	×	×	○	○	○	○
Muscles serving the ventral parts of the branchial arches										
Sphincter oesophagi	×	×	○	○	○	○	○	○	○	○
Obliqui ventrales	×	×	○	○	○	○	○	○	○	○
Transversi ventrales	×	×	○	○	○	○	○	○	○	○
Rectus communis	×	×	×	×	×	×	○	○	○	○
Recti ventrales	×	×	×	×	×	×	○	○	○	○
Muscles between the pectoral girdle and the skull, hyoid, and branchial arches										
Sternohyoideus	×	×	○	○	○	○	○	○	○	○
Pharyngoclavicularis externus	×	×	○	○	○	○	○	○	○	○
Pharyngoclavicularis internus	×	×	×	×	×	○	○	○	○	○
Protractor pectoralis	×	×	○	○	○	○	○	○	○	○
Levator pectoralis	×	×	×	×	×	×	×	×	×	○

×, no muscle fibers; ○, differentiated muscle fibers; ○(lbl1), detected as a larval branchial levator I; ○(lbl4&5), detected as a larval branchial levator IV and V

-* After 8 dph, I use the terms the “levator internus I” and the “levator posterior” instead of the “larval branchial levator I” and the “larval branchial levator IV and V ”, respectively.

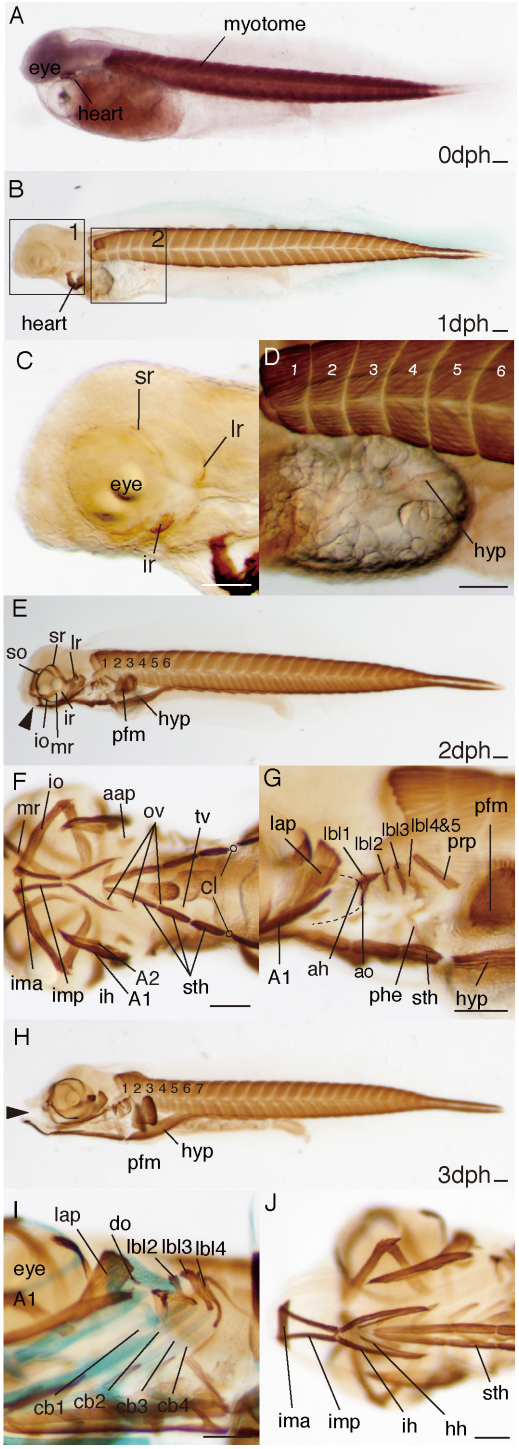
A
myotome
eye
heart
0dph
B
1
2
heart
1dph
C
sr
lr
eye
ir
D
1 2 3 4 5 6
hyp
E
so
sr
lr
1 2 3 4 5 6
ir
io
mr
pfm
hyp
2dph
F
io
mr
aap
ov
tv
cl
ima
imp
ih
A2
A1
sth
G
pfm
lap
lbl1
lbl2
lbl3
lbl4&5
prp
A1
ah
ao
phe
sth
hyp
H
1 2 3 4 5 6 7
pfm
hyp
3dph
I
lap
do
lbl2
lbl3
lbl4
eye
A1
cb1
cb2
cb3
cb4
J
sth
ima
imp
ih
hh

Figure 4-1

Figure 4-1. Larval musculature in the greater amberjack head and trunk regions at 0–3 dph. Muscles were labelled with anti-myosin antibody, and cartilage was stained with Alcian blue. (A) Lateral view of the musculature at 0 dph. (B) Lateral view of the musculature at 1 dph. (C) Magnification of the boxed area 1 in (B). Lateral view of the cranial musculature at 1 dph. (D) Magnification of the boxed area 2 in (B). Lateral view of the musculature at 1 dph. The figure shows the number of myotomes. (E) Lateral view of the musculature at 2 dph. The figure shows the number of myotomes. Black arrowhead shows the position of the mouth. (F) Ventral view of the cranial musculature at 2 dph. (G) Lateral view of the cranial musculature at 2 dph. (H) Lateral view of the musculature at 3 dph. The figure shows the number of myotomes. Black arrowhead shows the position of the mouth. (I) Ventrolateral view of the cranial musculature (brown) and cartilage (blue) at 3 dph. (J) Ventral view of the cranial musculature at 3 dph. aap, adductor arcus palatini; ah, adductor hyomandibulae; ao, adductor operculi; A1, adductor mandibulae A1; A2, adductor mandibulae A2; Cb, ceratobranchial cartilage; Cl, clavicle; do, dilatator operculi; hh, hyohyoidei; hyp, hypaxialis; ih, interhyoideus; ima, intermandibularis anterior; imp, intermandibularis posterior; io, inferior oblique; ir, inferior rectus; lap, levator arcus palatini; lbl, larval branchial levator; lr, lateral rectus; mr, medial rectus; ov, obliqui ventrales; pfm, pectoral fin muscle; phe, pharyngoclavicularis externus; prp, protractor pectoralis; so, superior oblique; sr, superior rectus; sth, sternohyoideus; tv, transversus ventralis. Scale bar = 0.1 mm.

---

appear to be present as a single muscle mass that branches into two parts at the ventral end (Fig. 4-1G). They pass anteroventrally between the larval branchial levators 1 and 2 and then insert into the hyosymplectic cartilage and the opercle, which have not yet become ossified. In the muscles located at the ventral part of the head, the intermandibularis posterior and interhyoideus are developing as paired small muscles, respectively (Fig. 4-1F), although they will become more deeply associated with each other to form the protractor hyoidei later in development. The intermandibularis anterior is also detected near the intermandibularis posterior (Fig. 4-1F). The larval branchial levators are clearly detected in the dorsal parts of the branchial arches (Fig. 4-1G). The larval branchial levator 1 is located anterior to the adductor hyomandibulae and operculi, whereas the other larval branchial levators are located posterior to the adductor hyomandibulae and operculi. The sphincter oesophagi, obliqui ventrales and transversi ventrales are detected in the ventral parts of the branchial arches (Fig. 4-1F). The obliqui ventrales and transversi ventrales are located on the ceratobranchial cartilage. The paired sternohyoideus has arisen lateral to the heart tube in the muscles between the pectoral girdle and the skull, hyoid and branchial arches (Fig. 4-1E, F, G). The sternohyoideus originates on the cranial face of the cleithrum and inserted into the hyoid. This muscle is composed of three subdivided muscles (Fig. 4-1F), and the protractor pectoralis is clearly detected (Fig. 4-1G). It appears to originate from the skull and pass downwards to attach to the cleithrum. The pharyngoclavicularis externus is also

detected, connecting ceratobranchial 5 with the cleithrum (Fig. 4-1G). A hypaxial muscle is attached to the sixth myotome in the body region and inserted on the posteroventral face of the cleithrum, opposite to the site where the sternohyoideus originates (Fig. 4-1E, G). Pectoral fin muscles are also detected and appear as two muscle fibre masses (Fig. 4-1E).

3 dph (3.8 mm TL)

This stage coincides with the first feeding; thus, all components of the cheek muscles are developed, with the exception of the levator operculi and the dilatator operculi in the opercular region. All six components of the extraocular muscles are clearly detected as at 2 dph (Fig. 4-1H). The dilatator operculi is newly located lateral to the levator arcus palatini in the cheek musculature and appeared as a very thin muscle band (Fig. 4-1I). The hyohyoideus is faintly detected as paired thin muscle bands between the interhyoideus and the sternohyoideus muscles on the ventral surface of the head (Fig. 4-1J). I define the hyohyoideus inferior, hyohyoidei abductors and hyohyoidei adductores as hyohyoideus muscle types because of confusion in the literature over the classification of muscles located in this region. The positions of the intermandibularis anterior, intermandibularis posterior and interhyoideus shift anteriorly, coinciding with the anterior shift of the mouth (Fig. 4-1H, J). Larval branchial levators are clearly detected in the dorsal parts of the branchial arches (Fig. 4-1I). With the exception of the larval branchial levator 1, these muscles originate from the lateral side of the otic vesicle and insert into the corresponding ceratobranchial cartilage along the branchial arch. The larval branchial levator 1 originates from the lateral side of the otic vesicle and points medially towards the region where epibranchial cartilage 1 or infrapharyngobranchial cartilages are to be formed. The muscles in the ventral parts of the branchial arches do not change their shape or position. The sternohyoideus also shifts anteriorly in the muscles between the pectoral girdle, the skull, hyoid and branchial arches, coinciding with the anterior shift of the mouth. No differences between 2 and 3 dph larvae are observed in the muscle composition of this region. In the body region, the hypaxial muscles are attached to the sixth myotome, and a new small hypaxial muscle mass is detected at the seventh myotome (Fig. 4-1H).

4 dph (3.7 mm TL)

The third adductor mandibulae portions Aω is recognised in the cheek musculature (Fig. 4-2A, B). The newly appearing adductor mandibulae muscle Aω is located anterior to adductor mandibulae A1. The dilatator operculi is clearly detected although this muscle is only rudimentary in 3-dph larvae (Fig. 4-2B). The composition of the other muscles has not changed.

5 dph (4.1 mm TL)

The levator operculi is detected in the cheek muscles (Fig. 4-2C, D) and develops behind the dilatator operculi. The larval branchial levator 2 gradually atrophies in the dorsal parts of the branchial arches, whereas the levatores externi and levator internus 2 have begun to develop (Fig. 4-2D, E). The retractor dorsalis is also detected at this stage (Fig. 4-2F). I identify this muscle clearly in samples cut off at the anterior somite because this muscle is positioned deeply in the body on the sphincter oesophagi. The pharyngoclavicularis internus is detected in the muscles between the pectoral girdle and the skull, hyoid and branchial arches (Fig. 4-2D). The composition of the other muscles has not changed.

6 dph (4.2 mm TL)

In the dorsal parts of the branchial arches, the larval branchial levator 2 atrophies completely, and the larval branchial levator 3 begin to atrophy, whereas the newly developed levatores externi muscles are positioned medial to the adductor operculi and the adductor hyomandibulae (Fig. 4-2G, H) and insert on each epibranchial cartilage. The obliqui dorsales, interbranchiales and obliqui posterior are detected (Fig. 4-2H, I). The rectus communis and recti ventrales are detected in the ventral parts of the branchial arches (Fig. 4-2J). The rectus communis connects the ceratobranchial of the respective arch to the hypobranchial of the preceding arch. The recti ventrales interconnects the fourth ceratobranchial to the fifth ceratobranchial. The hypaxial muscles are growing as three clear muscle bands and are inserted on the cleithrum and attached to the sixth to the eighth myotome (Fig. 4-2G).

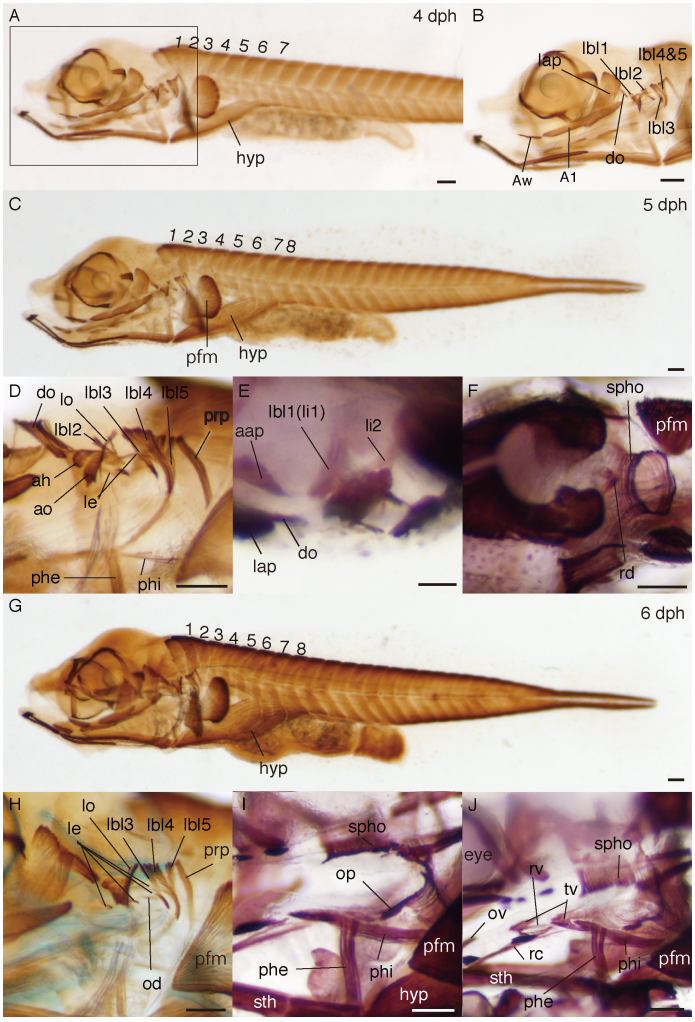

Figure 4-2. Larval musculature in the greater amberjack head and trunk regions at 4–6 dph. Muscles were labelled with anti-myosin antibody, and cartilage was stained with Alcian blue. (A) Lateral view of the musculature at 4 dph. The figure shows the number of myotomes. (B) Magnification of the boxed area in (A), focusing on the larval branchial levator and the adductor mandibulae Aω. (C) Lateral view of the musculature at 5 dph. The figure shows the number of myotomes. (D) Lateral view of the cranial musculature at 5 dph. Note that the larval branchial levator 2 is atrophying in part. (E) Dorsal view of the cranial musculature at 5 dph, focusing on the levatores interni. (F) Dorsolateral view of the musculature at 5 dph, focusing on the retractor dorsalis. Larva cut off at the anterior somite. (G) Lateral view of the musculature at 6 dph. The figure shows the number of myotomes. (H) Lateral view of the cranial musculature (brown) and cartilage (blue) at 6 dph, focusing on the muscles of the dorsal branchial arches. (I) Lateral view of the cranial musculature at 6 dph, focusing on the oblique posterior. A part of the head of a larva cut off to recognize the muscles more clearly. (J) Lateral view of the cranial musculature at 6 dph, focusing on the recti ventrales and rectus communis. A part of the head of the larva was cut off to recognize the muscles more clearly. aap, adductor arcus palatini; ah, adductor hyomandibulae; ao, adductor operculi; A1, adductor mandibulae A1; Aω, adductor mandibulae Aω; do, dilatator operculi; hyp, hypaxialis; lap, levator arcus palatini; lbl, larval branchial levator; le, levator externus; li, levator internus; lo, levator operculi; od, obliqui dorsales; op, obliquus posterior; ov, obliqui ventrales; pfm, pectoral fin muscle; phe, pharyngoclavicularis externus; phi, pharyngoclavicularis internus; prp, protractor pectoralis. rc, rectus communis; rd, retractor dorsalis; rv, recti ventrales; spho, sphincter oesophagi; sth, sternohyoideus; tv, transversus ventralis. Scale bar = 0.1 mm.

8 dph (4.5 mm TL)

The larval branchial levator 3 completely atrophies in the dorsal part of the branchial arches (Fig. 4-3A, B), whereas portions of the larval branchial levators 1, 4 and possibly 5 remain. The larval branchial levators, with the exception of larval branchial levator 1, are located lateral to the adductor operculi and the adductor hyomandibulae and insert at the ceratobranchial cartilages. The newly developed levatores externi muscles are positioned medial to the adductor operculi and the adductor hyomandibulae and insert at the epibranchial cartilages. Therefore, the levatores externi are clearly distinct from the larval branchial levators although the function of these muscles for lifting the branchial arches seems to be similar. By this stage, the levatores externi and the levator internus 2 are well developed. After this stage, I use the terms ‘levator internus 1’ and ‘levator posterior’ as designations for the muscles that until date are named ‘larval branchial levator 1’ and ‘larval branchial levator 4’ (and possibly 5), respectively (Table 4-1). The adductores newly appear (Fig. 4-3B); the hypaxial muscles increase in number and cover the abdominal region. These muscles are attached to the sixth to tenth myotomes (Fig. 4-3A).

10 dph (5.0 mm TL)

The hypaxial muscles in the body region increase in number and are attached to the sixth to eleventh myotomes (Fig. 4-3C). Several muscles near the 25th myotome in the caudal region partially extend from the trunk (Fig. 4-3C, D). These muscles are to become the caudal fin muscles in later stages of development. The position of muscle extension is coincident with the position of cell condensations that generate caudal cartilage tissue.

12 dph (5.8 mm TL)

The levator pectoralis has arisen from the epaxialis body musculature in the muscles between the pectoral girdle, the skull, hyoid and branchial arches (Fig. 4-3E, G). Pelvic, dorsal and anal fin muscles are developing in the body region (Fig. 4-3E, F, H, I, J).

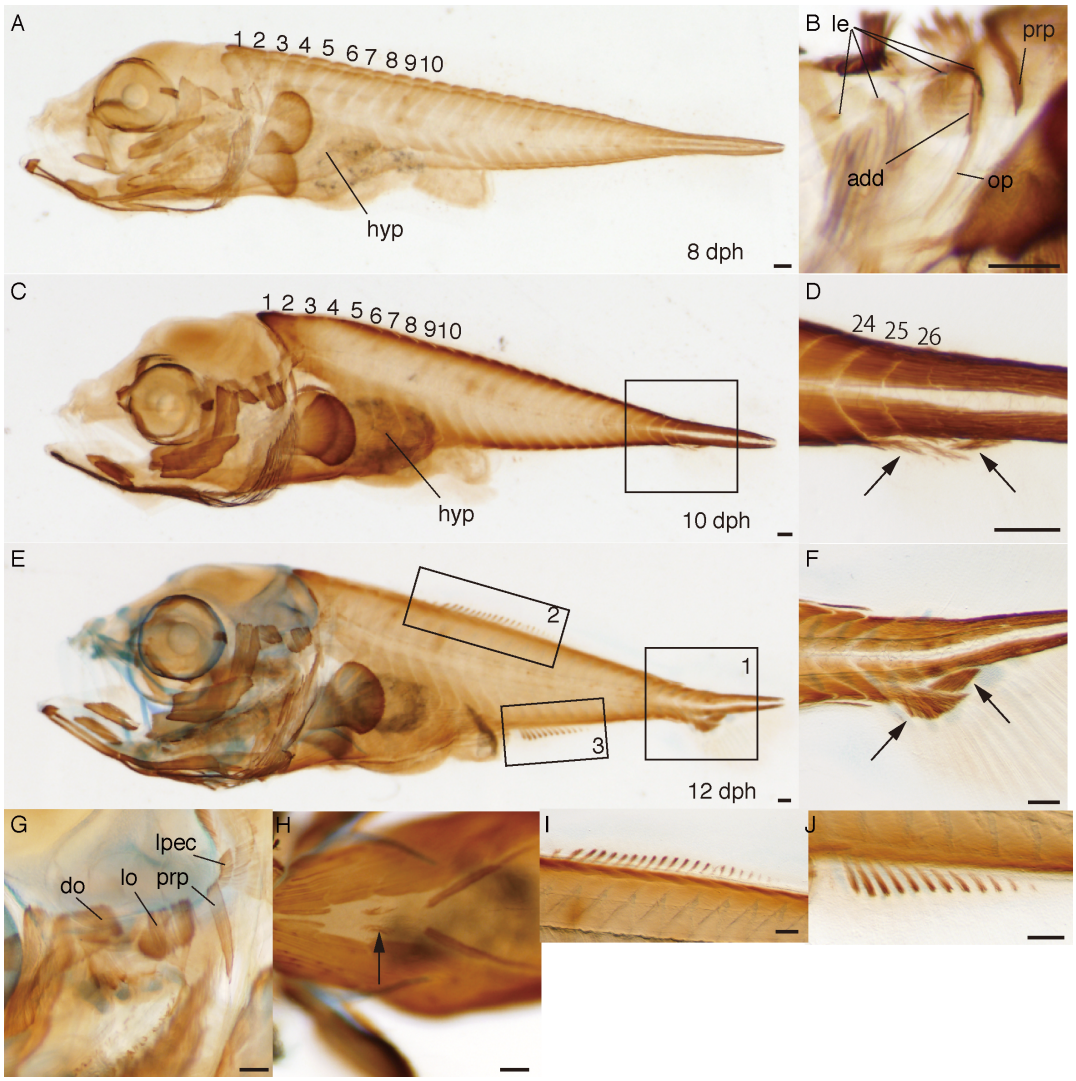

Figure 4-3. Larval musculature of the greater amberjack at 8, 10 and 12 dph. Muscles were labelled with anti-myosin antibody, and cartilage was stained with Alcian blue. (A) Lateral view of the cranial musculature at 8 dph. The figure shows the number of myotomes. (B) Ventrolateral view of the cranial musculature at 8 dph, focusing on the adductores. (C) Lateral view of the musculature at 10 dph. The figure shows the number of myotomes. (D) Magnification of the boxed area in (C). Arrows indicate muscles extending from the myotome. (E) Lateral view of the cranial musculature (brown) and cartilage (blue) at 12 dph. (F) Magnification of the boxed area 1 in (E). Arrows indicate muscles extending from the myotome. (G) Lateral view of the cranial musculature at 12 dph, focusing on the levator pectoralis. (H) Ventral view of the pelvic fin musculature (arrow) at 12 dph. (I) Magnification of the boxed area 2 in (E). (J) Magnification of the boxed area 3 in (E). add, adductores; do, dilatator operculi; hyp, hypaxialis; le, levator externus; lo, levator operculi; lpec, levator pectoralis; op, obliquus posterior; prp, protractor pectoralis. Scale bar = 0.1 mm.

Discussion

In this chapter, I described muscle development in the greater amberjack from hatching to 12 dph. I found that the muscle composition in the dorsal branchial arches changed to the adult form in the greater amberjack similar to the Japanese flounder during pre-flexion larval stage. This report provides fundamental information on greater amberjack muscle development, which will contribute towards the development of stable seed production. This report also provides a fundamental reference to study muscle development in fish.

Muscle development in the greater amberjack is very similar to that in the Japanese flounder, although these two fish belong to different orders of teleost. I reported in the greater amberjack that (1) the larval branchial levators are distinct from the levatores externi; (2) larval branchial levator 1 appears equal to the levator internus 1; (3) larval branchial levator 4, and possibly larval branchial levator 5, represent the levator posterior and (4) larval branchial levators 2 and 3, which are larval-specific muscles, atrophy soon after larval stages of development are complete. As larvae grow, the levatores externi and the levator internus 2 develop from the anterior region of the branchial arches. One difference between the Japanese flounder and the greater amberjack is that the greater amberjack has a recti ventralis, whereas the Japanese flounder does not. Although the number of recti ventrales varies in teleosts (Winterbottom, 1974) (reduced in number and represented only by a single pair in many taxa) (Stiassny, 2000), the recti ventrales are generally present in teleosts. Thus, the Japanese flounder, which has no recti ventrales, is an unusual fish.

Changes in feeding and respiratory mechanisms occur during pre-flexion larval stage in greater amberjack; the levator operculi, dilatator operculi and adductores develop, and the muscle composition in the dorsal branchial arches changes to the adult form during this stage. It is well known that changes in feeding and respiratory mechanisms occur during larval stages in fishes (Varres 1977; Otten 1982; Liem, 1991; Herbing *et al*, 1996a, b). These changes coincide with a rapid increase in relative size of the head. Ratios of head length, head depth and maxillary length to total or standard length rapidly increase in this stage in greater amberjack (Masuma *et al*., 1990; Tachihara *et al*., 1993). An increase in head depth is accompanied by a switch from ram feeding to suction feeding in *Amphiprion* (Liem, 1991).

The total length of larvae from hatching to about 7 dph hardly increases in hatchery-reared greater amberjack (Shiozawa *et al*. 2003, Teruya *et al*. 2009). The change from ram feeding to suction feeding occurs during this period. One reason larvae don't grow may be that larvae cannot obtain enough food/energy with ram feeding, at least in hatchery conditions. Ram feeding is not very efficient, and a lot of energy is required for the change from ram feeding to suction feeding. After about 7 dph, they start to grow steadily. The start of this growth depends most likely on the improvement of feeding and respiratory systems and not on the improvement of swimming ability, because the major fins develop after flexion larval stage.

The timing of ossification in cranial bones did not coincide with cranial muscle development in greater amberjack. Ossification in the cranial and axial bones proceeds from post-flexion larval stage to juvenile stage (Tachihara *et al*. 1993). Thus the muscle development is not related to ossification of bone, but rather to the cartilage development in greater amberjack as indicated in zebrafish (Kimmel *et al*. 1997) and Japanese flounder (the chapter II).

Skeletal deformities are mainly used to evaluate environmental conditions because it is possible to visualize skeletal structure. In this study, I clearly visualized the musculature of larvae in greater amberjack, although I did not observe abnormal musculature in the stained larvae in this lot. I described normal development of the muscular system of larval greater amberjack, which will allow the detection of abnormal cranial and axial muscles in larvae to improve larval rearing techniques by modifying environmental conditions. On the other hand, jaw malformations are often present in hatchery-reared yellowtail kingfish (*Seriola lalandi*) larvae (Cobcroft *et al*., 2004), which is closely related to the greater amberjack. They suggest the possibility that broodstock nutrition is a factor causing malformation of the jaw of kingfish larvae. This method also allows the evaluation of egg quality before first feeding and larval quality before bone formation.

CHAPTER V Development of the musculature and muscular abnormalities in larval seven-band grouper *Epinephelus septemfasciatus* (Thunberg)

The seven-band grouper, *Epinephelus septemfasciatus* (Thunberg), has been recognized as a potential new species for aquaculture in Japan. Although recent improvements in rearing techniques for this species have led to increases in larval survival under artificial rearing conditions (Tsuchihashi *et al*., 2003; Tanaka *et al*.., 2005; Sakakura *et al*., 2006; Sakakura *et al*., 2007a; Sakakura *et al*., 2007b; Teruya *et al*., 2008), high mortality in the early stages remains a problem for stable seed production. In addition, there is a concern regarding malformations in artificially reared fish (Nagano *et al*., 2007).

Malformations are not always caused by abnormalities in bone tissue (Sakaguchi *et al*., 1987; Yokoyama *et al*., 2005; Maeno *et al*., 1995) as described in the chapter IV. These findings suggest that the parasite and virus enter brain tissue and interfere with the nervous system, leading to myopathy of the axial muscles and asymmetrical changes in muscle tone, subsequently causing skeletal abnormalities. In addition, Akiyama *et al*. reported that deficiency of the amino acid tryptophan induced scoliosis in salmonids, including sockeye salmon *Oncorhynchus nerka*, rainbow trout *Oncorhynchus mykiss*, coho salmon *Oncorhynchus kisutch*, and chum salmon *Oncorhynchus keta* (Akiyama *et al*., 1986a; Akiyama *et al*., 1986b). These authors hypothesized that the scoliosis observed in these salmonids was induced by an abnormal muscular contraction because of a deficiency of serotonin, which is a tryptophan metabolite and brain neurotransmitter. Taken together, these observations suggest that it is reasonable to hypothesize that muscular abnormalities may also lead to skeletal deformity in the seven-band grouper. Unfortunately, despite the importance of the musculature in feeding, respiration, and swimming, little is known about the process of muscle development. I developed a modified whole mount immunohistochemical method that allows for the accurate identification of larval cranial muscles in the chapter II. The ability to document and detect abnormalities in body musculature, which has the same segmental structure as the vertebral skeleton, may lead to a better understanding of the processes leading to malformation of the vertebral skeleton.

In this chapter, I describe the process of muscle development in the seven-band grouper between 0–28 dph, when all cranial muscles appear, using the

modified whole mount immunohistochemical method. I also document the presence of larvae that have abnormal muscles in the jaw and body in cultured seven-band grouper. The utility of this method as a marker for improving the rearing techniques during larviculture is also discussed.

Materials and methods

Rearing conditions

For this study I used three males (mean length 77± 5.6 cm, mean weight 6.7± 1.6 kg) and a single female (69 cm, 5.3 kg) that were held at the Kamiura Laboratory, National Research Institute of Aquaculture, Fisheries Research Agency, Oita, Japan. Fertilized eggs were obtained by artificial insemination followed by injection with human chorionic gonadotropin (600 IU/kg of body weight; gonadotropin for injection 5000 U; ASKA Pharm.). The hatch rate was 93%. The floating eggs were transferred to a 1000 l tank with running seawater (2.5 l/ml, 23 °C) until they reached the somite stage. The eggs were then disinfected with ozonated seawater (0.3 ppm, 1 min) to prevent viral nervous necrosis, and were transferred into a 60 kl rearing tank for mass production. The water in the rearing tank was disinfected using ozone and there was no water exchange during seed production. The water temperature was maintained at 23 °C before hatching; thereafter, it was increased to 26 °C by 3 dph and held at this temperature during the remainder of the rearing period.

Larvae were fed S-type rotifers (Thai-strain, mean lorica length 136 μm) at a density of 10 individuals/ml from 3–7 dph and S-type rotifers (unknown strain obtained from the Oita Prefecture Public Fisheries Corporation, Oita, Japan, mean lorica length 155 μm) at a density of 10–15 individuals/ml from 8–51 dph. All rotifers were cultured with freshwater *Chlorell*a (Chlorella V12; Chlorella Industry) and were enriched with freshwater *Chlorella* enriched n-3 HUFA (Super Chlorella V12; Chlorella Industry) for 6–12 h prior to feeding. 500 ml Super Chlorella V12 was added to the rearing tank twice daily to prevent starvation of the rotifers. The seawater in the rearing tank was aerated through tubes (outer diameter 25 mm) that were placed at several locations on the bottom of tank and a rectangular aerator (2 × 2 × 15 cm) that was placed in the center of the tank. Before mouth opening, the aeration rate was controlled to maintain

the water velocity near the water surface (0.1–1.2 m depth) at 3–4cm/s; thereafter, the velocity was maintained at <2.9 cm/s. Twice daily, 20 g/kl of commercially available Fish Green (Pacific Trading), a fossil shell powder, was added to clear the seawater in the rearing tank.

Preparation of larvae

Larvae were sampled daily between 0 and 18 dph and 20, 23, 25, and 28 dph. The larvae (N = 30/day) were anesthetized with 3-aminobenzoic acid ethyl ester (Sigma) then fixed with 4% paraformaldehyde (PFA) in phosphate buffered saline (PBS) containing 0.3% Tween 20 (PBST), rinsed in PBST, dehydrated in a graded series of methanol (25, 50, 75, and 100%), and stored at –20 °C. The developmental stage of each specimen was identified following the description of Sabate *et al*. (2009) (Fig. 5-1). The fixed larvae (age, developmental stage, and total length (TL) as follows: 1 dph, A, 2.5 mm; 2 dph, A, 2.5 mm; 3 dph, B, 2.6 mm; 5 dph, B, 2.8 mm; 9 dph, B, 2.8 mm; 12 dph, C, 3.4 mm; 16 dph, D, 4.4 mm; 20 dph, D, 4.7 mm; 25 dph, E, 5.7 mm; and 28 dph, F, 8.9 mm) were used to document normal muscle development (Fig. 5-2, Fig. 5-3, Table5-1). Six of the fixed individuals (2 dph, A, 2.5 mm; 2 dph, A, 2.5 mm; 3 dph, B, 2.5 mm; 7 dph, B, 2.5 mm; 8 dph, B, 2.8 mm; 12 dph, B, 3.1 mm) were used to document abnormal muscle development (Fig. 5-4).

Immunohistochemistry

The larvae were subject to whole mount immunohistochemical staining following the methods described in the chapter II. Some larvae were cut with a sharp-edged razor before staining to clearly visualize the cranial muscles deeply positioned in the head. After staining, the samples were cleared in increasing concentrations of glycerol (25, 50, and 80%) and observed using a MZFL microscope (Leica) equipped with a combi III (Leica) or Eclipse 90i microscope (Nikon). Micrographs were captured using a CCD camera DP70 (Olympus) and processed using Adobe Photoshop CS3 (Adobe Systems). Digital measurements were obtained using ImageJ.

For fluorescence imaging of muscles and nerves, the tissues were simultaneously stained using a 1:200 dilution of primary antibodies against acetylated tubulin and myosin heavy chain. The primary antibodies were labelled with a Zenon tricolour labelling kit Mouse IgG2b (Invitrogen). The larvae were then stained for 5 min

with a 0.2 mg/ml solution of DAPI (4',6-diamidino-2-phenylindole) (Molecular Probes). After staining, the samples were cleared in increasing concentrations of glycerol (25 and 50%). Micrographs were captured using an Eclipse 90i microscope with Digital eclipse C1si (Nikon), and processed using Adobe Photoshop CS3 (Adobe Systems). The nomenclature of the muscles outlined in this study is based on that used in the chapter II.

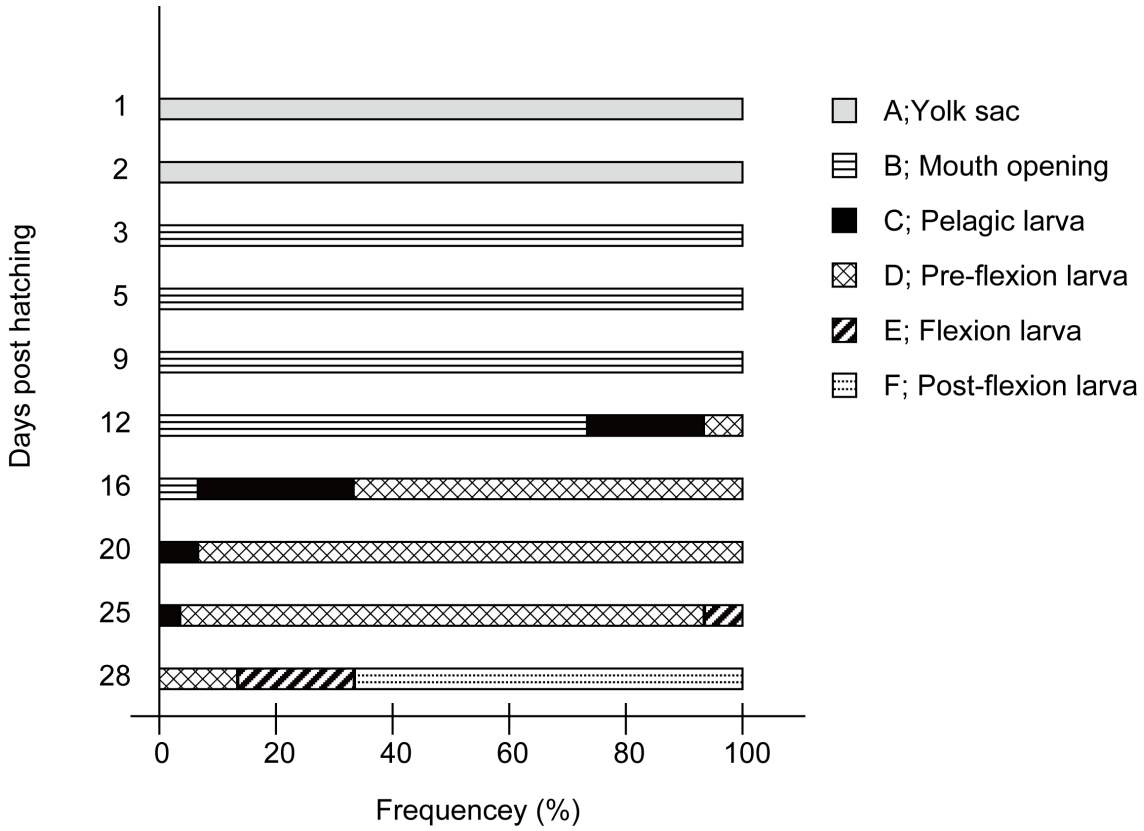

Figure 5-1 Developmental stages of the seven-band grouper used to document muscle development. Thirty larvae were checked at each sampling point. The developmental stage of each specimen was identified following the description of Sabate *et al.* (2009).

Results

Muscle development

I am unable to identify the presence of any cranial muscle tissue in larvae at 1 dph (stage A, 2.5 mm TL), even though the trunk myotomes and heart muscles are differentiated (Fig. 5-2A). At 2 dph (stage A, 2.5 mm TL), all six components of the extraocular muscles (superior oblique, inferior oblique, superior rectus, inferior rectus, medial rectus, and lateral rectus) are weakly stained, although the origin and insertion are not clear (Fig. 5-2B). The adductor mandibulae A1, levator arcus palatini, adductor arcus palatini, intermandibularis posterior, interhyoideus, and sternohyoideus are weakly stained in the head region (Fig. 5-2B, C). In the body, the hypaxialis appears to be growing rostrally (Fig. 5-2B). The pectoral fin muscles are also detected, and appear as two muscle fibre masses (Fig. 5-2B). The mouth has not yet shifted anteriorly and is not open. At 3 dph (stage B, 2.6 mm TL), the extraocular muscles are clearly visible. In addition, the intermandibularis anterior, the adductor mandibulae A2, and the complex of the adductor operculi and the adductor hyomandibulae has also developed (Fig. 5-2D, E). The mouth shifts anteriorly and is open at this stage. In the body region, a hypaxial muscle is attached to the sixth myotome and inserts on the posteroventral face of the cleithrum, opposite to the originating site of the sternohyoideus (Fig. 5-2D). At 5 dph (stage B, 2.8 mm TL), the hyohyoideus, obliqui ventralis, transversus ventralis, larval branchial levators, pharyngoclavicularis externus, but not the levatores interni, are detected (Fig. 5-2F, G). At 9 dph (stage B, 2.8 mm TL), the adductor mandibulae Aω, levator internus, and protractor pectoralis are first detected (Fig. 5-3A, B). In the body region, the hypaxial muscles increase in number and cover the abdominal region. The muscles are attached to the seventh to the ninth myotomes (Fig. 5-3A). At 12 dph (stage C, 3.4 mm TL), the pharyngoclavicularis internus is visible (Fig. 5-3C). The larval branchial levator 2 has thinned and is atrophying (Fig. 5-3C). At 16 dph (stage D, 4.4 mm TL), larval branchial levators 2 and 3 have disappeared completely and the levatores externi have developed in their place to control the branchial arches (Fig. 5-3D, E). In addition, the levator operculi has developed (Fig. 5-3E). In the dorsal region of the body, the muscles controlling the dorsal fin have developed (Fig. 5-3D), coinciding with development of the dorsal-fin spines. On the ventral side of the body, the muscles

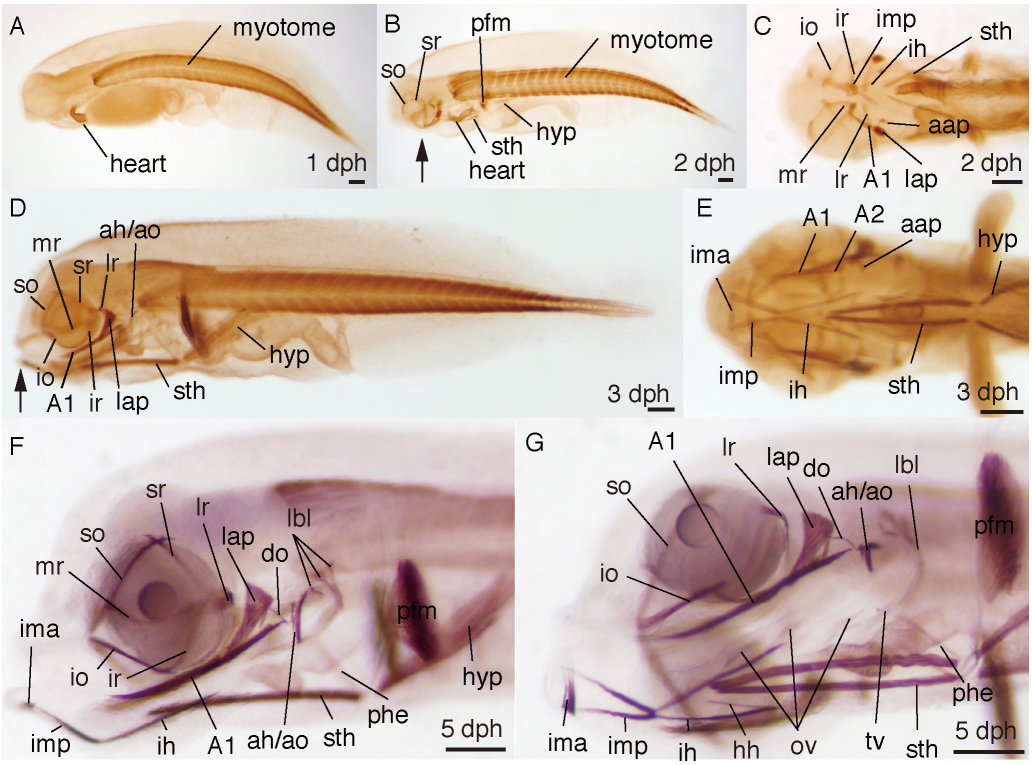

Figure 5-2 Larval musculature in the seven-band grouper head and trunk regions at 1–5 dph. Muscles were labelled with anti-myosin antibody. (A) Lateral view of the musculature at 1 dph. (B) Lateral view of the musculature at 2 dph. The black arrow indicates the position of the mouth. (C) Ventral view of the musculature at 2 dph. (D) Lateral view of the musculature at 3 dph. The black arrow indicates the position of the mouth. (E) Ventral view of the musculature at 3 dph. (F) Lateral view of the cranial musculature at 5 dph. (G) Ventrolateral view of the cranial musculature at 5 dph. aap, adductor arcus palatini; ah; adductor hyomandibulae, ao; adductor operculi; A1, adductor mandibulae A1; A2, adductor mandibulae A2; do, dilatator operculi; hh, hyohyoidei; hyp, hypaxialis; ih, interhyoideus; ima, intermandibularis anterior; imp, intermandibularis posterior; io, inferior oblique; ir, inferior rectus; lap, levator arcus palatini; lbl, larval branchial levator; lr, lateral rectus; mr, medial rectus; ov, obliqui ventrales; pfm, pectoral fin muscle; phe, pharyngoclavicularis externus; so, superior oblique; sr, superior rectus; sth, sternohyoideus; tv, transversus ventralis. Scale bar = 0.1 mm

controlling the pelvic fins are developing (Fig. 5-3D). At 20 dph (stage D, 4.7 mm TL), the rectus communis and obliquus posterior have developed (Fig. 5-3F, G). At 25 dph (stage E, 5.7 mm TL), several myotome groups are partially extended from the trunk in the caudal region (Fig. 5-3H). These muscles are destined to become the caudal fin muscles during later stages of development. At 28 dph (stage F, 8.9 mm TL), the adductor mandibulae A2 is visible as a thin rectangle (Fig. 5-3I).

Table 5-1. Timing of cranial muscle development in the seven-band grouper

	1dph	2dph	3dph	5dph	9dph	12dph	16dph	20dph	25dph	28dph
Muscles of the eye										
Superior oblique	×	○	○	○	○	○	○	○	○	○
Inferior oblique	×	○	○	○	○	○	○	○	○	○
Superior rectus	×	○	○	○	○	○	○	○	○	○
Inferior rectus	×	○	○	○	○	○	○	○	○	○
Medial rectus	×	○	○	○	○	○	○	○	○	○
Lateral rectus	×	○	○	○	○	○	○	○	○	○
Muscles of the cheek										
Adductor mandibulae	×	○	○	○	○	○	○	○	○	○
Levator arcus palatini	×	○	○	○	○	○	○	○	○	○
Dilatator operculi	×	×	×	○	○	○	○	○	○	○
Levator operculi	×	×	×	×	×	×	○	○	○	○
Adductor arcus palatini	×	○	○	○	○	○	○	○	○	○
Adductor operculi	×	×	○	○	○	○	○	○	○	○
Adductor hyomandibulae	×	×	○	○	○	○	○	○	○	○
Muscles serving the ventral surface of the head										
Intermandibularis anterior	×	×	○	○	○	○	○	○	○	○
Intermandibularis posterior	×	○	○	○	○	○	○	○	○	○
Interhyoideus	×	○	○	○	○	○	○	○	○	○
Hyohyoideus	×	×	×	○	○	○	○	○	○	○
Muscles serving the dorsal parts of the branchial arches										
Larval branchial levators	×	×	×	○	○	○	-*	-*	-*	-*
Levatores externi	×	×	×	×	×	○	○	○	○	○
Levatores interni	×	×	×	×	○(lbl1)	○(lbl1)	○	○	○	○
Levator posterior	×	×	×	○(lbl4&5)	○(lbl4&5)	○(lbl4&5)	○	○	○	○
Obliqui dorsales	×	×	×	×	×	×	○	○	○	○
Obliquus posterior	×	×	×	×	×	×	×	○	○	○

Adductores	×	×	×	×	×	×	×	○	○	○
Retractor dorsalis	×	×	×	×	×	×	×	×	×	○
Interbranchiales	×	×	×	×	×	×	×	○	○	○
Muscles serving the ventral parts of the branchial arches										
Sphincter oesophagi	×	×	×	×	○	○	○	○	○	○
Obliqui ventrales	×	×	×	○	○	○	○	○	○	○
Transversi ventrales	×	×	×	○	○	○	○	○	○	○
Rectus communis	×	×	×	×	×	×	×	×	○	○
Recti ventrales	×	×	×	×	×	×	×	○	○	○
Muscles between the pectoral girdle and the skull, hyoid, and branchial arches										
Sternohyoideus	×	○	○	○	○	○	○	○	○	○
Pharyngoclavicularis externus	×	×	×	○	○	○	○	○	○	○
Pharyngoclavicularis internus	×	×	×	×	×	×	○	○	○	○
Protractor pectoralis	×	×	×	○	○	○	○	○	○	○
Levator pectoralis	×	×	×	×	×	×	×	○	○	○

×, no muscle fibers; ○, differentiated muscle fibers; ○(lbl1), detected as a larval branchial levator I; ○(lbl4&5), detected as a larval branchial levator IV and V

-* After 16 dph, I use the terms the “levator internus I” and the “levator posterior” instead of the “larval branchial levator I” and the “larval branchial levator IV and V ”, respectively.

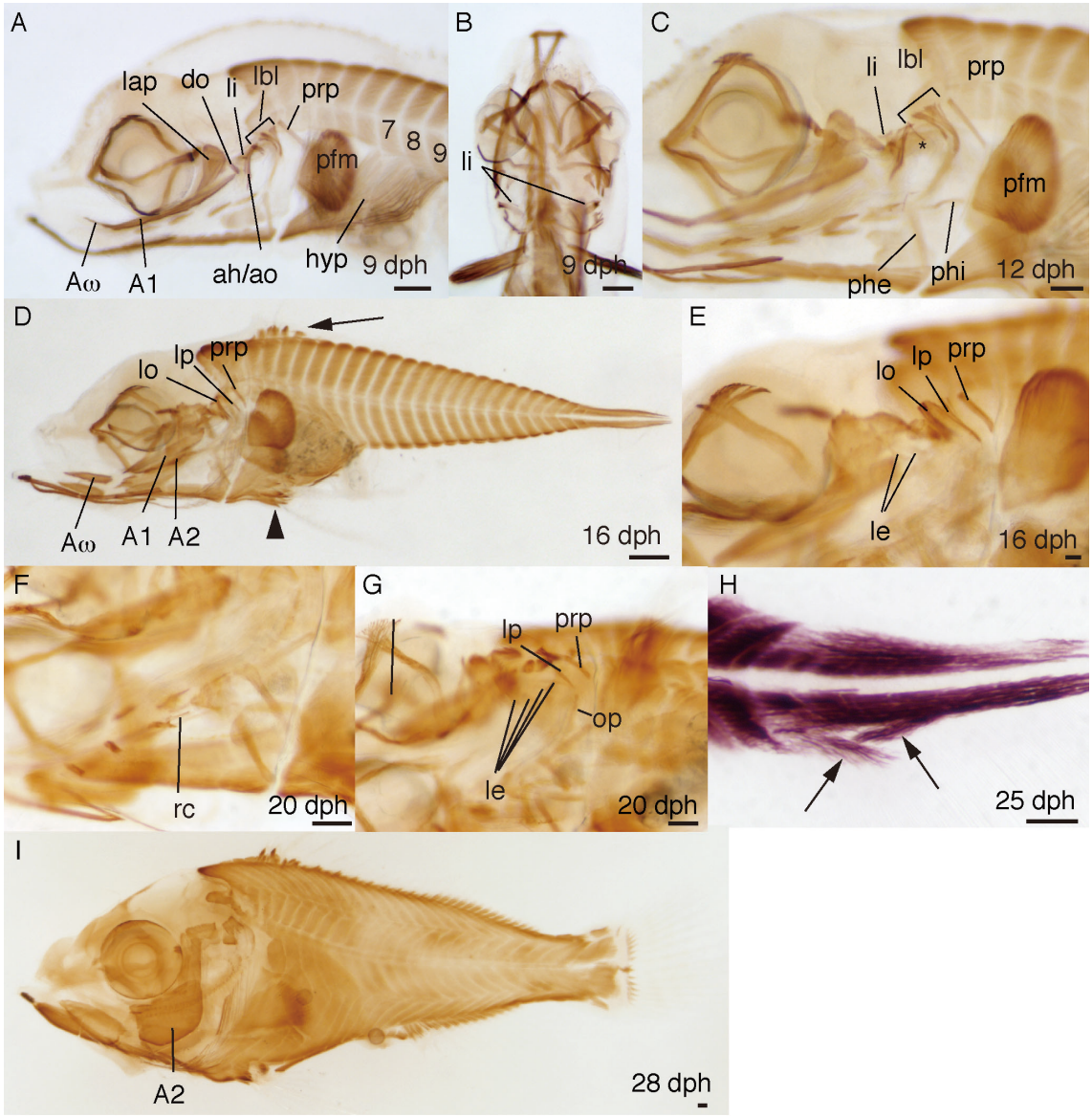

Figure 5-3 Larval musculature in the seven-band grouper head and trunk regions between 9–28 dph. Muscles were labelled with anti-myosin antibody. (A) Lateral view of the cranial musculature at 9 dph. The figures show the number of myotomes. (B) Dorsal view of the cranial musculature at 9 dph. (C) Lateral view of the cranial musculature at 12 dph. The asterisk indicates the atrophying larval branchial levator 2. (D) Lateral view of the musculature at 16 dph. The black arrow indicates the location of the dorsal fin muscles. The black arrowhead indicates the pelvic fin muscles. (E) Ventrolateral view of the cranial musculature at 16 dph. (F) Ventrolateral view of the musculature at 20 dph, focusing on the rectus communis. (G) Ventrolateral view of the musculature at 20 dph, focusing on the branchial muscles. (H) Lateral view of the caudal musculature at 25 dph. The black arrows indicate the muscles that extend from the ventral myotome. (I) Lateral view of the musculature at 28 dph. ah; adductor hyomandibulae, ao; adductor operculi; A1, adductor mandibulae A1; A2, adductor mandibulae A2; Aω, adductor mandibulae Aω; do, dilatator operculi; hyp, hypaxialis; lap, levator arcus palatini; lbl, larval branchial levator; le, levator externus; li, levator internus; lo, levator operculi; lp, levator posterior; op, obliquus posterior; pfm, pectoral fin muscle; phe, pharyngoclavicularis externus; phi, pharyngoclavicularis internus; prp, protractor pectoralis. rc, rectus communis; tv, transversus ventralis. Scale bar = 0.1 mm

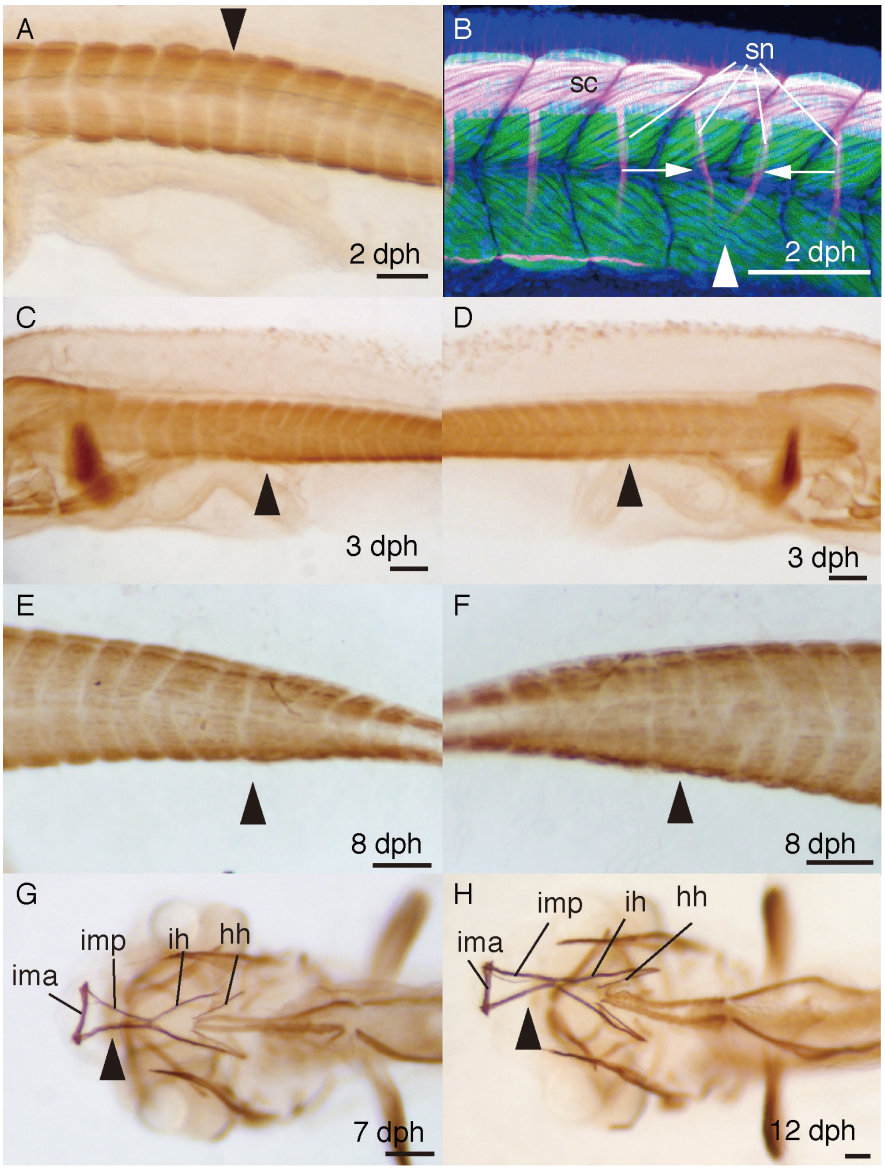

Figure 5-4 Muscular and nervous abnormalities in the seven-band grouper head and trunk regions between 2–12 dph. Muscles were labelled with anti-myosin antibody. Nerves were labelled with anti-acetylated tubulin antibody. (A) Lateral view of the trunk musculature 2 dph. Black arrowhead shows the position of muscular fusion at the dorsal side of body. (B) Lateral view of the trunk musculature and spinal nerves at 2 dph. White arrowhead shows the position of muscular fusion at the ventral side of body. White arrows show the spinal nerves which are bent. (C) Lateral view of the left trunk musculature at 3 dph. Black arrowhead shows the position of muscular disorder. (D) Lateral view of the right trunk musculature of the individual in (C). Black arrowhead shows the position where there is the muscular disorder at the left side. There is no muscular disorder in contrast with the left side. (E) Lateral view of the left trunk musculature at 8 dph. Black arrowhead shows the position of muscular disorder. (F) Lateral view of the right trunk musculature of the individual in (E). Black arrowhead shows the position of muscular disorder, which is the same position at the left side. (G) Ventral view of the cranial musculature at 7 dph. (H) Ventral view of the cranial musculature at 12 dph. hh, hyohyoidei; ih, interhyoideus; ima, intermandibularis anterior; imp, intermandibularis posterior. sc, spinal cord; sn, spinal nerve. Scale bar = 0.1 mm

Muscular malformations

I observed signs of fusion and disorder of muscles in the body musculature of several individuals. The phenotypes and location of the abnormalities differed between individuals (Figs. 4A-F). For example, the dorsal section of the body muscles were fused in a 2.5 mm TL stage A larva at 2 dph (Fig. 5-4A), whereas the ventral section of the body muscles were fused in another individual of the same size and age (Fig. 5-4B). In another instance, I observed disorder and fusion extending over four myotomes in a 2.5 mm stage B larva at 3 dph (Fig. 5-4C). Some disorders and fusion were visible only on one side of the body (Fig. 5-4C, D), while others were visible on both sides (Fig. 5-4E, F). In one individual (2 dph, stage A, 2.5 mm TL), the spinal nerves were abnormally positioned (i.e., bent) but had normal segmentation (Fig. 5-4B). In addition, the intermandibulae anterior and posterior and interhyoideus were abnormal in two individuals, one at 7 dph (stage B, 2.5 mm TL) and the other at 12 dph (stage C, 3.1 mm TL) (Fig. 5-4G, H). These muscles were thinner than those observed in normal larvae. I did not observe any abnormalities after 12 dph, except in one individual.

Discussion

The muscle development of seven-band grouper is very similar to that of Japanese flounder, although these two fish belong to different orders. One noteworthy difference between the seven-band grouper and in the Japanese flounder is that the development of the levator internus 1 occurs at a later stage in the former (6 days after first feeding vs. prior to first feeding, respectively). The levatores interni generally originates medial to the levatores externi on the lateral wall of the cranial vault and inserts onto the dorsal face of the second and third pharyngobranchials (Winterbottom, 1974; Stiassny, 2000). The levatores interni function primarily to adduct the upper pharyngeal jaw. However, the pharyngeal jaw is absent during the early larval stages. In Japanese flounder, the levator internus 1 (larval branchial levator 1) is supposed to pull the infrapharyngobranchials, as a single plate, against the larval branchial levators 2–5 during the early larval stages. Being the only muscles to adduct the branchial arches, they are thought to play a role in the expansion of the buccal chamber, a process that is critical for food intake during this stage. The effect of this delay in the timing of the

development of the levator internus 1 during early larval stages on feeding in the seven-band grouper is still unknown.

Based on variation in the pattern of the abnormal musculature, I hypothesized that multiple factors contribute to the development of abnormal musculature in the seven-band grouper (Fig. 5-4A-H). The occurrence of abnormal musculature on both sides of the same myotome indicates that the process was likely initiated at the somite stage during development of the myotome, and prior to first feeding. Thus, exposure to hypoxia and/or poor egg quality might have been contributing factors.

The occurrence of hypoxia during embryogenesis plays a role in inducing muscular abnormality in sea bream *Pagrus major* (Temminck and Schlegel) (Hattori *et al*.., 2004; Sawada *et al*., 2006b). Hypoxia can occur when the pelagic eggs are incubated at high densities in a rearing tank. Under these conditions, unless there is good mixing of the water column the eggs float to the surface, forming a dense layer in which the oxygen levels become depleted (Sawada *et al*., 2006b). The pelagic eggs of the seven-band grouper are typically incubated at high densities and are only gently aerated to prevent physical damage to eggs. These conditions may lead to hypoxia.

Conversely, egg quality affects mortality rates during the embryonic and larval stages and may also play a role in inducing embryonic and larval malformation (Kjørsvik *et al*., 1990; Brooks *et al*., 1997; Bromage *et al*., 1992; Bromage *et al*., 2001). In the seven band grouper, indices of egg quality, such as hatching rate and survival, are unstable (Tsuchihashi *et al*., 2003). Therefore, it is not possible to rule out poor egg quality as having an effect on musculature development.

The possible causes of abnormal musculature after first feeding include starvation and excess dietary docosahexaenoic acid (DHA) content. Protein degradation and separation of muscle fibres occur during starvation (Gisbert *et al*., 2008). However, the disorder and fusion observed in the trunk muscle of my sample does not reflect protein degradation or separation of muscle fibres (Fig. 5-4A-F); hence, these observed abnormalities cannot have been caused by starvation. In contrast, the abnormalities in the jaw are likely to be the result of protein degradation and, to some extent, separation of muscle fibres (Fig. 5-4H). Thus, my data suggest that starvation may be the cause of abnormalities in the jaw. Interestingly, an increase in dietary DHA content was associated with a dramatic increase in the incidence of muscular lesions in European sea bass *Dicentrarchus labrax* (Betancor *et al*., 2011; Betancor *et al*., 2012). The rotifers

standardly fed to seven-band grouper are also typically enriched with DHA using freshwater *Chlorella*; however, there is currently no information on the optimal levels of dietary DHA during early development for this species.

Vertebral deformities in artificially cultured fish have been described for many species. These deformities are caused by a number of factors, including temperature, velocity, salinity, feed, and the failure of the swim bladder to inflate (Dedi *et al*., 1995; Divanach *et al*., 1997; Takeuchi *et al*., 1998; Trotter *et al*., 2001; Kihara *et al*., 2002). However, little is known about the link between muscle abnormality and vertebral deformities. If the abnormal musculature of the trunk develops as a result of abnormal somitogenesis (described above), there is a potential for increased risk of developing vertebral deformities in seven-band grouper. This is because both the myotome and vertebral column are derived from the same somites (Morin-Kensicki *et al*., 2002). This phenomenon has been documented previously in sea bream *Pagrus major* (Temminck and Schlegel). In the sea bream, the occurrence of hypoxia during somitogenesis induces somatic disturbances and vertebral column defects (Hattori *et al*., 2004; Sawada *et al*., 2006b). I observed disorder and fusion only on one side of the body in some individuals. Vertebral deformities may also be induced by abnormal contraction of the abnormal musculature itself, a process which exerts an unbalanced force on the vertebral column in these individuals.

I did not observe abnormal musculature in the larvae after 12 dph, except in a single individual. Deformity can significantly affect mortality rate (Koumoundouros *et al*., 2002; Czesny *et al*., 2005). Therefore, this observation raises the possibility that the larvae that did exhibit abnormal musculature died by 12 dph, probably because of impaired swimming and feeding ability. Early mortality and malformation represent two of the largest barriers to mass larviculture of marine fishes. Given this, a number of researchers have investigated the causes of early mortality during larviculture and have documented a range of factors that contribute to the problem. Recognition of normal patterns of development and the ability to detect developmental defects provide a means of documenting conditions that improve larval survival and development. Such an approach can also be used to compare specimens from different egg batches. For example, poor egg quality or sub-optimal environmental conditions may be detected by monitoring for muscle abnormalities. This approach allows for rapid adjustment of rearing conditions.

CHAPTER VI Effect of temperature, hypoxia, and disinfection with ozonated seawater during somitogenesis on muscular development of the trunk in larval seven-band grouper, *Epinephelus septemfasciatus* (Thunberg)

I documented the existence of larvae with abnormal trunk muscles at two dph, prior to first feeding in the chapter V. In addition, some larvae had abnormal musculature on both sides of the same myotome. Together, these observations suggest that the abnormal development of the trunk muscles in the seven-band grouper larvae begins during somitogenesis, because somites are bilaterally paired blocks of mesoderm that form along the anterior-posterior axis of the developing embryo during somitogenesis, and give rise to myotomes. Environmental factors such as rearing temperature and oxygen concentration or intrinsic factors such as egg quality and/or genetic factors likely influence the rate of deformities. However, the mechanism(s) causing abnormal muscle development are poorly understood.

Embryonic development in teleosts, including muscular development, is influenced by environmental conditions, particularly temperature and dissolved oxygen (DO) concentrations. The rearing temperature directly and indirectly (via the brain) determines the rate of myogenesis, the composition of sub-cellular organelles, patterns of gene expression, and the number and size distribution of muscle fibres (reviewed in Johnston, 2006). Acute temperature changes of 9.5–13.5 °C during somitogenesis cause somitic segmental disturbance in zebrafish characterized by displacement of the borders of the affected myotomes (Roy *et al*., 1999; Kimmel *et al*., 1988). The muscle fibres in these segments are sometimes too short, or too long, and sometimes not correctly aligned. Similarly, though it is unclear how DO concentrations affect myogenesis, the occurrence of hypoxia (10-16.6% saturation) during somitogenesis also induces myogenic segmental disturbances in red sea bream *Pagrus major*, amberjack *Seriola dumerili* (Hattori *et al*., 2004; Sawada *et al*., 2006a; Sawada *et al*., 2006b). Hence it is possible that acute temperature changes and hypoxia during somitogenesis can cause somatic segmental disturbance in seven-band grouper. Given the uncertainties regarding the influence of environmental factors on somitogenesis, this chapter is focussed on elucidating these effects during juvenile production.

Based on observations in artificially cultured seven-band grouper larvae

during somitogenesis in the chapter V, exposure to changes in temperature, hypoxia or disinfection with ozonated seawater are strong candidates for causing the development of abnormal musculature of the trunk. In Japan, the juvenile production process for seven-band grouper typically involves holding fertilized eggs temporarily in an indoor ~1000 l tank with temperature controlled running seawater until they reach the somite stage. The eggs are then disinfected with ozonated seawater to prevent viral nervous necrosis (Teruya *et al*., 2008), and transferred into a large-scale rearing tank for mass production (Teruya *et al*., 2008). During this process, the seawater temperature cannot be strictly controlled in the temporary tanks, which are at ambient room temperature, or during the transfer between the temporary and large-scale tanks (range: ±1 °C). In addition, because the fertilized eggs are believed to be susceptible to physical stress, the temporary tank is typically only weakly aerated to minimize turbulence. Hypoxia can occur when the pelagic eggs are incubated at high densities with weak aeration in a small tank. Under these conditions, unless there is good mixing of the water column, the eggs float to the surface forming a dense layer in which the oxygen levels become too low. For example, the eggs of red sea bream float to the surface forming a dense layer of 18 mm thickness in which the oxygen levels decrease to ~3.7% after 10 minutes (Sawada *et al*., 2006b). This acute hypoxia induces muscular abnormality in red sea bream (Sawada *et al*., 2006b).

Although ozonated seawater is effective at inactivating nervous necrosis virus, it is also hazardous to embryos (Arimoto *et al*., 1996; Grotmol and Totland, 2000; Tsuchihashi *et al*., 2002). Exposure to ozonated seawater can delay hatching and reduce hatching rates. However, it is unknown whether muscular development is also affected.

In this chapter, I determine the effects of temperature, hypoxia, and exposure to ozonated seawater at environmentally realistic levels during somitogenesis on muscular development of the trunk in larval seven-band grouper.

Materials and methods

Preparation of eggs

Seven-band grouper eggs were obtained by artificial insemination as described in the chapter V. The hatching rate was 92.6%. The fertilized eggs were held in a 1000 l tank

with running seawater (21.6 °C) until the start of each experiment.

Effect of temperature

Fertilized eggs were transferred into a 48-well plate (Greiner bio-one) at 10 h post-fertilization (hpf). Each well contained 1 egg in 1 ml of sea water (22 °C) supplemented with 50000 IU/l of penicillin G (Wako), 0.05 g/l of streptomycin (Wako), and 0.0001% of bovine serum albumin (Wako). The plates were placed in a chamber containing paper soaked in distilled water to maintain humidity and the chambers were then placed in an incubator. The air in each chamber was exchanged daily. The temperature in each chamber was altered by moving the plates between two incubators that were maintained at 22 and 24 °C (Table 6-1). The eggs were divided into five groups (N= 48 eggs/group). Group 1 was maintained at 22 °C throughout the experiment. Prior to somitogenesis, the eggs in groups 2–5 were initially incubated at 22 °C. The eggs in group 2 were subsequently incubated at 24 °C for 3 h during the early somite stage (20 hpf) then at 22 °C until the end of experiment (92 hpf). The eggs in group 3 were incubated at 24 °C from early somitogenesis (20 hpf) to the end of the experiment. Groups 4 and 5 were exposed to the same temperature regimes as groups 2 and 3, but the change in temperature occurred at the mid-somite stage (24 hpf). All groups were performed in triplicate.

Effect of disinfection with ozonated seawater

Ozonated seawater was generated using a corona discharge ozone generator ESF-050 (Ebara). The concentration of total residual oxidants (TROs) was measured using a spectrophotometer DR-2010 (Hach) following the method of Mimura *et al*. (1999). A total of 500 - 1000 eggs were treated with ozonated seawater (0.3 mg TROs/l) for a total of 1 minute using three consecutive 20 l containers (treatment time per container = 10, 20, and 30 s). The eggs were exposed to ozonated seawater during the early (treatment group 1: 20 hpf) or mid- (treatment group 2: 24 hpf) somite stages. After disinfection, the eggs were rinsed twice in natural seawater (1 min/rinse). The control for each treatment group was treated in the same manner although natural seawater was substituted for ozonated seawater. All groups were performed in triplicate (Table 6-2). The treated eggs were transferred to a 500 ml airtight container containing 400 ml

natural seawater and kept in an incubator at 22 °C until the end of the experiment (92 hpf).

Effects of dissolved oxygen concentration

The seawater DO concentration was manipulated by nitrogen gas aeration. Oxygen levels were measured with an oxygen meter Oxi 3205 (WTW). A total of 500 – 1000 eggs per group were treated using a 500 ml airtight container containing 400 ml seawater. Treatment group 1 consisted of eggs that were exposed to hypoxia (22 % saturation) during the early somite stage (20 hpf) for 4 h. The eggs were then placed back into natural seawater (97% saturation) and held until the end of the experiment (92 hpf). Treatment group 2 consisted of eggs that were exposed to hypoxia (14 % saturation) during the mid-somite stage (24 hpf) for 4 h. The control for each treatment group was treated in the same manner although natural seawater was substituted for low DO seawater. All groups were performed in triplicate (Table 6-3). The treated eggs were transferred to a 500 ml airtight container containing 400 ml natural seawater and kept in an incubator at 22 °C until the end of experiment (92 hpf).

Immunohistochemistry and myotome observation

At two dph (92 hpf), the larvae were anesthetized with 3-aminobenzoic acid ethyl ester (Sigma-Aldrich) then fixed in 4% paraformaldehyde in phosphate buffered saline containing 0.1% Tween 20 (PBST), rinsed in PBST, dehydrated in a graded series of methanol (25, 50, 75, and 100 %), and stored at –20 °C for immunohistochemistry. The larvae were prepared for whole mount immunohistochemical staining with anti-myosin antibody A4. 1025 (Millipore) following the methods described in the chapter II. After staining, the samples were observed using a MZFL microscope (Leica) equipped with a Combi III (Leica) or Eclipse 90i digital microscope (Nikon). Normal 2 dph-larvae have v-shaped myotomes and myosepta, and a straight horizontal myoseptum (Fig. 6-1A). The vertices of the V-shaped myosepta are located along a straight horizontal myoseptum. Abnormal larvae have myosepta or horizontal myosepta that are absent, or vertices of V-shaped myosepta that are not located on the horizontal myoseptum (Fig. 6-1B). The proportion and frequency of abnormal larvae was calculated using 90 randomly selected specimens per treatment (30 per triplicate).

To evaluate the effect of DO concentration on the location of deformities, the

location along the trunk at which abnormal musculature was present during the early and mid-somite stage, was documented in 120 randomly selected specimens from both treatment groups 1 and 2.

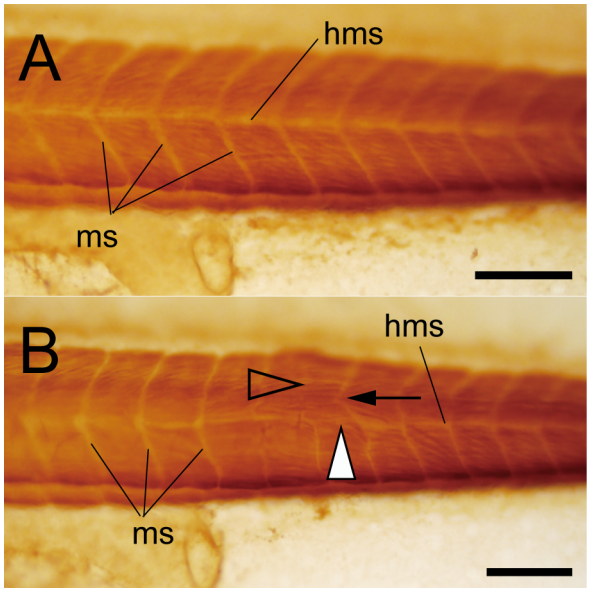

Figure 6-1 Photographs of seven-band grouper larvae trunk stained with anti-myosin antibody showing somitic defects. All larvae are shown with the anterior to the left and dorsal towards the top of page. (A) A normal larva. The vertices of V-shaped myosepta are all located on the straight horizontal myoseptum. (B) A larva exhibiting somitic defects following exposure to hypoxia. The arrow indicates the location of the abnormal myoseptum. The arrowhead indicates the location at which the myoseptum is absent. The white arrowhead indicates the location at which the horizontal myoseptum is absent. ms, myoseptum; hms, horizontal myoseptum. Scale bar = 100 μm.

Statistics

Differences between the control and treatment groups in the DO experiment and ozone disinfection experiment were determined using a G-test modified by William's correction. The G-test modified by William's correction was also used to analyse the effect of temperatures on malformation incidence. Differences with a $P < 0.05$ were considered significant.

Results

Effect of thermal regimes on muscle development

The mean (± S.E.) proportion of abnormal fish was 0.0±0%, 1.1±1.9%, 0.0±0%,

0.0±0%, and 1.1±1.9% in groups 1, 2, 3, 4 and 5, respectively. Thermal regimes during somitogenesis had no effect on the frequency of abnormality (G= 3.65, df=4, P>0.05) (Table 6-1).

Effect of disinfection with ozonated seawater on muscle development

The mean (± S.E.) proportion of abnormal fish was 0.0±0%, 0.0±0%, 3.3±5.8%, and 0.0±0% in control group 1, treatment group 1, control group 2, and treatment group 2, respectively. Disinfection with ozonated seawater during the early and mid-somite stages had no effect on the frequency of abnormality (early somite stage; G=0, df=1, P>0.05, mid-somite stage; G=3.61, df=1, P>0.05) (Table 6-2).

Effect of hypoxia on muscle development

The mean (± S.E.) proportion of abnormal fish was 0.0±0%, 48.9±36.7%, 0.0±0% and 47.8±38.6% in control group 1, treatment group 1, control group 2, and treatment group 2, respectively (Table 6-3). Exposure to low DO concentrations had a significant effect on the incidence of abnormalities during both the early and mid-somite stages (early somite stage; G=74.58, df=1, P<0.01, mid-somite stage; G=72.43, df=1, P< 0.01). All abnormal larvae had abnormalities on both sides of the trunk (Fig. 6-2A and B). The number of abnormal myotomes varied with each larva (Fig. 6-2C, D). The myotomal disturbances were localised in the region of myotomes 5–16 of larvae exposed to hypoxia during the early somite stage, with the majority of abnormalities occurring in the 11th myotome in treatment group 1 (Fig. 6-2E). Conversely, the myotomal disturbances were localized between myotomes 7–22 in larvae exposed to hypoxia during the mid-somite stage, and were most prevalent in the 13th myotome in treatment group 2 (Fig. 6-2E).

Table 6-1 Occurrence (count and % frequency) of abnormal seven-band grouper larvae in each triplicate (a, b, c) of groups of five different thermal regimes.

	N	A	total	% A	mean ± S.E. % A
Trt.1(a)	30	0	30	0.0	
Trt.1(b)	30	0	30	0.0	
Trt.1(c)	30	0	30	0.0	0.0±0
Trt.2(a)	29	1	30	3.3	
Trt.2(b)	30	0	30	0.0	
Trt.2(c)	30	0	30	0.0	1.1±1.9
Trt.3(a)	30	0	30	0.0	
Trt.3(b)	30	0	30	0.0	
Trt.3(c)	30	0	30	0.0	0.0±0
Trt.4(a)	30	0	30	0.0	
Trt.4(b)	30	0	30	0.0	
Trt.4(c)	30	0	30	0.0	0.0±0
Trt.5(a)	30	0	30	0.0	
Trt.5(b)	29	1	30	3.3	
Trt.5(c)	30	0	30	0.0	1.1±1.9

N, Number of normal larvae; A, Number of abnormal larvae

treatment 1 (trt.1: 22 °C), treatment 2 (trt.2: 22→24→22 °C during the early somite stage), treatment 3 (trt.3: 22→24 °C during the early somite stage), treatment 4 (trt.4: 22→24→22 °C during the mid-somite stage), treatment 5 (trt.5: 22→24 during the mid-somite stage).

Table 6-2 Effect of disinfection with ozonated seawater (0.3 mg TROs/l, 1 min) during the early (Exp. 1) or mid- (Exp. 2) somite stage on the occurrence (count and % frequency) of abnormal seven-band grouper larvae in each triplicate (a, b, c).

	N	A	total	% A	mean ± S.E. % A
Exp.1 control (a)	30	0	30	0.0	
Exp.1 control (b)	30	0	30	0.0	
Exp.1 control (c)	30	0	30	0.0	0.0±0
Exp.1 oxidants (a)	30	0	30	0.0	
Exp.1 oxidants (b)	30	0	30	0.0	
Exp.1 oxidants (c)	30	0	30	0.0	0.0±0
Exp.2 control (a)	27	3	30	10.0	
Exp.2 control (b)	30	0	30	0.0	
Exp.2 control (c)	30	0	30	0.0	3.3±5.8
Exp.2 oxidants (a)	30	0	30	0.0	
Exp.2 oxidants (b)	30	0	30	0.0	
Exp.2 oxidants (c)	30	0	30	0.0	0.0±0

N, Number of normal larvae; A, Number of abnormal larvae

The control groups for the respective experiments were treated in the same manner except normal seawater was substituted for the ozonated seawater.

Table 6-3 Effect of exposure to hypoxia during the early (Exp. 1: 22 % saturation) or mid- (Exp. 2: 14 % saturation) somite stage on the occurrence (count and % frequency) of abnormal seven-band grouper larvae in each triplicate (a, b, c).

	N	A	total	% A	mean± S.E.
Exp.1 control (a)	30	0	30	0.0	
Exp.1 control (b)	30	0	30	0.0	
Exp.1 control (c)	30	0	30	0.0	0±0%
Exp.1 hypoxia (a)	10	20	30	66.7	
Exp.1 hypoxia (b)	8	22	30	73.3	
Exp.1 hypoxia (c)	28	2	30	6.7	48.9±36.7%
Exp.2 control (a)	30	0	30	0.0	
Exp.2 control (b)	30	0	30	0.0	
Exp.2 control (c)	30	0	30	0.0	0±0%
Exp.2 hypoxia (a)	28	2	30	6.7	
Exp.2 hypoxia (b)	5	25	30	83.3	
Exp.2 hypoxia (c)	14	16	30	53.3	47.8±38.6%

N, normal muscle; A, abnormal muscle

The control groups for the respective experiments were treated in the same manner except natural seawater (97% saturation) was substituted for the low DO seawater

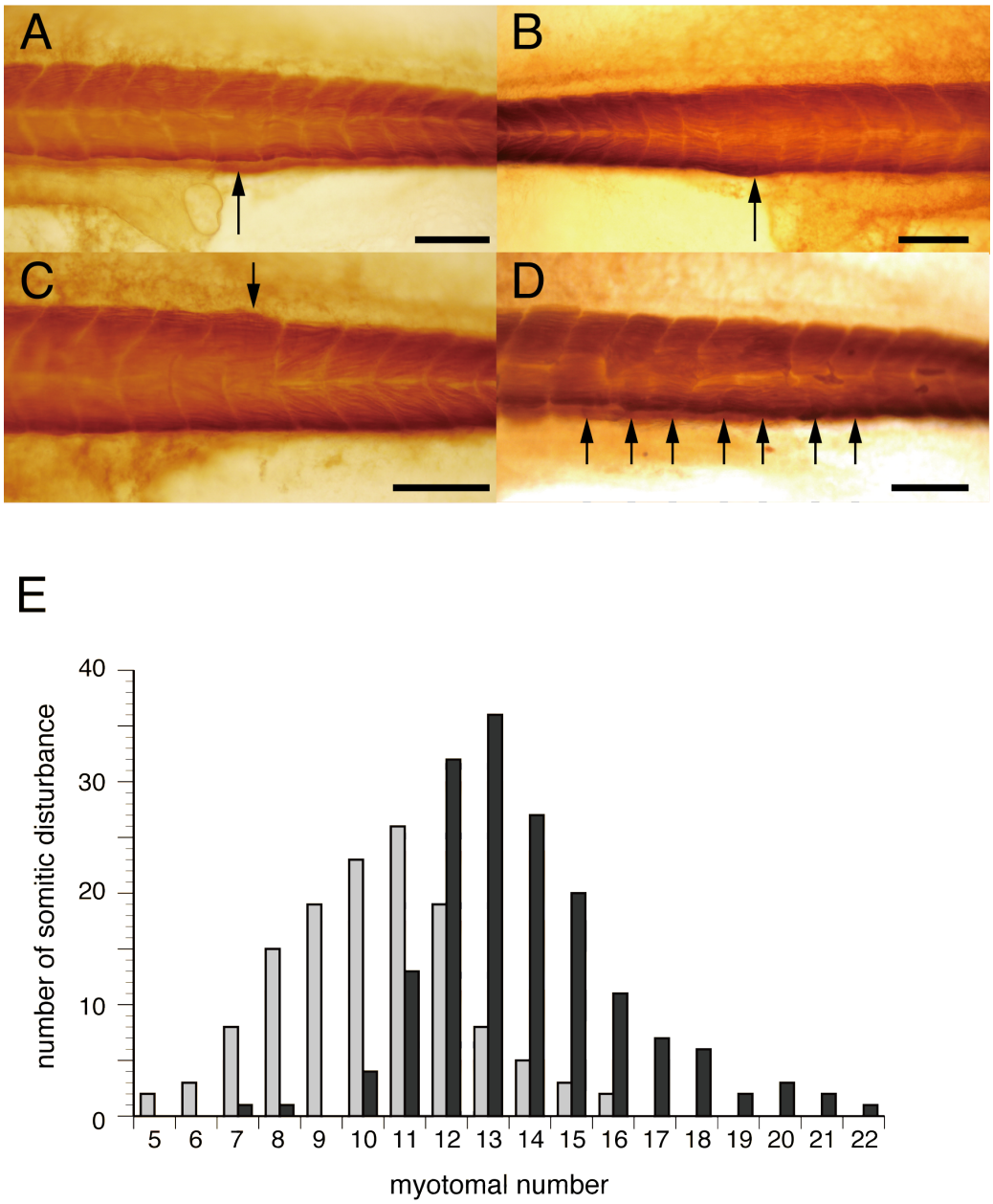

Figure 6-2 Muscular abnormalities caused by hypoxia in the seven-band grouper trunk regions. (A) Lateral view of the left trunk musculature. The black arrow indicates the position of muscular disorder. (B) Lateral view of the right trunk musculature of the individual in (A). The black arrow indicates the position of muscular disorder, which is the same position at the left side. (C) Lateral view of the trunk musculature. Two myotomes were fused at the dorsal side of myotomes (black arrow). (D) Lateral view of the trunk musculature. Seven myotomes exhibit muscular disorder (black arrows). (E) Distribution of somitic disturbances in seven-band grouper larvae exposed to hypoxia during the early somite stage (grey bars) and mid-somite stage (black bars). Scale bar = 100 μm.

Discussion

Levels of oxygen can vary dramatically in aquatic environments. Aquatic organisms, including fishes, have adapted accordingly to survive a wide range of oxygen concentrations, even during the embryonic stage. Under hypoxic conditions, fish exhibit changes in gene expression, and institute a variety of responses to hypoxia. These include shutting down of major energy-costly processes such as protein synthesis, and suppression of cell growth and proliferation (Padilla and Roth, 2001; Gracey *et al*., 2001; Ton *et al*., 2003; Kajimura *et al*., 2005; Terova *et al*., 2008). Under unfavourable hypoxic conditions that a fish cannot adapt to, these changes can lead to structural defects that affect the growth and survival of embryos (Hattori *et al*., 2004; Sawada *et al*., 2006a; Sawada *et al*., 2006b; Sawada *et al*., 2008; Sun *et al*., 2011). In this chapter, I demonstrated that exposure to hypoxia at environmentally realistic levels during somitogenesis can lead to abnormal muscle development in the trunk of seven-band grouper larvae. This is the first direct evidence linking exposure to hypoxia during somitogenesis and myogenic disturbances in *Serranidae*. These results highlight ways in which culturists can limit exposure of larvae to conditions that favour abnormal development, and thereby reduce the risk of mortality during juvenile production in seven-band grouper.

Hypoxia appears to induce malformation in muscular development in a range of fish species, and my results suggest that the embryos of seven-band grouper may have lower hypoxia tolerance than those of red sea bream and amberjack. Exposure to hypoxia during somitogenesis by nitrogen gas aeration, as in my experiments, plays a role in inducing muscular abnormality in red sea bream, amberjack, and striped jack (Hattori *et al*., 2004; Sawada *et al*., 2006a; Sawada *et al*., 2006b; Sawada *et al*., 2008). Of the seven-band grouper embryos that were exposed to low DO seawater (22% saturation) for 4 h, 48.9±36.7% had abnormal myotome development. In contrast, the embryos of red sea bream exposed to seawater with 25% saturation (22.5 °C) for 4 and 6 h had normal myotomes (Sawada *et al*., 2006b). Similarly, all amberjack embryos that were exposed to seawater with 23.5-25.5% saturation (19 °C) for 4 or 6 h exhibited normal myotome development (Sawada *et al*., 2006a).

Interestingly, the proportion of abnormal embryos produced following exposure to hypoxia (14% and 22% saturation) varied widely in seven-band grouper

(Table 6-3). I speculate that this is because unmeasured and uncontrolled environmental factors may also have influenced the results. For example, the concentration of dissolved carbon dioxide can affect the incidence of somatic disturbances in striped jack (Sawada *et al*., 2008). Exposure to hypercapnia (dissolved carbon dioxide concentration; 120 mg/l) during somitogenesis induces somatic disturbances but exposure to both hypercapnia and hypoxia during somitogenesis has a synergistic effect on somatic disturbances (Sawada *et al*., 2008). For example, exposure to hypoxia (25% saturation) and hypercapnia (concentration of dissolved carbon dioxide; 120mg/l) for 2.5 hours at 24 °C induces somatic disturbances in 100% of individuals, whereas hypoxia alone did not induce any disturbance. Although the concentrations of dissolved carbon dioxide were not investigated in this paper, the levels of dissolved carbon dioxide were not sufficient to induce any somitic disturbance in the absence of hypoxia because the abnormal rates of all control groups were 0% (Table 6-3). Thus, there is a need to discern not only the effect of hypoxia on muscle development at a wide range of DO concentrations and exposure times, but also to understand the synergistic effects of hypoxia and other environmental factors, including hypercapnia, in seven-band grouper.

The location of the myotomes that were affected by hypoxia varied with the timing of hypoxia treatment. The majority of abnormalities occurred in the 11th or 13th myotome in fish that were exposed during early and mid-somitogenesis, respectively. Three lines of evidence suggest that the development of abnormal myotomes is the result of somitic disturbance: 1) the abnormalities are induced in a stage specific manner during somitogenesis, 2) the abnormalities are induced on both sides of the myotome and 3) prior research in other vertebrates suggests somitic disturbances induce the abnormal development of myotomes. In addition, zebrafish mutants that develop defects during somitogenesis often have abnormal myotomes, an abnormal myoseptum, irregular primary motoneuron axon projections, and abnormal vertebrate (van Eeden *et al*., 1996). Taken together, these observations support my hypothesis that the occurrence of abnormal myotomes in larvae exposed to hypoxia are the result of somitic disturbances. Assuming this is true, there is also increased risk of larvae also having abnormal vertebral column development if they survive. This is because the somites give rise not only to skeletal muscle, but also to vertebrae and cartilage. Indeed, exposure to hypoxia during somitogenesis induces myogenic disturbances and vertebral column defects in other teleosts, such as red sea bream, amberjack, and striped jack

(Hattori *et al*., 2004; Sawada *et al*., 2006a; Sawada *et al*., 2008). The effects of hypoxia on somite formation and the underlying cellular and molecular mechanisms controlling this process in seven-band grouper embryos remain unknown. In mice, hypoxia disrupts FGF signalling, a trigger that induces the molecular oscillation system to promote formation of periodic somite segmentation in the presomitic mesoderm, leading to a failure of embryonic somitogenesis (Sparrow *et al*., 2012). Sparrow *et al*. (2012) also demonstrated that the degree of disruption is affected by a combination of genetic background and hypoxia. Further research is needed to determine how hypoxia affects somite formations in teleost embryos.

The maximum changes in temperature (2 °C) that occur during seven-band grouper mass production using temperature controlled running seawater did not increase the incidence of abnormalities of the trunk muscle. Rearing temperature is an important environmental variable influencing the rate of somitogenesis (Schroter *et al*., 2008) and the skeletal muscle phenotype of teleost fish (Johnston, 2006). Extreme temperature stress is recognized as a teratogenic factor that induces deformities during embryonic development in teleosts (Kimmel *et al*., 1988; Roy *et al*., 1999; Takle *et al*., 2005; Wargelius *et al*., 2005). Extreme changes in temperature (from 28.5 °C to 39–41 °C for 20 min) during somitogenesis, for example, are associated with increased somitic disturbance in zebrafish (Kimmel *et al*., 1988; Roy *et al*., 1999). Meanwhile, cellular mechanisms such as the heat-shock proteins act to minimize the damaging effects of thermal cellular stress in fish, even during the embryonic stage (Krone *et al*., 1997; Takle *et al*., 2005; Werner *et al*., 2007; Skjaerven *et al*., 2011). The induction of this protective mechanism against thermal stress by heat-shock proteins appears to prevent induction of abnormal development in the thermal experiment in this chapter. Although a more extreme change in temperature (10–12 °C) such as that tested in studies of zebrafish may induce somitic disturbances in this species, such variation is not typical during mass production.

Similarly, although the seven-band grouper embryos have low tolerance to ozonated seawater, for example the hatching rate is only 5% when exposed to ozone treatment at 0.5 mg TROs/l for 3 minutes (Tsuchihashi *et al*., 2002), the ozone treatment (0.3 mg TROs/l, 1 min) that is typically used in mass production had no negative effect on trunk muscle development in seven-band grouper larvae.

CHAPTER VII GENERAL DISCUSSION

Visualization of musculature using modified whole-mount immunostaining

Using a combination of potassium hydroxide, hydrogen peroxide, and trypsin to increase transparency, I was able to visualize the complete set of cranial muscles after whole mount immunostaining in four teleost species. This method allowed for the accurate identification of the larval cranial muscles. In addition to Japanese flounder, bamboo sole, greater amberjack, and seven-band grouper, I have successfully applied this immunohistochemical method to study a range of species, including Japanese amberjack *Seriola quinqueradiata*, Pacific bluefin tuna *Thunnus orientalis*, and Japanese eel *Anguilla japonica*. Further description of muscle development in other fish species using this method may allow for a better understanding of both the level of conservation in fish muscle development and the occurrence of unique and species specific muscle development processes.

This method renders the specimen more optically transparent when compared with previously reported whole mount immunostaining methods. However, both the new and old methods are limited in the sample thickness that can be visualized. Recently, new methods have been developed to render biological samples optically transparent, including Sca*l*e and CLARITY (Hama *et al*., 2011; Chung *et al*., 2013). It will be important to build on my modified whole-mount immunostaining method using these new approaches.

Similarity of muscle development in teleost fish larvae

There are a lot of similarities in muscles development among the four fishes, although these fishes belong to different orders of teleost. First, the eye muscles develop; next, all cheek muscles develop before first feeding. The muscles associated with the opercle develop gradually without relation to first feeding. The larval branchial levators regulate the branchial arches at first feeding. Later, the levatores externi and levator internus 2 develop and regulate the branchial arches, whereas larval branchial levator 2 and 3 atrophy. As a result, the larvae have the same branchial arch muscle composition as the adult.

The muscles required for feeding and respiration develop at this pre-flexion larval stage. Next, the dorsal, anal, pelvic and caudal fin muscles, which are required for

swimming, develop after pre-flexion larval stage. It is well known that changes in feeding and respiratory mechanisms occur during larval stages in fishes (Verraes, 1977; Otten 1982; Liem, 1991; Herbing *et al*., 1996a, b). Early in development, viscerocranial structures and functions are simple and nonintegrated, and respiration is cutaneous. During later ontogenetic stages, the opercular apparatus and levator operculi coupling occurs, facilitating the transition of cutaneous to branchial respiration. First-feeding larvae use a simple mechanism involving the hyoid-mandibule linkage to capture prey (ram feeding). During later ontogenetic stages, larvae capture prey using a more complex mechanism involving the hyoid- and opercular series-mandible linkages (suction feeding), thus becoming very efficient feeders. These reports were coincided with my observation; the levator operculi, dilatator operculi and adductores develop, and the muscle composition in the dorsal branchial arches changes to the adult form during pre-flexion larval stage.

Relationship between the larval branchial levators and the levatores externi, the levatores interni, and the levator posterior

I reported that (1) the larval branchial levators are distinct from the levatores externi. As larvae grow, the levatores externi and the levator internus 2 develop from the anterior region of the branchial arches; (2) larval branchial levator 1 appears equal to the levator internus 1; (3) larval branchial levator 4, and/or larval branchial levator 5, represent the levator posterior and (4) larval branchial levators 2 and 3, which are larval-specific muscles, atrophy soon after larval stages of development are complete.

Besides this study, there are only a few published reports that describe the development of the larval dorsal branchial muscles in zebrafish (e.g., Schilling & Kimmel, 1997; Hernandez *et al*., 2005). It remains unclear whether the larval branchial levators reported by me are homologous to the branchial levators identified in zebrafish. The anatomical term "branchial levator" was originally used in the myological description of larvae of zebrafish by Schilling & Kimmel (1997). These structures were not defined in the descriptive synonymy of Teleostei reported by Winterbottom (1974), or in the cranial muscle description reported by Edgeworth (1935). Although Schilling & Kimmel (1997) and Hernandez *et al*. (2005) described the morphology of the branchial levators (referring to them as termed branchial wall muscles) during development of zebrafish, the relationship between the branchial levators in larvae and

the levatores externi, levatores interni and levator posterior in adults remains poorly understood. In more recent anatomical studies focusing on the cranial muscles of adult fishes (Takata & Sasaki, 2005; Nakae & Sasaki, 2008), the terms levatores externi, levatores interni and levator posterior were used to describe the dorsal branchial muscles. Thus, the term branchial levators has previously been used only in the definition of larvae of zebrafish larvae.

Schilling & Kimmel (1997) define branchial levators as muscles that insert onto the ceratobranchial cartilages at 120 hpf, while Hernandez *et al*. (2005) define the branchial levators as muscles that insert onto the epibranchial elements at 6 dpf and 32 dpf in zebrafish. If the insertions of the branchial levators are translocated during development in zebrafish, the branchial levators at larval stage and levatores externi at adult stage are identical. That is, zebrafish may never have the muscles that are homologous to the larval branchial levators in Japanese flounder, bamboo sole, greater amberjack and seven-band grouper. Indeed, the position of the branchial levators in zebrafish is originally ventromedial to the adductor hyomandibulae and the adductor operculi. This topology is similar to that of in Japanese flounder, bamboo sole, greater amberjack and seven-band grouper after replacement. Additional study is required to precisely define branchial muscle development in other fishes, including zebrafish.

It is unclear why the larval branchial levators atrophy and the levatores externi subsequently develop. The positioning of the adductor hyomandibulae and the adductor operculi muscles resulting from this replacement appears advantageous, as the adductor hyomandibulae and the adductor operculi seem to act more effectively against the dilatator operculi and the levator operculi. In other words, replacing these muscles may be associated with development of the opercle and the appearance of the dilatator operculi and the levator operculi muscles to feed and respire more effectively.

Relationship between the levatores externi and the levator posterior

In teleosts, the levator posterior originates from one or more of the prootic, pterotic, epiotic, intercalary or exoccipital bones and usually inserts on some or all of epibranchial 4, ceratobranchial 5 and the cartilaginous remains of epibranchial 5 (Winterbottom, 1974). Although Edgeworth (1935) defines the levator posterior as the fifth levator externus, a later report by Winterbottom (1974) indicates that the levator posterior represents only the levator externus 5, only a part of the levator externus 4 or

actually a combination of these two muscles in some cases. In addition, the levator posterior is generally separated from the levator externus series by a distinct hiatus.

I found that the levator posterior and the levatores externi exhibited different origins. The levator posterior develops as part of the larval branchial levators prior to first feeding. The larval branchial levators 2 and 3 atrophy, and the majority of the posterior muscle mass of the larval branchial levators remains as the levator posterior. In other words, the insertion of the levator posterior may depend on which posterior muscle mass of the larval branchial levators remains during development. This hypothesis helps explain the variation of the insertion observed in the different fish species outlined above. In contrast, the levatores externi develop in the more anterior portion of the branchial region, located under the adductor hyomandibulae and the adductor operculi later. Based on these results, the levator posterior does not represent the levator externus 5, even though its function and approximate position may be identical to the levator externus 5. Considering the observation that the levator posterior does not represent the levator externus 5 in four species of fish that are taxonomically distinct from each other, there is a possibility that this is common in fish.

Visualization tool to identify muscle abnormalities

Early mortality and malformation represent two of the biggest barriers to mass larviculture of marine fishes. Given this, a number of researchers have investigated the causes of early mortality during larviculture and have documented a range of factors that contribute to the problem (Tsuchihashi *et al*, 2003; Tanaka *et al*., 2005; Sakakura *et al*., 2006; Sakakura *et al*., 2007a; Sakakura *et al*., 2007b; Teruya *et al*., 2008).

Recognition of normal patterns of development and detection of developmental defects can be used to improve larval rearing techniques through modification of environmental parameters (Koumoundouros *et al*., 2001; Sfakianakis *et al*., 2004; Sfakianakis *et al*., 2006; Cobcroft & Battaglene 2009; Georgakopoulou *et al*., 2010). Skeletal deformities are often used to evaluate the influence of environmental conditions because of the relative simplicity in visualizing skeletal structure.

In this study, I developed a method which was used to clearly visualize the musculature of larvae of the Japanese flounder, bamboo sole, greater amberjack, and seven-band grouper. The development of this method allows for the detection of abnormal cranial and axial muscles in larvae. This information can be used to improve

larval rearing techniques by modifying environmental conditions. Indeed, using this method, I demonstrated that hypoxia affects muscle development in seven-band grouper. Early detection of muscle abnormalities may allow for selective culling of a population, thereby eliminating waste of human resources, money, and time in raising abnormal fish to a sufficient size to allow examination. Additionally, such an approach can be used to compare specimens from different egg batches. For example, poor egg quality may be detected by monitoring of muscle abnormalities.

SUMMARY

Muscle development in the Japanese flounder *Paralichthys olivaceus* was investigated, focusing primarily on the cranial muscles, using a whole mount immunohistochemical staining method. It is well established that during the very early stages of morphogenesis, until 4 dph, muscles required for feeding develop. Later, between 8 and 16 dph, the muscle composition in the dorsal branchial arches changes to the adult form. I discovered the presence of larval-specific muscles in this ontogenetic period, termed the larval branchial levators 2 and 3, located in the dorsal branchial arches. The larval branchial levators 2 and 3 disappear during the course of development, whereas the others remain as levator internus 1 and levator posterior, which have also been described in adult fish. In place of these regressed muscles, the levatores externi and levator internus 2 develop and regulate the branchial arches. In addition, I found that the levator posterior, which is thought to represent the fifth levator externus, and the levatores externi exhibit different origins. I also found that at least a part of the caudal fin musculature develops from the trunk myotome.

Muscle development in the bamboo sole *Heteromycteris japonicus* was investigated, focusing primarily on the cranial muscles, using an improved whole mount immunohistochemical staining method. Larvae of bamboo sole were found to have larval branchial levators, but not all of them are retained in adults, a condition also seen in the Japanese flounder. In particular, larval branchial levators 2 and 3 disappear during the course of development, while 1 and 4 remain to become the levator internus 1 and levator posterior, which are well defined muscles in adults. In place of the atrophied muscles, levatores externi and levator internus 2 develop and regulate the branchial arches. The results show that the muscle composition in the dorsal branchial arches changes to the adult form before metamorphosis in the bamboo sole, as seen in the Japanese flounder, and this transformation may be common to all members of that group.

The presence of larval-specific muscles in the Japanese flounder and bamboo sole has been shown, but it is unclear whether larval-specific muscles are common to all fish or unique to flatfish. Muscle development in the greater amberjack *Seriola dumerili* was investigated, focusing primarily on the cranial muscles from 0 dph to 12 dph, using an improved whole mount immunohistochemical staining method. I found that the

muscles required for feeding develop by 3 dph, when the larvae begin to feed. Subsequently, muscle composition in the dorsal branchial arches changes to the adult form between 5–8 dph. At 8 dph, all the muscles required for feeding and respiration appear, whereas the dorsal, pelvic and caudal fin muscles required for swimming develop later. The results show that the muscle composition in the dorsal branchial arches changes to the adult form in the greater amberjack, as seen in the flatfish, and this transformation may be common to all members of teleost fishes.

I have documented muscle development in the seven-band grouper, *Epinephelus septemfasciatus*, focusing primarily on the cranial muscles from 0 dph to 28 dph, using a modified whole mount immunohistochemical staining method. The eye muscles developed first followed by the cheek muscles, which completed development prior to first feeding. The muscles associated with the opercle and the levator internus 1 developed gradually and were not linked to first feeding. Later, between 12 and 16 dph, the muscle composition in the dorsal branchial arches changed to the adult form. I observed a number of cultured larvae that exhibited abnormal musculature in the body and jaw. The results provide the first documentation of muscle development in larval seven-band grouper. This information can be used to detect abnormalities during development and provide a marker to assess the effect of changes in larval rearing techniques.

The cause of abnormal musculature on both sides of the same myotome in artificially cultured seven-band grouper *Epinephelus septemfasciatus* (Thunberg) larvae is unclear. I respectively evaluated the effects of three factors: changes in temperature (between 22 and 24 °C), disinfection with ozonated seawater (0.3 mg TROs/l, 1 min), and hypoxia (22 or 14 % saturation) during the early (20 h post-fertilization, hpf) and mid- (24 hpf) somite stages on trunk muscular development in larval seven-band grouper. The thermal regimes and disinfection with ozonated seawater had no effect on muscle development ($P>0.05$, G-test). In contrast, exposure to hypoxia during both the early and mid-somite stages increased the incidence of abnormal musculature in the trunk ($P<0.01$, G-test). These larvae have abnormal musculature on both sides of the trunk. In addition, the number of abnormal myotomes is different among these larvae. Exposure in the early and mid-somite stages resulted in the highest frequency of abnormalities in the 11th and 13th myotome, respectively. These results suggest that hypoxia during somitogenesis can lead to abnormal muscle development in the trunk of

artificially cultured seven-band grouper larva.

ACKNOWLEDGMENTS

The author expresses sincere gratitude to Dr. Yoh Yamashita, Dr. Tatsuya Sugawara, and Dr. Masatomo Tagawa, Kyoto University for their critical reading of the thesis.

The author wishes to express special thanks to Dr. Tohru Suzuki, Tohoku University, Dr. Satoshi Miwa, Dr. Masanori Okauchi, and Dr. Koichi Okuzawa, National Research Institute of Aquaculture (NRIA) for their insights, suggestions, and support.

The author sincerely thanks Dr. Tadahide Kurokawa, Tohoku National Fisheries Research Institute, for technical advice on immunohistochemistry, Dr. Kunio Sasaki of Kochi University, for expert guidance in Japanese flounder dissection, Dr. Takashi Yoshimatsu, Mie University, for technical advice on rotifer culture, Dr. Kazuhisa Teruya, Seikai National Fisheries Research Institute, for technical advice on larval culture, Dr. Tadahisa Seikai, Fukui Prefectural University, for technical advice on fish culture, Dr. Hisashi Hashimoto, Nagoya University, for technical advice on a variety of laboratory procedures, suggestions, and encouragement, Dr. Kiyoshi Kikuchi, The University of Tokyo, for discussion, Mr. Masaharu Tsuji and Dr. Yasushi Tsuchihashi, Mie Prefectural Science and Technology Promotion Center, Mr. Keiichi Hirasawa, Mr. Makoto Shirakashi, Dr. Shizumasa Onoue, Oita Prefectural Agriculture, and Mr. Yoichi Yamashita, Oita Prefecture Public Fisheries Corporation, for technical advice and suggestion, Mr. Hideyuki Shibahara, Tokyo University of Marine Science and Technology, for his technical assistance, and Ms. Ayako Yoshimura and Dr. Katsuyuki Hamasaki, Tokyo University of Marine Science and Technology for their assistance in fish sampling.

The author sincerely thanks Dr. Hideki Tanaka, Dr. Takuji Okumura, Dr. Masahiko Awaji, Dr. Keisuke Yamano, Dr. Toshiya Yamaguchi, Dr. Mitsuo Nyuji, NRIA, Mr. Hiroshi Hashimoto, Seikai National Fisheries Research Institute, Mrs. Tomiko Fujiwara, Mrs. Yuko Hashikawa, Mrs. Izumi Okai, Mrs. Miwako Seko, and Mrs. Ari Tsujino, for their support and encouragement.

REFERENCES

Akiyama T., Murai T. & Mori K. (1986a) Role of tryptophan metabolites in inhibition of spinal deformity of chum salmon fry caused by tryptophan deficiency. *Bull Jpn Soc Sci Fish* 52, 1255-1259.

Akiyama T., Murai T. & Nose T. (1986b) Oral administration of serotonin against spinal deformity of chum salmon fry tryptophan deficiency. *Bull Jpn Soc Sci Fish* 52, 1249-1254.

Andrades J.A., Becerra J. & Fernández-Llebrez P. (1996) Skeletal deformities in larval, juvenile and adult stages of cultured gilthead sea bream (*Sparus aurata* L.). *Aquaculture* 141, 1-11.

Arimoto M., Sato J., Maruyama K., Mimura G. & Furusawa I. (1996) Effect of chemical and physical treatments on the inactivation of striped jack nervous necrosis virus (SJNNV). *Aquaculture* 143, 15-22.

Azevedo M.F.C., Oliveira C., Pardo B.G., Martínez P. & Foresti F. (2008) Phylogenetic analysis of the order Pleuronectiformes (Teleostei) based on sequences of 12S and 16S mitochondrial genes. *Genet Mol Biol* 31, 284-292.

Barahona-Fernandes M.H. (1982) Body deformation in hatchery reared European sea bass *Dicentrarchus labrax* (L). Types, prevalence and effect on fish survival. *J Fish Biol* 21, 239-249.

Betancor M.B., Atalah E., Caballero M., Benítez -Santana T., Roo J., Montero D. & Izquierdo M. (2011) α-Tocopherol in weaning diets for European sea bass (*Dicentrarchus labrax*) improves survival and reduces tissue damage caused by excess dietary DHA contents. *Aquac Nutr* 17, e112-e122.

Betancor M.B., Caballero M.J., Benítez -Santana T., Saleh R., Roo J., Atalah E. & Izquierdo M. (2012) Oxidative status and histological changes in sea bass larvae muscle in response to high dietary content of docosahexaenoic acid DHA. *J Fish Dis* DOI: 10.1111/j.1365-2761.2012.01447.x

Blaxter J.H.S. (1988) Pattern and variety in development. In: Hoar W.S. & Randall D.J., editors. Fish Physiology 11A, Academic Press, New York, pp 1-58.

Boglione C., Gisbert E., Gavaia P., Witten P.E., Moren M., Fontagné S. & Koumoundouros G. (2013) Skeletal anomalies in reared European fish larvae and juveniles. Part 2: main typologies, occurrences and causative factors. *Rev Aquacult* 5, S121-S167.

Bromage N., Jones J., Randall C., Thrush M., Davies B., Springate J., Duston J. & Barker G.

(1992) Broodstock management, fecundity, egg quality and the timing of egg production in the rain bow trout (*Oncorhynchus mykiss*). *Aquaculture* 100, 141-166.

Bromage N., Porter M. & Randall C. (2001) The environmental regulation of maturation in farmed finfish with special reference to the role of photoperiod and melatonin. *Aquaculture* 197, 63-98.

Brooks S., Tyler C.R. & Sumpter J.P. (1997) Egg quality in fish: what makes a good egg? *Rev Fish Biol Fish* 7, 387-416.

Chapleau F. (1993) Pleuronectiform relationships: a cladistic reassessment. *Bull Mar Sci* 52, 516-540.

Chung K., Wallace J., Kim S-Y., Kalyanasundaram S., Andalman A.S., Davidson T.J., Mirzabekov J.J., Zalocusky K.A., Mattis J., Denisin A.K., Pak S., Bernstein H., Ramakrishnan C., Grosenick L., Gradinaru V. & Deisseroth K. (2013) Structural and molecular interrogation of intact biological systems. *Nature* 497, 332-337.

Cobcroft J.M. & Battaglene S.C. (2009) Jaw malformation in striped trumpeter *Latris lineata* larvae linked to walling behaviour and tank colour. *Aquaculture* 289, 274-282.

Cobcroft J.M., Pankhurst P.M., Poortenaar C., Hickman B. & Tait M. (2004) Jaw malformation in cultured yellowtail kingfish (*Seriola lalandi*) larvae. *New Zeal J Mar Fresh* 38, 67-71.

Czesny S.J., Graeb B.D.S. & Dettmers J.M. (2005) Ecological consequences of swim bladder noninflation for larval yellow perch. *Trans Am Fish Soc* 134, 1011-1020.

Dedi J., Takeuchi T., Seikai T. & Watanabe T. (1995) Hypervitaminosis and safe levels of vitamin A for larval flounder (*Paralichthys olivaceus*) fed *Artemia* nauplii. *Aquaculture* 133, 135-146.

Diogo R., Hinits Y. & Hughes S.M. (2008) Development of mandibular, hyoid and hypobranchial muscles in the zebrafish: homologies and evolution of these muscles within bony fishes and tetrapods. *BMC Dev Biol* 8. DIO:10.1186/1471-213X-8-24

Divanach P., Papandroulakis N., Anastasiadis P., Koumoundouros G. & Kentouri M. (1997) Effect of water currents on the development of skeletal deformities in sea bass (*Dicentrarchus labrax* L.) with functional swimbladder during postlarval and nursery phase. *Aquaculture* 156, 145-155.

Edgeworth F.H. (1935) The Cranial muscles of vertebrates, Cambridge University Press, Cambridge.

Geerinckx T. & Adriaens D. (2007) Ontogeny of the intermandibular and hyoid musculature in the suckermouth armoured catfish *Ancistrus* cf. *triradiatus* (Loricariidae, Siluriformes). *Anim*

Biol 57, 339-357.

Geerinckx T. & Adriaens D. (2008) Ontogeny of the suspensorial and opercular musculature in the suckermouth armoured catfish *Ancistrus* cf. *triradiatus* (Loricariidae, Siluriformes). *Zoomorphology* 127, 83-95.

Georgakopoulou E., Katharios P., Divanach P. & Koumoundouros G. (2010) Effect of temperature on the development of skeletal deformities in Gilthead seabream (*Sparus aurata* Linnaeus, 1758). *Aquaculture* 308, 13-19.

Gisbert E., Ortiz-Delgado J.B. & Sarasquete C. (2008) Nutritional cellular biomarkers in early life stages of fish. *Histol Histopathol* 23, 1525-1539.

Gracey A.Y., Troll J.V. & Somero G.N. (2001) Hypoxia-induced Gene Expression Profiling in the Euryoxic Fish *Gillichthys mirabilis*. *Proc Natl Acad Sci U S A* 98, 1993-1998.

Grotmol S. & Totland G.K. (2000) Surface disinfection of Atlantic halibut *Hippoglossus hippoglossus* eggs with ozonated sea-water inactivates nodavirus and increases survival of the larvae. *Dis Aquat Organ* 39, 89-96.

Hama H., Kurokawa H., Kawano H., Ando R., Shimogori T., Noda H., Fukami K., Sakaue-Sawano A. & Miyawaki A. (2011) Sca*l*e: a chemical approach for fluorescence imaging and reconstruction of transparent mouse brain. *Nat Neurosci* 14, 1481-1488.

Hamasaki K., Tsuruoka K., Teruya K., Hashimoto H., Hamada K., Hotta T. & Mushiake K. (2009) Feeding habits of hatchery-reared larvae of greater amberjack *Seriola dumerili*. *Aquaculture* 288, 216-225.

Hattori M., Sawada Y., Kurata M., Yamamoto S., Kato K. & Kumai H. (2004) Oxygen deficiency during somitogenesis causes centrum defects in red sea bream, *Pagrus major* (Temminck et Schlegel). *Aquac Res* 35, 850-858.

Herbing I.H.V., Miyake T., Hall B.K. & Boutilier R.G. (1996a) Ontogeny of feeding and respiration in larval Atlantic cod *Gadus morhua* (Teleostei, Gadiformes): I. Morphology. *J Morphol* 227, 15-35.

Herbing I.H.V., Miyake T., Hall B.K. & Boutilier R.G. (1996b) Ontogeny of feeding and respiration in larval Atlantic cod *Gadus morhua* (Teleostei, Gadiformes): II. Function. *J Morphol* 227, 37-50.

Hernandez L.P., Patterson S.E. & Devoto S.H. (2005) The development of muscle fiber type identity in zebrafish cranial muscles. *Anat Embryol* 209, 323-334.

Hirata Y., Hamasaki K., Imai A., Teruya K., Iwasaki T., Hamada K. & Mushiake K. (2009) Effects of different photoperiods and water temperatures on survival, growth, feeding and initial

swim bladder inflation of greater amberjack S*eriola dumerili* larvae. *Nippon Suisan Gakkaishi* 75, 995-1003.

Huysentruyt F., Geerinckx T. & Adriaens D. (2007) A descriptive myology of *Corydoras aeneus* (Siluriformes: Callichthyidae), with a brief discussion on adductor mandibulae homologies. *Anim Biol* 57, 433-452.

Imai A., Iwasaki T., Hashimoto H., Hirata Y., Hamasaki K., Teruya K., Hamada K. & Mushiake K. (2011) Mechanism for initial swim bladder inflation in larvae of greater amberjack *Seriola dumerili* inferred from larval rearing experiments and ontogenetic development of a swim bladder. *Nippon Suisan Gakkaishi* 77, 845-852.

Javidan Y. & Schilling T.F. (2004) Development of cartilage and bone. In: Detrich H.W. III, Westerfield M. & Zon L.I., editors. The Zebrafish: Cellular and Developmental Biology, 2nd Ed Methods Cell Biol, Elsevier Academic Press, California, pp 415-436.

Johnston I.A. (2006) Environment and plasticity of myogenesis in teleost fish. *J Exp Biol* 209, 2249-2264.

Kajimura S., Aida K. & Duan C. (2005) Insulin-like growth factor-binding protein-1 (IGFBP-1) mediates hypoxia-induced embryonic growth and developmental retardation. *Proc Natl Acad Sci U S A* 102, 1240-1245.

Kihara M., Ogata S., Kawano N., Kubota I. & Yamaguchi R. (2002) Lordosis induction in juvenile red sea bream, *Pagrus major*, by high swimming activity. *Aquaculture* 212, 149-158.

Kimmel C.B., Sepich D.S. & Trevarrow B. (1988) Development of segmentation in zebrafish. *Development* 104, 197-207.

Kjørsvik E., Mangor-Jensen A., Holmefjord I., Blaxter J.H.S. & Southward A.J. (1990) Egg Quality in Fishes. Advances in Marine Biology, Academic Press, London, pp 71-113.

Kolkovski S. & Sakakura Y. (2007) Yellowtail kingfish, from larvae to mature fish - problems and opportunities. *World Aquaculture* 38, 44-48.

Koumoundouros G., Divanach P. & Kentouri M. (2001) The effect of rearing conditions on development of saddleback syndrome and caudal fin deformities in *Dentex dentex* (L.). *Aquaculture* 200, 285-304.

Koumoundouros G., Maingot E., Divanach P. & Kentouri M. (2002) Kyphosis in reared sea bass (*Dicentrarchus labrax* L.): ontogeny and effects on mortality. *Aquaculture* 209, 49-58.

Krone P.H., Sass J.B. & Lele Z. (1997) Heat shock protein gene expression during embryonic development of the zebrafish. *Cell Mol Life Sci* 53, 122-129.

Laggis A., Sfakianakis D.G., Divanach P. & Kentouri M. (2010) Ontogeny of the body skeleton in

Seriola dumerili (Risso, 1810). *Ital J Zool* 77, 303-315.

Liem K.F. (1991) A functional approach to the development of the head of teleosts: Implications on constructional morphology and constraints. In: Schmidt-Kittler N. & Vogel K., editors. Constructional morphology and evolution, Springer-Verlag, Berlin, pp 231-249.

Liu C.H. (2001) Early osteological development of the yellow tail *Seriola dumerili* (Pisces: Carangidae). *Zool Stud* 40, 289-298.

Maeno Y., Sorimachi M. & Egusa S. (1995) Histopathology of viral deformity in yellowtail fingerling, *Seriola quinqueradiata*. *Fish Pathol* 30, 53-58.

Masuma S., Kanematu M. & Teruya K. (1990) Embryonic and morphological development of larvae and juveniles of the Amberjack, *Seriola dumerili*. *Ichthyol Res* 37, 164-169.

Matsuoka M. (1987) Development of the skeletal tissues and skeletal muscles in the red sea bream. *Bull Seikai Reg Fish Res Lab* 65, 1-113.

Minami T. (1982) The early life history of flounder *Paralichthys olivaceus*. *Bull Jpn Soc Sci Fish* 48, 1581-1588.

Minami T. (1981) The early life history of a sole *Heteromycteris Japonicus*. *Bull Jpn Soc Sci Fish* 47, 857-862.

Morin-Kensicki E.M., Melancon E. & Eisen J.S. (2002) Segmental relationship between somites and vertebral column in zebrafish. *Development* 129, 3851-3860.

Nagano N., Hozawa A., Fujiki W., Yamada T., Miyaki K., Sakakura Y. & Hagiwara A. (2007) Skeletal development and deformities in cultured larval and juvenile seven-band grouper, *Epinephelus septemfasciatus* (Thunberg). *Aquac Res* 38, 121-130.

Nakae M. & Sasaki K. (2008) Branchial arch muscle innervation by the glossopharyngeal (IX) and vagal (X) nerves in Tetraodontiformes, with special reference to muscle homologies. *J Morphol* 269, 674-690.

Norman J.R. (1934) A systematic monograph of the flatfish (Heterosomata). British Museum, London.

Ochiai A. (1966) Studies on the comparative morphology and ecology of the Japanese soles. *Misaki Marine Biological Institute Kyoto University Special Report* 3, 1-97 (in Japanese).

Otten E. (1982) The development of a mouth-opening mechanism in a generalized *Haplochromis* species:*H.elegans* Trewavas 1933(Pisces, Cichlidae). *Neth J Zool* 32, 31-48.

Padilla P.A. & Roth M.B. (2001) Oxygen deprivation causes suspended animation in the zebrafish embryo. *Proc Natl Acad Sci U S A* 98, 7331-7335.

Pardo B., Machordom A., Foresti F., Porto-Foresti F., Azevedo M., Bañon R., Sánchez L. &

Martínez P. (2005) Phylogenetic analysis of flatfish (Order Pleuronectiformes) based on mitochondrial 16s rDNA sequences. *Sci Mar* 69, 531-543.

Patterson S.E., Mook L.B. & Devoto S.H. (2008) Growth in the larval zebrafish pectoral fin and trunk musculature. *Dev Dyn* 237, 307-315.

Roy M.N., Prince V.E. & Ho R.K. (1999) Heat shock produces periodic somitic disturbances in the zebrafish embryo. *Mech Dev* 85, 27-34.

Sabate F.S., Sakakura Y., Shiozaki M. & Hagiwara A. (2009) Onset and development of aggressive behavior in the early life stages of the seven-band grouper *Epinephelus septemfasciatus*. *Aquaculture* 290, 97-103.

Sakaguchi S., Hara T., Matsuzato T., Shibahara K., Yamagata Y., Kawai H. & Maeno Y. (1987) Scoliosis of cultured yellowtail caused by parasitic *Myxobolus buri*. *Bull Natl Res Inst Aquac* 12, 79-86.

Sakakura Y., Shiotani S., Chuda H. & Hagiwara A. (2006) Improvement of the survival in the seven-band grouper *Epinephelus septemfasciatus* larvae by optimizing aeration and water inlet in the mass-scale rearing tank. *Fish Sci* 72, 939-947.

Sakakura Y., Shiotani S., Chuda H. & Hagiwara A. (2007a) Flow field control for larviculture of the seven-band grouper *Epinephelus septemfasciatus*. *Aquaculture* 268, 209-215.

Sakakura Y., Shiotani S., Shiozaki M. & Hagiwara A. (2007b) Larval rearing without aeration: a case study of the seven-band grouper *Epinephelus septemfasciatus* using a wave maker. *Fish Sci* 73, 1199-1201.

Sawada Y., Hattori M., Iteya M., Takagi Y., Ura K., Seoka M., Kato K., Kurata M., Mitatake H., Katayama S. & Kumai H. (2006a) Induction of centrum defects in amberjack *Seriola dumerili* by exposure of embryos to hypoxia. *Fish Sci* 72, 364-372.

Sawada Y., Hattori M., Sudo N., Kato K., Takagi Y., Ura K., Kurata M., Okada T. & Kumai H. (2006b) Hypoxic conditions induce centrum defects in red sea bream *Pagrus major* (Temminck and Schlegel). *Aquac Res* 37, 805-812.

Sawada Y., Higuchi K., Haga Y., Ura K., Ishibashi Y., Kurata M., Miyatake H., Katayama S. & Seoka M. (2008) Effects of hypoxia and hypercapnia on the embryonic development of striped jack, *Pseudocaranx dentex*. *Nippon Suisan Gakkaishi* 74, 144-151.

Schilling T.F. & Kimmel C.B. (1997) Musculoskeletal patterning in the pharyngeal segments of the zebrafish embryo. *Development* 124, 2945-2960.

Schilling T.F., Piotrowski T., Grandel H., Brand M., Heisenberg C.P., Jiang Y.J., Beuchle D., Hammerschmidt M., Kane D.A., Mullins M.C., van Eeden F.J., Kelsh R.N.,

Furutani-Seiki M., Granato M., Haffter P., Odenthal J., Warga R.M., Trowe T. & Nusslein-Volhard C. (1996) Jaw and branchial arch mutants in zebrafish I: branchial arches. *Development* 123, 329-344.

Schroter C., Herrgen L., Cardona A., Brouhard G.J., Feldman B. & Oates A.C. (2008) Dynamics of zebrafish somitogenesis. *Dev Dyn* 237, 545-553.

Sfakianakis D.G., Georgakopoulou E., Papadakis I.E., Divanach P., Kentouri M. & Koumoundouros G. (2006) Environmental determinants of haemal lordosis in European sea bass, *Dicentrarchus labrax* (Linnaeus, 1758). *Aquaculture* 254, 54-64.

Sfakianakis D.G., Koumoundouros G., Divanach P. & Kentouri M. (2004) Osteological development of the vertebral column and of the fins in *Pagellus erythrinus* (L. 1758). Temperature effect on the developmental plasticity and morpho-anatomical abnormalities. *Aquaculture* 232, 407-424.

Shiozawa S., Takeuchi H. & Hirokawa J. (2003) Improved seed production techniques for the amberjack, *Seriola dumerili*. *Saibai Giken* 31, 11-18.

Skjaerven K.H., Olsvik P.A., Finn R.N., Holen E. & Hamre K. (2011) Ontogenetic expression of maternal and zygotic genes in Atlantic cod embryos under ambient and thermally stressed conditions. *Comp Biochem Physiol A Mol Integr Physiol* 159, 196-205.

Smith M., Hickman A., Amanze D., Lumsden A. & Thorogood P. (1984) Trunk neural crest origin of caudal fin mesenchyme in the zebrafish Brachydanio rerio. *Proc R Soc Lond B* 256, 137-145.

Sparrow D.B., Chapman G., Smith A.J., Mattar M.Z., Major J.A., O'Reilly V.C., Saga Y., Zackai E.H., Dormans J.P., Alman B.A., McGregor L., Kageyama R., Kusumi K. & Dunwoodie S.L. (2012) A mechanism for gene-environment interaction in the etiology of congenital scoliosis. *Cell* 149, 295-306.

Stiassny M.L.J. (2000) Muscular System. In: Bullock G. & Bunton T.E., editors. Gross functional anatomy, Academic Press, London, pp 119-128.

Sun C., Tao Y., Jiang X. & Zou S. (2011) IGF binding protein 1 is correlated with hypoxia-induced growth reduce and developmental defects in grass carp (*Ctenopharyngodon idellus*) embryos. *Gen Comp Endocr* 172, 409-415.

Tachihara K., Ebisu R. & Tukashima Y. (1993) Spawning, eggs, larvae and juveniles of the purplish amberjack *Seriola dumerili*. *Nippon Suisan Gakkaishi* 59, 1479-1488.

Takahashi N. (1917) On the homology of the median longitudinal muscles - supracarinalis and infracarinalis - with the fin-muscles of the dorsal and anal fins, and their functions. *J Coll*

Sci Tokyo Imp Univ 6, 199-213, 192 pls.

Takata Y. & Sasaki K. (2005) Branchial structures in the Gasterosteiformes, with special reference to myology and phylogenetic implications. *Ichthyol Res* 52, 33-49.

Takemaru I., Kashio N. & Maeno K. (2009) Kyphosis and lordosis observed in yellowtail and amberjack cultured in Kagoshima Bay. *Aquac Sci* 52, 255-264 (in Japanese with English abstract).

Takeuchi T., Dedi J., Haga Y., Seikai T. & Watanabe T. (1998) Effect of vitamin A compounds on bone deformity in larval Japanese flounder (*Paralichthys olivaceus*). *Aquaculture* 169, 155-165.

Takle H., Baeverfjord G., Lunde M., Kolstad K. & Andersen Ø. (2005) The effect of heat and cold exposure on HSP70 expression and development of deformities during embryogenesis of Atlantic salmon (*Salmo salar*). *Aquaculture* 249, 515-524.

Tanaka Y., Sakakura Y., Chuda H., Hagiwara A. & Yasumoto S. (2005) Food selectivity of seven-band grouper *Epinephelus septemfasciatu*s larvae fed different sizes of rotifers. *Nippon Suisan Gakkaishi* 71, 911-916 (in Japanese with English abstract).

Terova G., Rimoldi S., Corà S., Bernardini G., Gornati R. & Saroglia M. (2008) Acute and chronic hypoxia affects HIF-1αmRNA levels in sea bass (*Dicentrarchus labra*x). *Aquaculture* 279, 150-159.

Teruya K., Yoseda K., Oka M., Nishioka T., Nakano S., Mori K. Sugaya T. & Hamasaki K. (2008) Effects of photoperiod on survival, growth and feeding of seven band grouper *Epinephelus septemfaciatus* larvae. *Nippon Suisan Gakkaishi* 74, 645-652 (in Japanese with English abstract).

Teruya K., Hamasaki K., Hashimoto H., Katayama T., Hirata Y., Tsuruoka K., Hayashi T. & Mushiake K. (2009) Ontogenetic changes of body density and vertical distribution in rearing tanks in greater amberjack *Seriola dumerili* larvae. *Nippon Suisan Gakkaishi* 75, 54-63 (in Japanese with English abstract).

Ton C., Stamatiou D. & Liew C.C. (2003) Gene expression profile of zebrafish exposed to hypoxia during development. *Physiol Genomics* 13, 97-106.

Trotter A.J., Pankhurst P.M. & Hart P.R. (2001) Swim bladder malformation in hatchery-reared striped trumpeter *Latris lineata* (Latridae). *Aquaculture* 198, 41-54.

Tsuchihashi Y., Kuriyama I., Kuromoiya Y., Kashiwagiw M. & Yoshioka M. (2003) Effects of water temperature, illumination and feed oil addition on the survival of larvae in the mass seed production of the sevenband grouper, *Epinephelus septemfasciatus*. *Suisan Zoshoku*

51, 49-54 (in Japanese with English abstract).

Tsuchihashi Y., Kuriyama I., Kuromiya Y., Kashiwagi M. & Yoshioka M. (2002) Control of Viral Nervous Necrosis (VNN) in seedling production of sevenband grouper, *Epinephelus septemfasciatu*s. *Aquaculture* 50, 355-361.

van Eeden F.J., Granato M., Schach U., Brand M., Furutani-Seiki M., Haffter P., Hammerschmidt M., Heisenberg C.P., Jiang Y.J., Kane D.A., Kelsh R.N., Mullins M.C., Odenthal J., Warga R.M., Allende M.L., Weinberg E.S. & Nusslein-Volhard C. (1996) Mutations affecting somite formation and patterning in the zebrafish, *Danio rerio*. *Development* 123, 153-164.

Verraes W. (1977) Postembryonic ontogeny and functional anatomy of the ligamentum mandibulo-hyoideum and the ligamentum interoperculo-mandibulare, with notes on the opercular bones and some other cranial elements in *Salmo gairdneri* Richardson, 1836 (Teleostei: Salmonidae). *J Morphol* 151, 111-119.

Wargelius A., Fjelldal P.G. & Hansen T. (2005) Heat shock during early somitogenesis induces caudal vertebral column defects in Atlantic salmon (*Salmo salar*). *Dev Genes Evol* 215, 350-357.

Werner I., Linares-Casenave J., Eenennaam J. & Doroshov S. (2007) The effect of temperature stress on development and heat-shock protein expression in larval green sturgeon (*Acipenser mirostris*). *Environ Biol Fish* 79, 191-200.

Winterbottom R. (1974) A descriptive synonymy of the striated muscles of the teleostei. *Proc Acad Nat Sci (Phil)* 125, 225-317.

Yokoyama H., Freeman M.A., Itoh N. & Fukuda Y. (2005) Spinal curvature of cultured Japanese mackerel *S. japonicus* associated with a brain myxosporean, *Myxobolus acanthogobii*. *Dis Aquat Organ* 66, 1-7.